ICR ANNUAL REPORT 1997(Volume 4)

ICR

ANNUAL REPORT 1997

Kyoto University
Institute for Chemical Research

Volume 4

***ICR* ANNUAL REPORT 1997 (Volume 4)**
For the calendar year 1 January 1997 to 31 December 1997

Editors:
Professor Minoru KANEHISA (Editor in chief)
Professor Naoki SATO
Professor Toshinobu YOKO

Managing editor:
Hiroyuki HARA

Published and distributed by:
Institute for Chemical Research (*ICR*), Kyoto University
http://www.kuicr.kyoto-u.ac.jp/

Note: *ICR* Annual Report available from the *ICR* Library,
Institute for Chemical Research, Kyoto University,
Uji, Kyoto 611-0011, Japan.
Tel: +81-(0)774-38-3009
Fax: +81-(0)774-38-4370

ISSN 1342-0321

Printed by
Nakanishi Printing Co. Ltd.
Shimotachiuti-dori Higashi-iru, Kamigyo-ku, Kyoto 602-8048, Japan.
TEL:+81-(0)75-441-3155. FAX:+81-(0)75-417-2050;441-3159.
E-mail:HBE02610@niftyserve.or.jp hide@nacos.com
http://www.nacos.com/

31 March 1998

Front cover: *Historical remarks to the Institute for Chemical research(ICR)*

The chemical structure shown on the front cover represents cellulose which is a raw material of Viscose Rayon, the first man-made fiber.

In the late 1930s, during the course of studies being made of the development of a new two-bath stretch spinning process of viscose fibers, the late professor Masao Horio and his collaborators succeeded in producing a viscose rayon staple with a fine crimp similar to that of wool at the Horio Laboratory of the Institute, Takatsuki, Osaka (at that time). The cross section of crimped rayon staple can be distinguished with two different parts by a boundary line x, as shown in Fig. 1 a and b. The upper part A shows finer serrations and is characterized by a thick skin. On the other hand, the serrations of the lower part B are coarser and deeply notched, and the skin is thinner. Such a structure they called "bilateral structure". The motive force of the crimp formation is the coiling nature of fibers coming from the bilateral structure. The total shipment of rayon staple of Japan in 1963 was 284,000 tons, of which about 186,000 tons were the crimped staple manufactured by the process developed by Horio et al.

Wool is a typical bilateral fiber which is composed of an acidic part (para-cortex) and a basic part (ortho-cortex) (Fig 2). This dichotomy of the wool fiber was also first realized by Horio et al., although later these terms were more generally called as "paracortex" and "orthocortex".

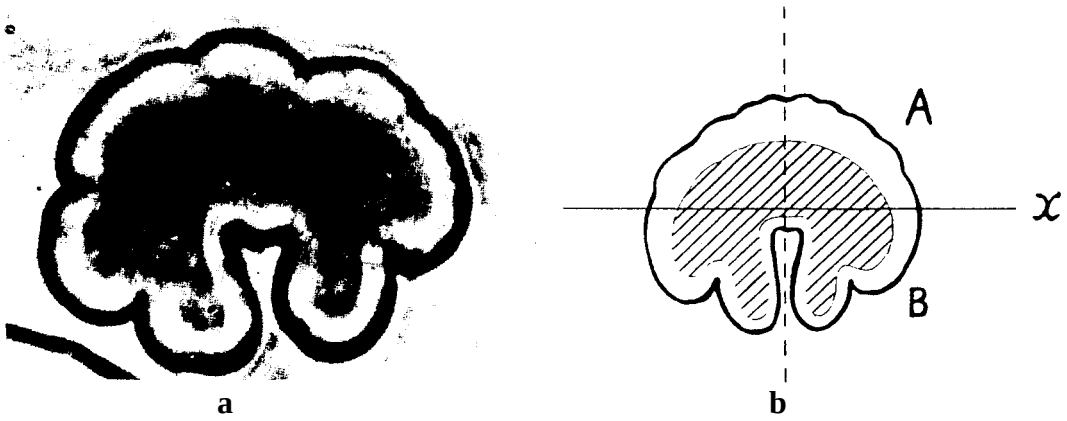

Fig 1. (a) Cross section of standard crimped rayon staple. (b) Schematic representation of a cross section of a standard crimped staple. x = boundary line.

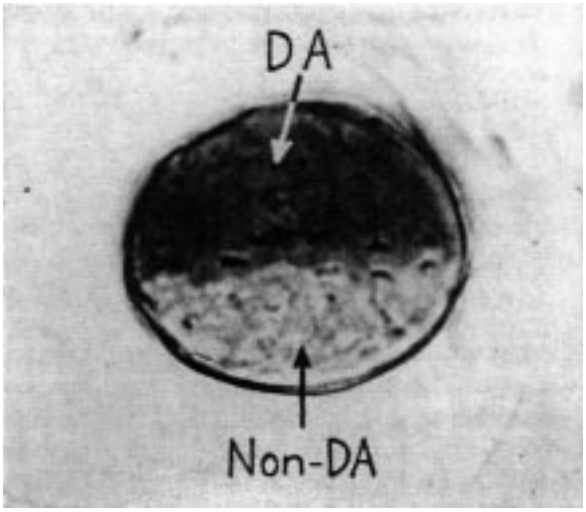

Fig 2. Differentially stained cross section of a wool fiber by Janus Green. DA : Dye-accessible (paracortex), Non-DA : Non-dye-accessible (orthocortex).

CONTENTS

Preface

100 years has passed since the establishment of Kyoto University. Various events to celebrate the centenary of the University have been held in 1997. As a part of the program, open house of research institutes in Uji campus has been carried out in November, for the first time.

Now the second century of the University has started. 13 research instututes are belonging to Kyoto University, and among them the Institute for Chemical Research (ICR) has the longest history and the greatest number of research staffs. ICR is expected to act as a leader of research institutions in the new era of the University. This booklet is the 1997 edition of the ICR Annual Report including the summaries of the scientific works by 27 laboratories in 1997, and the list of publications of the research staffs. It is recognized that the activities of ICR cover very extensive fields. Currently, 26 full professors, 23 associate professors and 47 instructors are working in the ICR. At the end of March, 1997, Professor Y.Bando of the Solid State Chemistry Laboratory has retired and Professor J.Oda of the Function Molecular Conversion Laboratory will retire in March, 1998. The selection of the successors is now in the course.

Each professor in ICR is belonging to one of the graduate schools of Science, Medicine, Pharmaceutical Sciences, Engineering and Agriculture. Namely, ICR is accepting graduate students from these 5 schools and the total number of graduate students in 1997 has attained to 220. This is an evidence that ICR is covering very broad research fields. ICR is offering an ideal circumstance for young scientists to cultivate their abilities for research by contacting with experts in other fields.

ICR has organized an international symposium, International Colloquium on Magnetic Films and Surfaces held at Sunshine Coast, Australia, in August 4-8, 1997. T.Shinjo has served as the chairperson of the organizers. From 20 countries in the world, 170 scientists, including 60 Japanese, have attended. Participants have enjoyed the exciting discussions on recent topics in thin film magnetism. Two Research Projects on Priority Areas sponsored by Monbusho has started in 1997, of which leaders are professors of ICR, K.Tamao and T.Shinjo. The titles of projects are "The Chemistry of Inter-element Linkage" and "Nanoscale Magnetism and Transport."

It is a pleasure for me to inform that a new building of ICR is now under construction and will be completed by the end of this year. The new building with the area of about 900m^2 will be used by several groups and also be able to supply the spaces for pioneering joint works. The new laboratories will be utilized to promote collaborations in the Institute and also those with outside people. Fruitful results obtained using this new atmosphere will be introduced in forthcoming issues of this Report.

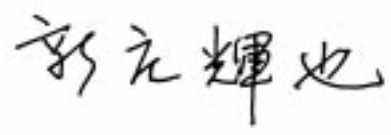

Teruya SHINJO

January,1998 DIRECTOR

TOPICS AND INTRODUCTORY COLUMNS OF LABORATORIES

Key to headline in the columns

RESEARCH DIVISION – Laboratory (Subdivision)*

*** See also "Organization and Staff" on page 83.**

Abbreviations used in the columns

Prof Em	Professor Emeritus	GS	Graduate Student
Prof	Professor	DC	Doctor's Course (Program)
Vis Prof	Visiting Professor	MC	Master's Course (Program)
Assoc Prof	Associate Professor	UG	Undergraduate Student
Lect	Lecturer	RF	Research Fellow
Lect(pt)	Lecturer (part-time)	RS	Research Student
Instr	Instructor		
Assoc Instr	Associate Instructor	D Sc	Doctor of Science
Techn	Technician	D Eng	Doctor of Engineering
Guest Scholar	Guest Scholar	D Agr	Doctor of Agricultural Science
Guest Res Assoc	Guest Research Associate	D Pharm Sc	Doctor of Pharmaceutial Science
Univ	University	D Med Sc	Doctor of Medical science

Detailed *L* Emission Spectra and Satellites of $_{74}$W

Aurel-Mihai Vlaicu, Tatsunori Tochio, Takashi Ishizuka, Daisuke Ohsawa, Yoshiaki Ito, and Takeshi Mukoyama

The *L*α and *L*β spectra of tungsten were measured using a high resolution single crystal x-ray spectrometerand were fitted into Lorentzians. The fit residuals of the *L*α and *L*β spectra indicate satellites in the vicinity of each spectrum, which are originated from Coster-Kronig transitions. Linewidths, energies, and intensities were estimated for each diagram line.

Keywords : *L*α,β satellite lines/ Coster-Kronig transition / spectator hole / natural linewidth / multiplet fitting/

It is generally difficult to analyse *L* x-ray emission spectra induced by electron impact because all the three *L* subshells can be ionized and the redistribution of initial vacancies due to Coster-Kronig transitions produce additional inner-shell vacancies. The existence of two or more holes in atomic inner shells gives rise to satellite lines with energies which are shifted from the diagram lines. The study of L x-ray satellites in high-Z elements has not been performed by many workers. There have been reported only a few papers on tungsten $_{74}$W [1,2,3] for the last 20 years. The widths of some *L* x-ray lines of W were measured as part of a program for compiling the *L* series linewidths in heavy elements [4,5,6]. They suggested that the disagreement between theory and experiment without the analysis of hidden satellites was due to the large values of *M*- and *N*- subshells partial widths reported in the work of McGuire [7].

In the present study, we investigated the line width, energies and intensities including satellites of W *L*α,β emission lines generated by electron bombardment using a single-crystal high resolution x-ray spectrometer for the evaluation on the correctness of the theoretical calculation of different types of transition rates.

The tungsten *L* spectral lines were excited by electron bombardment in a rotating anode at tube voltage of 49 kV and 150-180 mA. The spectral measurements were carried out with a single-crystal spectrometer with symmetrical Si(440), Si(444) and Ge (444) perfect crystals in which x-ray topography showed no dislocation. A double slit collimator of 100 mm length and the vertical width of 10 or 20 mm was used for the measurement.

The natural linewidths (Γ_n) of the emission spectra were evaluated from the measured spectral linewidths (Γ_o) including the energy dispersion due to the slit (δE_{slit}) and the crystal ($\delta E_{crystal}$), as follows:

$$\Gamma_{nat}^{(n)} = \Gamma_{obs}^{(n)} - (\delta E_{slit} + \delta E_{crystal})^{(n)}$$

where (n) is the correction parameter, which was determined for each spectral line by numerically solving the above equations using two different experimental conditions of collimator slit or Bragg reflection. The obtained correction parameter (n) values between $1.4 < n < 1.6$ were considered as reasonable in our experiment.

STATES AND STRUCTURE — Atomic and Molecular Physics —

Scope of Research

In order to obtain fundamental information on the property and structure of materials, the the electronic states of atoms and molecules are investigated in detail using X-ray, SR, ion beam from accelerator and nuclear radiation from radioisotopes. Theoretical analysis of the electronic states and development of new radiation detectors are also performed.

Professor
MUKOYAMA, Takeshi
(D Eng)

Assoc. Prof
ITO, Yoshiaki
(D Sc)

Instructor
KATANO, Rintaro
(D Eng)

Instructor
NAKAMATSU, Hirohide
(D Sc)

Guest Res Assoc
TURGUT, Bastug (D Sc)
Students:
YAMAGUCHI, Kouichirou (DC)
OHSAWA, Daisuke (DC)
SHIGEMI, Akio (DC)
SUZUKI, Chikashi (DC)
TOCHIO, Tatsunori (DC)
VLAICU, A.Mihai (DC)
MASAOKA, Sei (DC)
ISHIZUKA, Takashi (MC)
NAKANISHI, Yoshikazu(RF)
YASUI, Jun (RF)

The natural width of an x-ray line originated from a transition from an atomic level (A) to a level (B) is represented as the sum of the width of the initial and final levels: $\Gamma(A \rightarrow B) = \Gamma(A) + \Gamma(B)$

Theoretical values of natural width of atomic vacancy states were reported for *L*-shell [8], and *M*-shell [8] using the relativistic calculations, and for *N*-shell with nonrelativistic calculations [9].

The relative intensities of Coster-Kronig satellite transitions are calculated assuming that the radiative transition rate $\omega_{i=1,2,3}$ has the same value for single vacancy states and multiple vacancy states. For the transitions to the initial vacancy state L_2, the relative intensities of the spectator hole satellite lines to the diagram line can be calculated as follows:

$$Is(L_2)=(\sigma_1/\sigma_2)\, f_{1,2}\, P(L_1L_2X)$$

where $\sigma_{i=1,2,3}$ is the ionization cross section by electrons for the L_i subshell; $f_{i,j}$ is the partial Coster-Kronig transition probability from L_i to L_j level; $P(L_iL_jX)$ is the probability of the radiationless transition $L_i \rightarrow L_jX$, for which the double vacancy state L_jX is created, where *X* is either *M* or *N* shell. In the transitions to the initial vacancy state L_3, there are two possible Coster-Kronig transitions: $L_1 \rightarrow L_3X$ and $L_2 \rightarrow L_3X$. The relative intensities of the spectator hole satellite lines to the diagram line has two terms:

$$Is(L_3) = (\sigma_1/\sigma_3)\, f_{1,3}\, P(L_1L_3X) + (\sigma_2/\sigma_3)\, f_{2,3}\, P(L_2L_3X).$$

We used for ω_i the values reported by Krause [10], for σ_i the values reported by Reusch [11] for $_{73}$Ta at 50 kV, and for $P(L_iL_jX)$ the values reported by Chen *et al.* [12].

In Table 1 we compare our results with the previous experimental values by Salem *et al.*[4,5]. The values derived from theoretical linewidth as the sum of the two levels involved in the transition are shown for a comparison with the experimental values obtained with the multiplet fitting method by Deutsch *et al.* [13] by considering the satellite structure: the relative intensities and the relative energy position of the satellite lines to the diagram lines were fixed in the fitting. The energies of the satellites were taken from the table by Parente [14].

In the transitions involving *L*-shell levels and *M*-shell levels, such as $L\alpha_1$, $L\alpha_2$, $L\beta_1$, $L\beta_3$, and $L\beta_4$, we have a good agreement between the values obtained by multiplet fitting and the theoretical values which are obtained using the relativistic calculations. On the other hand, for the transitions involving *L*-shell levels and *N*-shell levels, such as $L\beta_2$, $L\beta_{15}$, $L\gamma_1$, the widths obtained from theoretical calculations are all larger than those from the experiments, the difference being between 2.7 eV and 3.3 eV. This disagreement between theory and experiment for $L_i \rightarrow N_j$ transitions can be attributed to the values for the *N* shell vacancy states obtained from nonrelativistic calculations. Although Gokhale *et al.* [6] and Salem & Lee [4] also suggested

this, they did not considered the satellite structure for each spectra.

The relative intensities derived from the radiative transition probabilities published by Scofield [15] are shown in Table 1 together with the experimental values reported by Salem *et.al* and our experimental values obtained by single Lorentzian fitting.

The structure left in the residue of fitting by using single Lorentzians may be attributed to the presence of the hidden satellites. Even after considering the satellite structure, by using the multiplet fitting, there still remains some structure in the residue. This situation has appeared for all analysed spectra, excluding $L\beta_{2,15}$, when the residue was completely solved. This can be due to the fact that we could not include in the multiplet fitting model the contribution of the: *O* and *P* shell spectator hole, and the shake-off processes.

References

[1] L.Salgueiro, M.L.Carvalho, and F.Parente, *Journal de Physique*, colloque C9, **48**, 609 (1987)

[2] A.N.Nigam, R.B.Mathur *Chemical Physiscs Letters* **28**, 41 (1974)

[3] A.N.Nigam, R.B.Mathur, and R.Jain, *J.Phys.***B7**, 2489

[4] S.I.Salem, and P.L.Lee, *Phys.Rev*.**A10**, 2033 (1974)

[5] S.I.Salem, S.L.Panossian, and R.A.Krause, *At. Data Nucl. Data Tables* **14**, 91 (1974)

[6] B.G.Gokhale *et. al*, *Phys.Rev.***A28**, 858 (1983)

[7] E.J.McGuire, *Phys.Rev.***A5**, 1043 (1972); **A6,** 851 (1972); **A10** 13 (1974)

[8] M.S.Chen, B.Crasemann, and H.Mark, *Phys.Rev.***A24**, 177 (1981); **A27**, 2989 (1983); **A21**, 449 (1980)

[9] E.J.McGuire, *Phys.Rev.***A9**, 1840 (1974)

[10] M.O.Krause, *J.Phys.Chem.Ref.Data* **8**, 307 (1979)

[11] S.Reusch, H.Genz, W.Low, A.Richter, *Z.Phys.***D3**, no.4, 379 (1986)

[12] M.H.Chen, B.Crasemann, H.Mark, M.Aoyagi, and H.Mark, *At.Data and Nuclear Data Tables*, **24**, 13 (1979)

[13] M.Deutsch, G.H"olzer, J.H"artwig, J.Wolf, M.Fritsch, and E.F"orster, *Phys.Rev.***A51**, 283 (1995)

[14] F.Parente, *At.Data Nucl.Data Tables* **26**, 383 (1981)

[15] J.H.Scofield, *At. Data Nucl. Data Tables* **14**, 121 (1974)

Table 1

Line	Transition	Linewidth							Relative Intensity		
		Experimental			Theoretical				Theoretical	Experiment	
		Salem [eV]	Present work	(n corr.) [eV]	Γi [eV]	Γf [eV]	Γi+Γf	Multiplet fitting	Scofield	Salem	Present work
$WL\alpha_1$	L3-M5	7.84	7.022	(1.33)	4.812	1.795	6.607	6.675	100	100	100
$WL\alpha_2$	L3-M4	5.27	7.27	(2.25)	4.812	1.868	6.680	6.784	11.34	11.16	11.43
$WL\beta_2$	L3-N5	9.26	10.572	(1.603)	4.812	7.720	12.53	9.616	17.74	-	20.79
$WL\beta_{15}$	L3-N4	-	7.73	(1.65*)	4.812	7.89	12.70	9.43	1.98	-	1.55
$WL\ \beta_{2,15}$									19.64	22.74	22.34
$WL\beta_6$	L3-N1	-	11.65	-	4.812	15.00	19.81	-	1.246	1.25	1.25
$WL\beta_1$	L2-M4	7.82	6.941	(1.54)	4.821	1.868	6.689	6.620	100	100	100
$WL\gamma_1$	L2-N4	10.20	10.626	(1.96)	4.821	7.89	12.71	10.07	18.61	18.80	23.16
$WL\beta_3$	L1-M3	12.6	12.72	(1.52)	5.959	10.560	16.519	-	100	100	100
$WL\beta_4$	L1-M2	13.20	14.66	(1.22)	5.959	11.90	17.859	-	79.88	67.8	77.32

Crystal Structure Analysis of C_{60} Low Temperature Phase by Electron Crystallography with Cryo-TEM

Tetsuya Ogawa, Seiji Isoda and Takashi Kobayashi

The crystal structure of C_{60} at liquid helium temperature was examined by electron diffraction method using an imaging plate and cryo-TEM. The R factor could be reduced to a certain amount by assuming a multi-component crystal. Disorder in the crystal might be an important factor as well as dynamical scattering effect to be considered in electron crystallography for analyzing structures of thin crystals.

Keywords: Electron crystallography / C_{60} / Cryo-TEM / Imaging plate

A transmission electron microscope (TEM) is a useful tool for studying crystal structures of ultra-thin organic specimens. Recently, Dorset and coworkers [1] demonstrated the possibility of crystal structure analysis by the electron diffraction technique. However, the kinematical treatment gives only 0.2-0.3 as the R factor, which is worse compared with the results of X-ray or neutron scattering methods. The reason is considered to be the existence of dynamical scattering and the lack of quantitative response of the conventional recording medium. In this work, we investigated the electron diffraction pattern of thin C_{60} crystals at liquid helium temperature using a 400 kV cryo-TEM and an imaging plate (IP) to analyze the structure and revealed a disordered structure in the thin crystal. An IP exhibits wide dynamic range, high sensitivity and good linear response to electron dose. These excellent properties make it possible to obtain precise electron diffraction intensities and to analyze crystal structure in atomic resolution.

The thin crystalline sample was prepared by vacuum deposition of C_{60}. The TEM used was JEM-4000SFX, which is equipped with a cryo-stage cooled by liquid helium so that the sample is observed at the temperature of 4.2 K. An electron diffraction pattern with the incident beam along <111> was observed and recorded on an IP. Forty-six integral intensities of symmetrically independent reflections were estimated and compared with those calculated from model structures.

Several workers have carried out the crystal structure analysis on C_{60} below its glass transition point (86K) by X-ray and neutron scattering, where the fitting of the intensity profile was carried out using a rotational angle ϕ as a parameter for the model [4,5], see Fig. 1(a). The best fit was found at ϕ~98°. David [6] analyzed neutron scattering data below the first-order transition point (260K) in detail and pointed out that there are two crystal modifications, which they called the major and the minor orientations, corresponding to different ϕ values. Below the

STATES AND STRUCTURES — Crystal Information Analysis —

Scope of research

Structures of materials and their structural transition associated with chemical reactions are studied through the direct observation of atomic or molecular imaging by high resolution microscopy. It aims to explore new methods for imaging with high resolution and for obtaining more detailed chemical information. The following subjects are studied: direct structure analysis of ultrafine crystallites and ultrathin films, crystal growth and adsorption states of organic materials, and development on high resolution energy filtered imaging as well as electron energy-loss spectroscopy.

Prof KOBAYASHI, Takashi (D Sc)

Assoc Prof ISODA, Seiji (D Sc)

Instr OGAWA, Tetsuya (D Sc)

Instr NEMOTO, Takashi (D Sc)

Assoc Instr MORIGUCHI, Sakumi

Guest Scholars:
NEHER, Dieter (D Sc)
FLOERSHEIMER, Mathias (D Sc)

Students:
IRIE, Satoshi (DC)
KUWAMOTO, Kiyoshi (DC)
KOSHINO, Masanori (DC)
YAJI, Toyonari (DC)
SUGA, Takeo (DC)
FUJIWARA, Eiichi (DC)
TSUJIMOTO, Masahiko (MC)
YOSHIDA, Kaname (MC)
FURUKAWA, Chieko (MC)
AKAGI, Nozomu (MC)
TERADA, Shohei (MC)
HAHAKURA, Seiji (MC)

glass transition point the hopping between them is frozen. From their neutron scattering data, the ratio of the major and minor orientations was determined to be ~0.64 at 200 K, which is increased to ~0.84 at the glass transition temperature and becomes constant below that temperature.

At the first step, we discuss the least-squares fit of the observed scattering intensities from the thin C_{60} crystal at liquid helium temperature with those calculated kinematically from a model structure in which all molecules have the same rotation of ϕ. The least-squares fit by the model with a rotation angle was carried out for every degree of the rotation angle. As a result, the R factor reaches the minimum value of 0.23 at ϕ~99°. The rotation angle ϕ~99° coincides well with that of major orientation (97.62°) already reported, which indicates that the C_{60} molecule in thin film tends to have mainly the major orientation at liquid helium temperature.

As the second step of analysis we tried to estimate the coexisting ratio between the major and minor orientations by the least-squares fitting of observed intensities as in the case of David and coworkers. The minimum *R* factor of 0.17 is obtained at major:minor = 0.74:0.26. The ratio of the major orientation, 0.74, is slightly different from the value of 0.84 obtained for the bulk by David and coworkers. The *R* factor is decreased from 0.23 to 0.17 by assuming the coexistence of major and minor orientations.

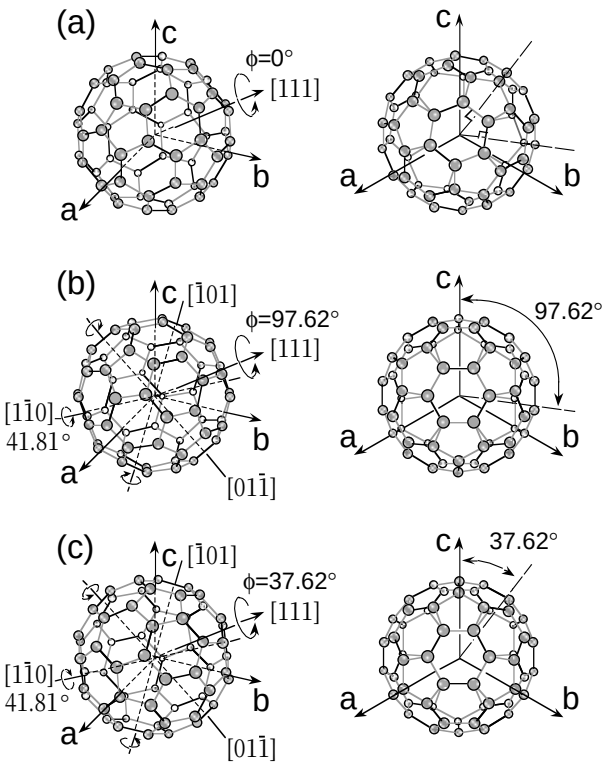

Figure 1. Orientation of the molecule at the origin of the unit cell in the low-temperature phase of C_{60} (left) and their projections on (111) (right). (a) Initial setting, ϕ=0°, where three mirror planes of the molecule is normal to the three unit-cell axes; (b) major orientation, ϕ=97.62°; (c) minor orientation, ϕ=37.62°.

Since the *R* factor of 0.17 still seems unsatisfactory, an extra parameter to be minimized has to be considered. That is, the existence of the f.c.c. component in the sample was considered, where f.c.c. component means an additional disordered region of molecular orientation due to the rapid freezing of molecules at each random orientational angle. The minimum value of *R* factor (0.12) is obtained at the f.c.c.:major:minor ratio of 0.47:0.46:0.07. Accordingly, some molecules are expected to transform into a glassy state without passing through the ordered phase. The major:minor ratio of 0.46:0.07 (= 0.87:0.13) corresponds well to the results of neutron scattering experiment by David and coworkers. The R factor is reduced to 0.12 considering the existence of some fraction of f.c.c.

The specimen used in this work is thin enough and contains no heavy atoms. Therefore the dynamical scattering effect is negligible. However, the *R* factor does not fall lower than 0.23 when an attempt was made to fit the observed intensities only with those calculated based on one structural component structure, *i.e.* major orientation. By assuming the coexistence of minor orientation crystal and also f.c.c. crystal with the random molecular orientation, the *R* factor could be reduced to 0.17 and furthermore to 0.12. The minor orientation and random orientation of f.c.c. structure are regarded as disordered structures in the major orientation crystal. Thus, the structural disorder in a specimen may be one key factor to be considered in structure analysis by electron crystallography.

References

1. Dorset D. L.: *Structural electron crystallography*. New York and London: Plenum Press, (1995)
2. Ogawa, T., Moriguchi, S., Isoda, S. and Kobayashi, T.: *Polymer* **35**, 1132-1136, (1994).
3. Ogawa, T., Moriguchi, S., Isoda, S. and Kobayashi, T.: *Proceedings of the thirteenth international congress on electron microscopy*, **1**, 965-966, (1994)
4. Heiney, P. A., Fischer, J. E., McGhie, A. R., Romanow, W. J., Denenstein, A. M., McCauley, Jr. J. P., Smith, III A. B. and Cox, D. E.: *Phys. Rev. Lett.* **66**, 2911-2914, (1991)
5. David, W. I. F., Ibberson, R. M., Matthewman, J. C., Prassides, K., Dennis, T. J. S., Hare, J. P., Kroto, H. W., Taylor, R. and Walton, D. R. M.: *Nature* **353**, 147-149, (1991)
6. David, W. I. F., Ibberson, R. M. and Matsuo, T.: *Proc. R. Soc. Lond.* **A442**, 129-146, (1993)

Edge-on Lamellae of Polyoxymethylene Crystallized from Solutions Epitaxially onto Alkali Halides

Masaki Tsuji, Masahiro Fujita, Masatoshi Tosaka and Shinzo Kohjiya

Edge-on crystalline lamellae of polyoxymethylene (POM) were isothermally grown onto the (001) face of NaCl or KCl from 0.1 wt% solutions (solvent: nitrobenzene, acetophenone, benzyl alcohol, *m*-cresol). The thickness of crystalline core in the edge-on lamella increased with decreasing supercooling (ΔT), but was inevitably smaller than the corresponding lamellar thickness for any ΔT. Accordingly, the POM edge-on lamella should have a surface layer (20~25% of the lamellar thickness) containing folds on each side of its crystalline core.

Keywords : POM/ Epitaxy/ Transmission electron microscopy/ TEM/ Electron diffraction/ Dark-field image/ Lamellar thickness/ Crystalline core

Epitaxy of polyoxymethylene (POM) onto various alkali halides has been studied extensively [1-6]. In analogy with polyethylene (PE) [7], typical morphology of POM on the (001) face of an alkali halide observed by transmission electron microscopy (TEM) is characterized by rodlike crystals oriented in the <110> directions of the substrate. Electron diffraction (ED) revealed that the chain stems in such rodlike crystals lie parallel to the substrate surface and are also oriented in the <110> directions of the substrate [4,5]. Recently, it was proposed that the chain stems in the rodlike crystal of POM grown epitaxially on NaCl might be set parallel to the long axis of the rod with a triangular cross-section [6]. Before this proposal, it had been postulated that the stems in the rod should be packed perpendicular to its long axis, *i.e.*, each of the rodlike crystals of POM had been regarded as an "edge-on" lamella [5], without any conclusive evidences. Here, we will report the morphology of the rodlike crystals of POM grown on alkali halides which was studied by TEM in bright- and dark-field imaging modes, and also will discuss the dependence of the crystalline-core thickness on the crystallization temperature (Tc).

POM (TENAC 5010, M≅40,000; Asahi Chemical Industry Co., Ltd.) was utilized. Substrates used here were NaCl and KCl, the (001) faces of which were freshly cleaved just before use, because only the hexagonal form of POM is expected to grow on both of them [4]. Nitrobenzene, acetophenone, benzyl alcohol, and *m*-cresol were used as a solvent. At desired Tc's, epitaxy was performed isothermally (Tc ±1˚C) for 60 seconds in every 0.1 wt% solution of POM under an N_2 atmosphere. TEM was carried out with a JEOL JEM-200CS operated at 160 or 200 kV. For ED and dark-field imaging, a specimen-rotating holder was utilized.

On both of the substrates, the rodlike crystals were surely oriented in the [110] and [-110] directions of the substrate, being perpendicular to each other [8, 9]. By ED experiments, the crystal form of the rodlike crystals of POM grown on NaCl and KCl was confirmed to be hexagonal (9/5 helix: a = 0.447 nm, c (chain axis) = 1.739 nm) [10]. Evidently, the crystals on KCl were nucleated much more densely than those on NaCl, prob-

STATES AND STRUCTURES — Polymer Condensed States —

Scope of research

Attempts have been made to elucidate the molecular arrangement and the mechanism of structural formation/change in crystalline polymer solids, polymer gels and elastomers, polymer liquid crystals, and polymer composites, mainly by electron microscopy and/or X-ray diffraction/scattering. The major subjects are: synthesis and structural analysis of polymer composite materials, preparation and characterization of polymer gels and elastomeric materials, structural analysis of crystalline polymer solids by direct observation at molecular level resolution, and in situ *studies on structural formation/change in crystalline polymer solids.*

Prof KOHJIYA, Shinzo (D Eng)

Assoc Prof TSUJI, Masaki (D Eng)

Instr URAYAMA, Kenji (D Eng)

Instr TOSAKA, Masatoshi

Instr MURAKAMI, Syozo (D Eng)

Students:
HIRATA, Yoshitaka (DC)
SHIMIZU, Toshiki (DC)
MURAKAMI, Takeshi (DC)
BEDIA, Elinor L.(DC)
FUJITA, Masahiro (MC)
KAWAMURA, Takanobu (MC)
KAMIJO, Takashi (MC)
KASAI, Yutaka (MC)
HORIGUCHI, Nariatsu (UG)
NAKANO, Shin-ichi (UG)
YOKOYAMA, Keisuke (UG)
ANDREA, Barbetta (RF)
TERAKAWA, Katsumi (RF)
LUO, Zhaohui (RS)
NOVILLO, Fernando A. (RS)

ably because KCl has a nearly perfect lattice-matching with the hexagonal POM than other alkali halides [4]. In contrast, nucleation took place less frequently on NaCl, and accordingly, most of the resulting rodlike crystals could grow much longer.

It was not easy to measure correctly the width of rodlike crystal. Occasionally, however, we could do so for some crystals giving adequate mass-thickness contrast only in the bright-field image of Pt-Pd- shadowed rodlike crystals grown on KCl at 125˚C. In this case, the average width of the rodlike crystals was estimated at 9.1 (±1.7) nm. This value is approximately compatible with the lamellar thickness measured before by small-angle X-ray scattering (SAXS) of single crystal mats [11,12], as shown in Fig.1.

In the ED patterns obtained here, two *hhl* net-patterns of the hexagonal lattice, which are perpendicular to each other, were recognized. Therefore, it can be concluded that the chain axis in the rodlike crystal is oriented in either [110] or [-110] direction of the substrates and the contact plane of the rodlike crystal, *viz.* the plane in contact with the substrate surface is the (100) plane of hexagonal POM [8,9]. In order to determine the direction of chain axis in the rodlike crystals, the 100 dark-field image of them was taken after tilting the specimen by |30˚| around the axis perpendicular to the long axis of the rod [8]. From the image, it was determined that POM chain stems are set perpendicular to the long axis of the rodlike crystal, strictly speaking, to that of the crystalline core in the rodlike crystal. These results definitely revealed that each of the rodlike crystals grown epitaxially on KCl and NaCl is an edge-on folded-chain lamella of POM, taking into account the lateral width of the crystals and the molecular weight of POM [8,9]. Each bright striation in the dark-field image, therefore, corresponds to the crystalline core in the edge-on lamella [7-9]. Using the present dark-field imaging technique by TEM, we can directly estimate the crystalline-core thickness, *viz.* the stem length in an edge-on lamella. For this purpose, KCl was used as a substrate.

It is well known that the lamellar thickness increases approximately linearly with increasing reciprocal of the supercooling, $1/\Delta T$ [12]. Here, $\Delta T \equiv Td^0 - Tc$, where Td^0 is the equilibrium dissolution temperature for each solvent. The values of Td^0 and of the lamellar thickness of POM single crystals grown isothermally at various Tc's were quoted from literature [11] for each solvent used in this report.

Figure 1 shows the $1/\Delta T$-dependence of the crystalline-core thickness, which was obtained by the dark-field TEM [9], and also that of the lamellar thickness of single crystals grown from solutions, which was estimated by SAXS [11,12]. Obviously, the crystalline-core thickness is smaller than the corresponding lamellar thickness and is about half the lamellar thickness at any $1/\Delta T$, though it increases with increasing $1/\Delta T$. Accordingly, the POM edge-on lamella should have a surface layer (20~25% of the lamellar thickness) containing folds on each side of its crystalline core: the layer is presumed to be composed of adjacent-reentrant folds with some fluctuation in contour length and its resultant fluctuation in comformation as in the solution-grown lamellae of PE [7], by taking into account the results of surface decoration [9,13] and atomic force microscopy [14] of the POM single crystals.

From only the present results, however, it was difficult to determine whether the crystalline-core thickness increases linearly with $1/\Delta T$ or not, though in our temperature range in Fig.1 the lamellar thickness increases fairly linearly with increasing $1/\Delta T$ [12]. For more accurate estimation of crystalline-core thickness, lattice imaging by high-resolution TEM (HRTEM) seems to be the best method. It is, however, difficult to take an HRTEM image of the edge-on lamellae of POM, because they are vulnerable to electron irradiation and in addition their orientation is not appropriate. HRTEM studies on other polymers, which are less sensitive against electron irradiation and have adequate crystallite orientation, are in progress [15].

References

1. Koutsky J A, et al. *J. Polym. Sci: Part B (Polym. Lett.)*, **5**, 177 (1967); Kiss K, et al. *ibid.*, **5**, 1087 (1967).
2. Carr S H, et al. *J. Polym. Sci.: A-2*, **8**, 1467 (1970).
3. Mauritz K A, et al. *J. Polym. Sci.: Polym. Phys. Ed.*, **13**, 787 (1975); Mauritz K A, et al. *J. Polym. Sci.: Macromol. Rev.*, **13,** 1 (1978).
4. Rickert S E, et al. *J. Appl. Phys.*, **47**, 4304 (1976).
5. Balik C M, et al. *J. Polym. Sci.: Polym. Phys. Ed.*, **20**, 2003 / 2017 (1982).
6. Sato Y *J. Polym. Sci.: Part B: Polym. Phys.*, **28**, 1163 (1990).
7. Tsuji M, et al. *Bull. Inst. Chem. Res., Kyoto Univ.*, **72**, 429 (1995).
8. Fujita M, et al. *J. Macromol. Sci. -Phys.*, **B36**, 681 (1997).
9. Fujita M, et al., submitted to *Macromolecules*.
10. Uchida T, et al. *J. Polym. Sci.: A-2*, **5**, 63 (1967).
11. Korenaga T, et al. *Polym. J.*, **3**, 21 (1972).
12. Nakajima A, et al. *Pure & Appl. Chem.*, **31**, 1 (1972).
13. Wittmann J C, et al. *J. Polym. Sci.: Polym. Phys. Ed.*, **23**, 205 (1985).
14. Nisman R, et al. *Langmuir*, **10**, 1667 (1994).
15. Fujita M, et al. *Sen'i Gakkai Prepr.*, F-103 (1997).

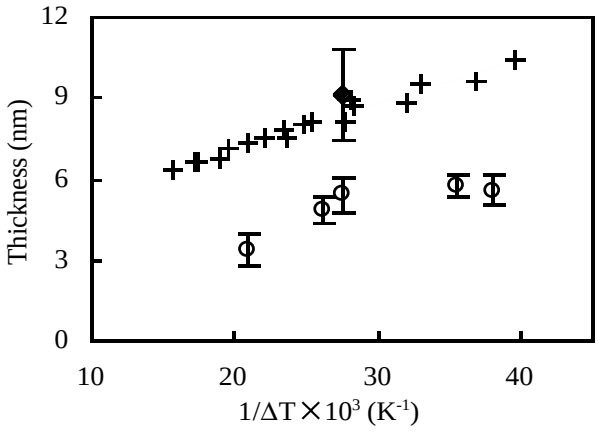

Figure 1. Crystalline-core thickness (o) and lamellar thickness (+, ♦) plotted against the reciprocal of the supercooling (ΔT). The values of lamellar thickness (+), which were measured by SAXS, were quoted from ref 11, and that (♦) was estimated by bright-field TEM. The vertical bars represent standard deviations.

^{14}N NMR Spectra Sensitive to Membrane Curvature and Segmental Motions of Phospholipid Headgroup

Emiko Okamura, Chihiro Wakai, Nobuyuki Matubayasi, and Masaru Nakahara

Surface curvature dependence of the dynamical structure of the headgroups of phospholipids was studied by ^{14}N NMR on liposomes and micelles. When the diameter was increased from 55 to 100 nm in unilamellar vesicles, ^{14}N NMR signals, for the first time observed for the micelles and unilamellar vesicles with high surface curvatures, suddenly vanished.

Keywords : Bilayer/ Liposome/ Micelle/ Dynamics/ Quadrupole

Molecular level study of the structure and dynamics of phospholipid membranes is of great importance for a better understanding of various biomembrane functions. In order to elucidate the correlation between the dynamical structures and functions of the membranes at an atomic-site level, we now apply multinuclear NMR spectroscopy to model membranes like phospholipid liposomes, micelles, and emulsions. We especially pay attention to the membrane curvature dependence of the dynamical structures of these membranes. This is because the membrane curvature can be an important factor controlling biomembrane function and integrity. For example, plasma lipoproteins regulate apoprotein binding in the metabolism process by controlling their surface curvatures. Morover, we think the molecular level study of the curvature effect is also crucial for the potential utilization of the functions of the liposomes and emulsions such as solubilization, drug delivery, and so on.

The effect of the curvature is expected to be most significant for hydrophilic headgroups at surfaces. In plasma lipoproteins described above, lipid headgroups at surfaces are considered to play an important role for the apoprotein binding. So far, however, there have been no systematic studies of the curvature effect. We first succeeded in applying ^{14}N NMR to probe the surface curvature dependence of the fluctuation of the headgroup structure [1].

We focus on uni- (**I**, **II**) and multilamellar liposomes (**III**, **IV**) of 1,2-dipalmitoylphosphatidylcholine (DPPC) with different diameters from 55 nm (**I**) to 1-30 μm (**IV**). The schematic structure of the liposome (**I**) is depicted in Figure 1. We also compare the ^{14}N NMR spectra with those of the spherical micelles of 1-palmitoyl-lysophosphatidylcholine (PaLPC) with diameter of 5 nm as given in Figure 2.

Figure 3 shows the ^{14}N NMR spectra in four types of liposomes. The spectra of aqueous phosphorylcholine and PaLPC solutions are also given. A sharp symmetric peak

INTERFACE SCIENCE — Solutions and Interfaces —

Scope of research

Structure and dynamics of a variety of ionic and nonionic solutions of physical, chemical, and biological interests are systematically studied by NMR under extreme conditions. High pressures and high temperatures are employed to shed light on microscopic controlling factors for the structure and dynamics of solutions. Vibrational spectroscopic studies are carried out to elucidate structure and orientations of organic and water molecules in ultra-thin films. Crystallization of protein monolayers, advanced dispersion systems at liquid-liquid interfaces, and biomembranes are also investigated.

Prof
NAKAHARA, Masaru
(D Sc)

Assoc Prof
UMEMURA, Junzo
(D Sc)

Instr
MATSUMOTO, Mutsuo
(D Sc)

Instr
MATUBAYASI, Nobuyuki
(Ph D)

Assoc Instr
OKAMURA, Emiko
(D Pharm Sci)

Assoc Instr
WAKAI, Chihiro
(D Sc)

Research Assistants(pt)
KIMURA, Noriyuki (D Sc)
SAKAI, Hiroshi

Students
TANO, Takanori (DC)
BOSSEV, Dobrin (DC)
KONISHI, Hirofumi (MC)
TOYA, Hiroshi (MC)
AKIYAMA, Hisashi (MC)
IMADA, Tomokatsu (MC)
KAWAI, Kunichika (MC)
TSUJINO, Yasuo (MC)
MCNAMEE, Cathy (RS)

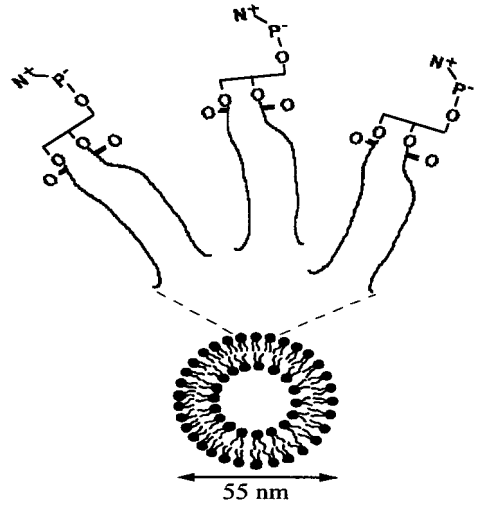

Figure 1. Schematic structure of the unilamellar liposome (**I**).

at -329 ppm is assigned to the choline N^+-methyl group (a, b). The ^{14}N NMR spectra of the DPPC liposomes depend remarkably on the surface curvature and temperature. This is most evident for the highly curved liposomes (**I**) (traces c-f). The observed chemical shifts are, however, the same as those of the isotropic (a) and micellar solution (b). Further, the increase in the liposome diameter from 55 (**I**) to 100 nm (**II**) strongly affects the spectral feature of the choline signal (g).

The chemical shift values indicate the conformation of the choline N^+-methyl sites are essentially similar. This is quite reasonable, considering that the choline N^+-methyl groups are surrounded by many water molecules and that the conformation is mainly dominated by the hydration force irrespective of the surface curvature.

The rotational motion of the choline N^+ is restricted and that the fluctuation of the P-N vector is permitted only in the direction along the molecular axis (parallel to the chain axis) in the liposomes with small curvatures. Note that the appearance of the NMR signal is only due to the rotational motion of the quadrupole ^{14}N nucleus inducing orientation relaxation.

We discuss the dynamics of the headgroup choline N^+ site. We strictly measure the spin-lattice and spin-spin relaxation times (T_1 and T_2, respectively) of the liposomes (**I**) and the micelles. As a result, we succeed in the unique determination of the rotational correlation time (τ) and the quadrupolar coupling constant (QCC) from the following two equations (where $\omega=2\pi$ 19 MHz):

$$\frac{1}{T_1} = \frac{3\pi^2}{10}(QCC)^2\,\tau\left(\frac{1}{1+\omega^2\tau^2} + \frac{4}{1+4\omega^2\tau^2}\right)$$

$$\frac{1}{T_2} = \frac{3\pi^2}{20}(QCC)^2\,\tau\left(3 + \frac{5}{1+\omega^2\tau^2} + \frac{2}{1+4\omega^2\tau^2}\right).$$

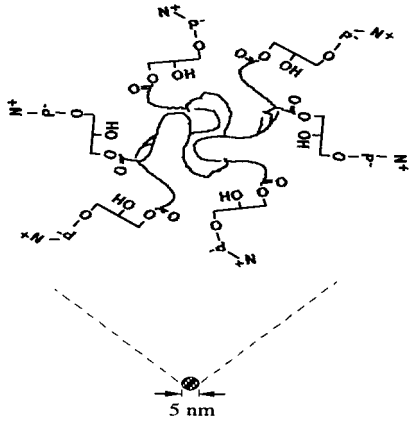

Figure 2. Schematic structure of the PaLPC micelle.

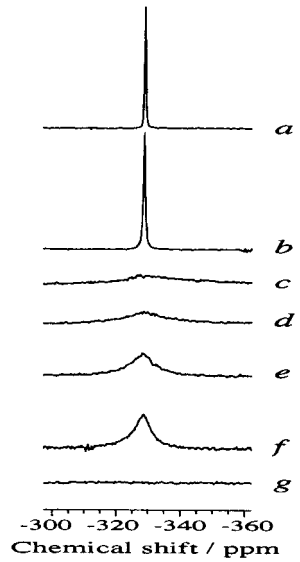

Figure 3. ^{14}N NMR spectra of the DPPC liposomes. For comparison, the spectra of aqueous phosphorylcholine and micellar PaLPC solutions at 30 ˚C are given by the traces a and b, respectively. The traces c, d, e, and f denote the spectra of the liposomes (**I**) at 30, 36, 40, and 50 ˚C, respectively; the trace g representing the spectra of the liposomes (**II**-**IV**) at 50 ˚C. Saturated KNO_3 in D_2O was used as an external reference.

It is concluded that the surface curvature dominates the segmental motions of the hydrophilic choline groups. The ^{14}N NMR spectroscopy is, therefore, proven to sensitively reflect surface curvature dependence in bilayers and micelles. Molecular level studies of the dynamical structure of the lipoprotein surfaces and the apoprotein binding mechanisms are now in progress, by combining site-selective NMR and the surface curvature effect.

Reference

1. E. Okamura et al., *Chem. Lett.*, **1997**, 1061-1062 .

Photoemission and Inverse Photoemission Studies on Organic Semiconductor Thin Films

Naoki Sato, Hiroyuki Yoshida and Kiyohiko Tsutsumi

Ultraviolet photoemission (PE) and inverse photoemission (IPE) spectra were measured for evaporated thin films of perylene-3,4,9,10-tetracarboxylic dianhydride (PTCDA) and *N,N'*-dimethylperylene-3,4,9,10-bis(dicarboximide) (DM-PBDCI), the latter known as an *n*-type organic semiconductor and the semiconducting nature of the former still unidentified. The electronic structure around the energy gap, obtained from the combination of PE and IPE spectra observed, turns out to be almost common between the two compounds, indicating that PTCDA could be grouped into the *n*-type semiconductor.

Keywords : Photoemission/ Inverse photoemission/ Organic semiconductor/ Thin film/ PTCDA

The reliable information of the electronic structure of both occupied and unoccupied states, in particular, around the energy gap, is indispensable for the elucidation of electronic properties of solids and/or the design of new electronic materials. Ultraviolet photoemission (PE) spectroscopy is widely known as one of the most useful methods to obtain direct information of valence electronic structure in solids, even in the case of organic ones, and, in contrast, there has been no efficient method to observe directly their unoccupied states. However, inverse photoemission (IPE) spectroscopy has largely been developed as a method to detect such states very recently. In this context we have built an apparatus for the purpose of IPE measurements in the vacuum ultraviolet region particularly for organic solids and have so far applied it to thin films of a few organic semiconductors.

On the one hand, perylene-3,4,9,10-tetracarboxylic dianhydride (PTCDA) is one of organic semiconductors, often used as a material in the studies viewing the development of so-called molecular electronic devices, while its electronic nature has not completely been clarified, in particular, about the semiconducting behavior as *n*- or *p*-type. Here, *N,N'*-dimethylperylene-3,4,9,10-bis(dicarboximide) (DM-PBDCI) is its analogous compound and has already been confirmed to be an *n*-type organic semiconductor from several different experiments. In this work, PE and IPE spectra were measured for evaporated thin films of PTCDA and DM-PBDCI to compare their valence and lower vacant electronic structures for checking the semiconducting characteristics of PTCDA.

The sample materials were purified by repeated sublimation at a pressure lower than 5×10^{-5} Pa. The specimen films of PTCDA and DM-PBDCI were deposited at a thickness of 3-20 nm on polycrystalline copper substrates and were measured in situ on two separate home-built apparatus, each for PE or IPE. The apparatus for PE measurements was an upgraded version

INTERFACE SCIENCE — Molecular Aggregates —

Scope of research

The research at this subdivision is devoted to correlation studies on structures and properties of both natural and artificial molecular aggregates from two main standpoints: photoelectric and dielectric behaviors. The electronic structure of molecular and/or polymeric thin films is studied using photoelectron spectroscopies in connection with the former, and its results are applied to create novel molecular systems with characteristic electronic functions. The latter is concerned with heterogeneous structures in microcapsules, biopolymers, biological membranes and biological cells, and the nonlinearity in their dielectric properities is also studied in relation to molecular motions.

Professor
SATO, Naoki
(D Sc)

Associate Professor
ASAMI, Koji
(D Sc)

Instructor
KITA, Yasuo
(D Sc)

Instructor
YOSHIDA, Hiroyuki
(D Sc)

Students
ODA, Masao (DC)
SAKUMA, Taro (DC)
YANO, Setsuko (MC)
SHIMADA, Kenji (MC)
TSUTSUMI, Kiyohiko (MC)
NAGAI, Yasuaki (MC)

of that reported in detail previously [1]. That for IPE, consisting of two ultra-high vacuum chambers, was equipped with an Erdman-Zipf type gun supplying an electron beam of a particular kinetic energy distribution in the range from 4 to 15 eV and a bandpass detector with the maximum sensitivity at 9.8 eV fabricated from a Cu-BeO photomultiplier as well as optical crystal plates; such a combination of the electron gun and the detector lead to an overall energy resolution of about 0.8 eV. Reliable IPE spectra, free of charging and/or radiation damage, were obtained in a few tens of minutes after starting irradiation on a specimen film.

Ultraviolet PE spectra of DM-PBDCI and PTCDA measured using the same excitation energy were very similar to each other. Such spectra, recorded by using a spherical retarding-field analyzer, permitted to determine accurate values of threshold ionization energy and work function, to be $I_s^{th} = 6.1_5$ eV and $\phi = 4.4_1$ eV, respectively, for PTCDA and to be $I_s^{th} = 6.1_0$ eV and $\phi = 4.5_6$ eV, respectively, for DM-PBDCI. The good correspondence observed for the energy parameters as well as the spectral lineshapes indicates that the electronic structure in the valence electronic states is largely common for the two compounds in the thin films.

IPE spectra of DM-PBDCI and PTCDA thin films were obtained to be almost the same under the given spectral resolution. This suggests that the electronic structure in lower unoccupied states is also common for the two compounds. Besides, the spectrum of PTCDA can be compared with the recent result by Hirose et al. [2]; the two independent spectra are regarded to essentially coincide with each other.

Semiempirical MO calculations using the PM3 method showed that most MOs around the energy gap for both molecules are predominantly characterized by the perylene skeleton, so that the corresponding MOs for them are of almost identical nature. This supports that almost the same electronic structure observed for the two films for both highest occupied and lowest unoccupied states can basically be understood, on the basis of the polarization model of the electronic structure in organic molecular solids.

The combinations of the respective PE and IPE spectra obtained for PTCDA and DM-PBDCI show the resemblance of the electronic structure around the energy gap for both compounds, and it is notable that the Fermi level could be positioned close to the edge of the unoccupied states, by considering the values of work function above. These observations lead, therefore, to the conclusion that the semiconductive characteristics of the two compounds are largely common, so that both could be of *n*-type; this corresponds to the results of charge carrier mobilities in both crystals.

References

1. Hirooka T, Tanaka K, Kuchitsu K, Fujihira M, Inokuchi H and Harada Y, *Chem. Phys. Lett.*, **18**, 390 (1973).
2. Hirose Y, Wu C I, Aristov V, Soukiassian P and Kahn A, *Appl. Surf. Sci.*, **113/114**, 291 (1997).

Electrical and Morphological Changes of Human Erythrocytes under High Hydrostatic Pressure Followed by Dielectric Spectroscopy

Koji Asami

Dielectric spectroscopy was applied for studying electrical and structural properties of human erythrocytes under high hydrostatic pressure, which revealed that erythrocytes undergo a change of cell shape, hemolysis, vesiculation and membrane thinning at pressure ranging from 3000 to 5000 atm.

Keywords : Dielectric spectroscopy/ Biological cell/ Hydrostatic pressure/ Membrane

It is well known that biological cells are damaged and killed by high hydrostatic pressure. However, the underlying mechanism has not been clearly understood. This is because there are few studies on properties of cells under high hydrostatic pressure, although many kinds of cells treated by high hydrostatic pressure have been studied at atmospheric pressure. Dielectric spectroscopy that can elucidate electrical and structural properties of cells in non-invasive way is suited for in situ measurements under high hydrostatic pressure because it needs only a pair of electrodes for measurements, which are easily installed in a pressure cell.

Dielectric relaxation spectra have been measured on suspensions of three types of human erythrocytes (normocyte, spherocyte and ghost) under high hydrostatic pressure up to 5000 atm. Around 3000 atm a change of the cell shape from biconcave to spherical occurred accompanying with hemolysis, which was suggested from the sharpening of the relaxation spectra. At pressure between 3000 and 4000 atm, a new dielectric dispersion appeared at frequencies below 30 kHz, which could be due to microvilation followed by vesiculation. At 5000 atm, the capacitance of the plasma membrane increased, which may indicate thinning of the lipid bilayer and/or intrusion of water into the lipid bilayer.

The present results demonstrated that dielectric spectroscopy is a useful tool for in situ and real-time monitoring of cells under high hydrostatic pressure and can contribute to better understanding of the effects of pressure on cells.

Arsenic Biogeochemistry Affected by Eutrophication in Lake Biwa, Japan

Yoshiki Sohrin, Masakazu Matsui, Munetsugu Kawashima, Masashi Hojo and Hiroshi Hasegawa

The seasonal variations of arsenic species were studied in the mesotrophic northern and eutrophic southern basins of Lake Biwa in Japan. The variations of arsenic species in lake water largely depend on biological processes, such as the metabolism of phytoplankton, decomposition of organic matter by bacteria, and microbial reduction of iron and manganese oxides in sediments. These results show that eutrophication affects the concentration and speciation of arsenic in the lake water.

Keywords : Arsenic/Methylarsenic/Organoarsenic/Lake water/Eutrophication/Biogeochemistry

Aquatic organisms metabolize arsenic, forming organoarsenic compounds such as non-toxic arsenic-containing ribofuranosides and arsenobetaine. The metabolism results in the occurrence of thermodynamically unstable arsenite and methylarsenic compounds in natural waters. So far, mainly four arsenic species have been determined in natural waters. Arsenate [$AsO(OH)_3$; As(V)] is the thermodynamically stable form under oxic conditions, of which one or two protons are dissociated at natural pHs. As(V) is a chemical analogue of phosphate and may interfere with oxidative phosphorylation. Monomethylarsonic acid [$CH_3AsO(OH)_2$; MMAA(V)] and dimethylarsinic acid [$(CH_3)_2AsO(OH)$; DMAA(V)] also form anions in natural water but are much less toxic than As(V). Arsenite [$As(OH)_3$; As(III)] is a neutral species at natural pHs and inhibits the activity of enzymes by binding to thiol groups. Since there are large differences in chemical behavior and toxicity among the arsenic species, the determination of speciation is very important in the study of the biogeochemistry of arsenic.

We have studied the seasonal variations of arsenic speciation in Lake Biwa in order to elucidate the effect of eutrophication on the biogeochemistry of arsenic [1, 2]. Lake Biwa is geographically divided into two parts, the mesotrophic northern and the eutrophic southern basins (Figure 1). In addition, the new analytical technique used in this study allowed us to determine trivalent methyl arsenicals, that is, monomethylarsonous acid, [$CH_3As(OH)_2$; MMAA(III)] and dimethylarsinous acid [$(CH_3)_2AsOH$; DMAA(III)] [3]. MMAA(III) and DMAA(III) have high toxicity, since they are lipophilic and inhibit the activity of enzymatic SH-groups. They are assumed to be intermediates in the biosynthesis of organoarsenicals. This is the first report of the distribu-

INTERFACE SCIENCE — Separation Chemistry —

Scope of research

Our research activities are concerned in the behavior of chemical substances in geochemistry and the biochemical reactions. Major subjects of the reserch are followings: (1) Biogeochemistry of trace elements in the hydrosphere. Analytical methods for trace elements are developed using the selective complex formation systems. The behavior of trace elements in hydrosphere is explored to realize the significance of them for ecosystem. (2) Design and synthesis of the selective complex formation systems. Ligands (host molecules) that have novel functions in separation of metal ions and guest molecules are designed and synthesized.

Prof MATSUI, Masakazu (D Sc) | Assoc Prof UMETANI, Shigeo (D Sc) | Instr SASAKI, Yoshihiro (D Sc) | Instr HASEGAWA, Hiroshi (D Sc) | Techn SUZUKI, Mitsuko (D Sc)

Lect(pt):
SOHRIN, Yoshiki (D Sc)

Students:
YOSHIDA, Yumi (DC)
MITO, Saeko (DC)
TOKUTOME, Chikako (MC)
MORI, Koji (MC)
AZUMA, Yohei (MC)
NAITO, Kanako (MC)
NORISUE, Kazuhiro (MC)

tion of trivalent methyl arsenicals in lake water.

Figure 2 shows the seasonal variations of arsenic species in Lake Biwa. Within the surface water of the northern basin, arsenic speciation changed seasonally. As(III) increased in spring and fall, and DMAA(V) increased and became the dominant species in summer. The concentration of As(III) and DMAA(V) reached 94% and 64% of total arsenic, respectively. Though MMAA(V) also increased in the euphotic zone during summer and fall, it was usually an order of magnitude less than DMAA(V). In the hypolimnion of the southern basin, the concentration of total arsenic greatly increased in summer with the depletion of DO. Although the species of arsenic most contributing to the increase were As(V) and As(III), high concentration of DMAA(V) was also observed in the hypolimnion.

DMAA(V) and As(III) originate from phytoplankton. Uptake of As(V) by algae and subsequent increase in the concentration of As(III) and methylarsenic(V) species in water have been observed in culture and during the development of blooms in enclosure experiments. However, the correlation of DMAA(V) and Chl. a in Figure 1 suggests that the relation between the DMAA(V) concentration and primary productivity is very dependent on the sampling time. It is not clear whether methylarsenic(V) species are produced directly by living phytoplankton or indirectly as a degradation product of organoarsenicals by bacteria. In the southern basin, high concentrations of DMAA(V) are observed in the low DO ranges. The results suggest that DMAA(V) could be produced by the anaerobic decomposition of algal matter sinking from the surface [1].

In both basins, MMAA(III) and DMAA(III) were minor components, of which concentrations usually did not exceed 0.3 nM. They were distributed not only in the epilimnion but also in the hypolimnion and did not show a clear seasonal change. MMAA(III) and DMAA(III) have been thought to be in the form of $(CH_3AsO)_x$ and $(CH_3)_2As\text{-}O\text{-}As(CH_3)_2$. However, we confirmed through liquid-liquid distribution experiments that MMAA(III) and DMAA(III) are monomeric below the concentrations of 10^{-3} and 10^{-8} M, respectively. Data for ^{1}H-NMR chemical shift suggested that MMAA(III) and DMAA(III) are undissociated at pH values around neutral. Thus, we presume their chemical forms to be $CH_3As(OH)_2$ and $(CH_3)_2AsOH$ [2, 3].

Eutrophication affects the concentration and speciation of arsenic in the lake water. The total arsenic concentration was increased by 2-4 times in the southern basin in summer, while it was nearly constant in the northern basin. The enhancement of total arsenic was due to the increase of As(V) from the sediment, which was accompanied by the increase of iron, manganese and phosphorous [4]. Arsenicals adsorbed onto iron and manganese oxides are redissolved, when the iron and manganese oxides are reduced under anoxic condition. Phosphate, which is a chemical analogue of As(V), is concurrently released from the sediment. Another distinction between the northern and southern basins is the efficiency of methylarsenic formation. The large load of phosphorus in the southern basin may have decreased the arsenic metabolism efficiency of phytoplankton. The variations of arsenic species depend on biological processes, such as the metabolism of phytoplankton, decomposition of organic matter by bacteria, and microbial reduction of ferromanganese oxides in sediments.

References

1. Sohrin Y, Matsui M, Kawashima M, Hojo M, Hasegawa H *Environ. Sci. Technol.* **31**, 2712 (1997).
2. Hasegawa H *Appl. Organomet. Chem.*, **11**, 305 (1997).
3. Hasegawa H, Sohrin Y, Matsui M, Hojo M, Kawashima M *Anal. Chem.*, **66**, 3247 (1994).
4. Sohrin Y, Tateishi T, Mito S, Matsui M, Maeda H, Hattori A, Kawashima M, Hasegawa H *Lakes Reservoirs* , **2**, 77 (1996).

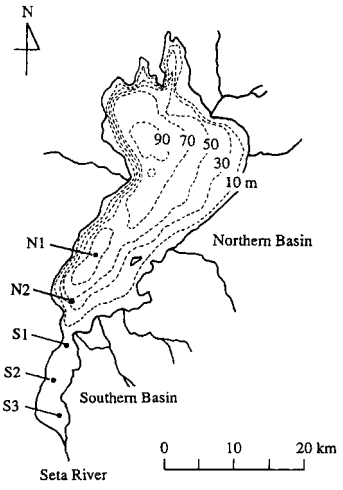

Figure 1. Sampling stations in Lake Biwa.

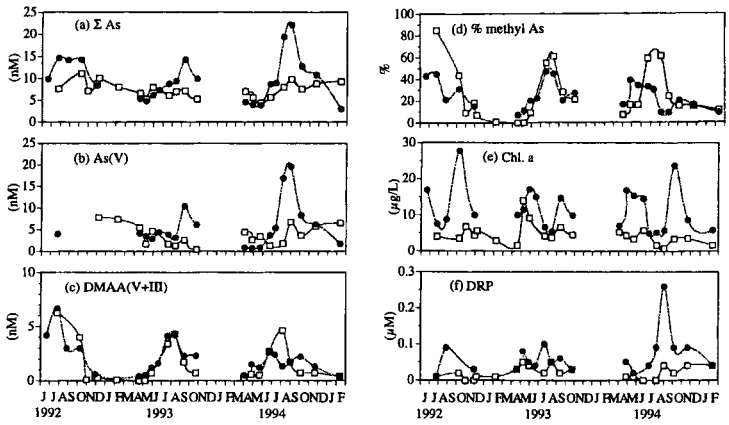

Figure 2. The seasonal variation in the average concentrations of arsenic species, Chl. a and DRP in the epilimnion (0–10 m for N1, 0–4 m for S3). Total methyl As is the sum of DMAA(V+III) and MMAA(V+III). □, station N1; ●, station S3.

Magnetoresistance of Bloch-Wall-Type Magnetic Structures Induced in NiFe/CoSm Exchange-Spring Bilayers

Ko Mibu, Taro Nagahama, Teruo Ono and Teruya Shinjo

The magnetoresistance (MR) originating from a magnetic structure with gradually rotating magnetic moments was studied using soft-magnetic (NiFe)/hard-magnetic (CoSm) bilayers. The main feature of the MR curves was explained as anisotropic magnetoresistance (AMR) effect. It was found that a giant-magnetoresistance-(GMR)-type effect coexisted, although the effect was very small in comparison with the AMR effect.

Keywords: exchange-spring multilayers/ Bloch wall/ anisotropic magnetoresistance/ giant magnetoresistance

It has been known that magnetic domain walls contribute to the electric resistance in ferromagnetic metals. The mechanism is, however, not well-elucidated yet. In order to get information about the domain wall resistance, we have investigated the magnetoresistance due to a magnetic structure with gradually rotating magnetic moments, like a Bloch wall. Such magnetic structures can be realized in "exchange-spring" bilayers, which consist of soft magnetic and hard magnetic layers with a magnetic coupling at the interface [1]. When an inverse magnetic field is applied to the saturated state, the magnetic moments in the soft magnetic layer start to rotate reversibly at a certain magnetic field (H_b), showing a magnetic structure with gradually rotating magnetic moments (Figure 1). The rotation angles can be controlled by increasing the external magnetic field, until an irreversible magnetization process due to domain wall dis-

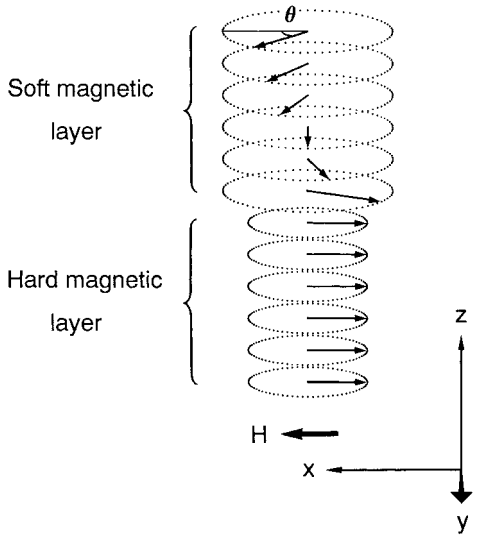

Figure 1. Illustration of an exchange-spring state in a soft-magnetic/hard-magnetic bilayer.

SOLID STATE CHEMISTRY — Artificial Lattice Alloys —

Scope of research

By using vacuum deposition method, artificial multilayers have been prepared by combining various metallic elements. The recent major subject is an interplay of magnetism and electric transport phenomena such as the giant magnetoresistance effect. Fundamental magnetic properties of metallic multilayers have been studied by various techniques including Mössbauer spectroscopy using Fe-57, Sn-119, Eu-151 and Au-197 as microprobes, and neutron diffraction. Preparation of microstructured films is attempted and novel magnetic and transport properties are investigated.

Prof
SHINJO, Teruya
(D Sc)

Assoc Prof
HOSOITO, Nobuyoshi
(D Sc)

Instr
MIBU, Ko
(D Sc)

Techni
KUSUDA, Toshiyuki

Guest Research Associate:
HASSDORF, Ralf (D Sc)

Students:
NAGAHAMA, Taro (DC)
HAMADA, Sunao (DC)
SHIGETO, Kunji (DC)
ITO, Takahiro (MC)
NISHIDA, Keisuke (MC)
TANAKA, Satsuki (MC)

placement in the CoSm layer occurs at H_c. The magnetization curve reflects the magnetization process as shown for a NiFe(300Å)/CoSm(1000Å) bilayer in Figure 2. The magnetization process between H_b and H_c is completely reversible. The direction of the magnetic moments at each magnetic field during this reversible process is calculated from the condition that gives the minimum in the total magnetization energy. The reversible magnetization curve is also reproduced using the directions calculated for each magnetic field [1].

Magnetoresistance was measured with a magnetic field parallel to the axis of easy magnetization (the *x* direction) and with electric currents parallel (ρ_{xx}) and perpendicular (ρ_{yy}) to the magnetic field. The magnetoresistance in these configurations corresponds to the magnetoresistance due to electric currents along a Bloch wall. In NiFe/CoSm bilayers, the resistivity of the CoSm layer is about 100 times larger than that of the NiFe layer. Therefore, when the magnetoresistance is measured in current-in-plane geometries, the electric current mostly flows in the NiFe layer.

The magnetoresistance curves of the NiFe(300Å)/CoSm(1000Å) bilayer in the two geometries, ρ_{xx} and ρ_{yy}, at 5.0 K are shown in Figure 3 (a). A reversible change is observed in the magnetic field range where the reversible magnetization process takes place. The observed magnetoresistance shows a characteristic shape; the resistance changes drastically right above H_b, has an extremum, then recovers gradually. The curves measured in the two geometries appear to be a mirror image of each other relative to the average value. This fact implies that the effect is mainly due to anisotropic magnetoresistance (AMR), i.e. magnetoresistance dependent on the angle between the magnetization and the electric current. In the present system, each atomic layer has different direction of magnetic moment relative to the direction of electric current. If the phenomenological equation for AMR, which is valid for uniformly magnetized films, is applied to such a system, the local resistivity is distributed as a function of the depth from the interface. The AMR of the NiFe layer as a whole is estimated from the parallel circuit of the distributed local resistivity. The calculated resistivity reproduces the feature of the reversible parts in Figure 3 (a) well [1].

If the magnetoresistance due to the electric current flowing in a twisted magnetic structure is only from the AMR effect, the average of ρ_{xx} and ρ_{yy} should be almost constant, independent of the rotation angles. The experimental average (ρ_{av}) of ρ_{xx} and ρ_{yy} for NiFe(300Å)/CoSm(1000Å) shows a small positive effect as shown in Figure 3 (b). The result indicates that a positive magnetoresistance effect that cannot be explained with the

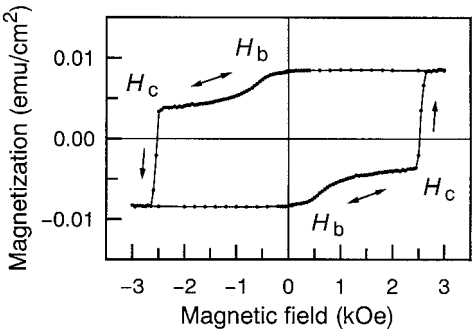

Figure 2. Magnetization curve of NiFe(300Å)/CoSm(1000Å) at 5.0 K.

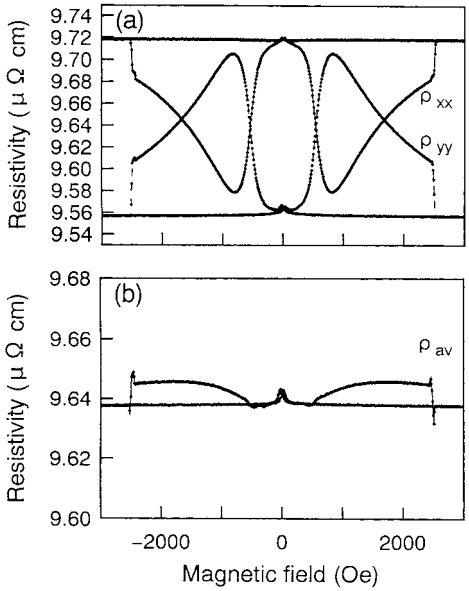

Figure 3. Magnetoresistance curves of NiFe(300Å)/CoSm(1000Å) at 5.0 K: (a) ρ_{xx} and ρ_{yy}, and (b) ρ_{av}.

AMR effect exists in ρ_{xx} and ρ_{yy}. The average resistance ρ_{av} increases as the relative angle between the magnetic moments in the NiFe layer increases. Therefore, the effect is thought to be due to a giant-magnetoresistance-(GMR)-type effect, i.e. magnetoresistance dependent on the relative configuration of magnetic moments [2].

In this way, magnetoresistance when an electric current flows in a twisted magnetic structure was studied using NiFe/CoSm exchange-spring bilayers. It was found that a GMR-type effect of less than 0.1 % coexists with an AMR-type effect of several %.

REFERENCES

1. Mibu K, Nagahama T and Shinjo T, *J. Magn. Magn. Mater.*, **163**, 75-79 (1996); Nagahama T, Mibu K and Shinjo T, *J. Phys. D: Appl. Phys.*, **31**, 42-48 (1998).
2. Mibu K, Nagahama T, Ono T and Shinjo T, *J. Magn. Magn. Mater.*, to be published (1998); *J. Magn. Soc. Jpn.* (in Japanese), to be published (1998).

Growth of heavily Pb-substituted Bi-2201 single crystals by a floating zone method

Takahito Terashima, Iksu Chong and Mikio Takano

Single crystals of the heavily Pb-substituted Bi-2201 phase were grown to a typical planar shape of 6 x 3 x 0.03 mm^3 by using a floating zone method [1]. These crystals with the highest Pb content ever reported are free from any structural modulation as examined by transmission electron microscopy, and the orthorhombic lattice parameters are a = 5.300(3) Å, b = 5.392(3) Å, and c = 24.603(5) Å (V = 703.2 $Å^3$). Their superconducting properties can be modified within the over-doped region in such a way that the transition temperature, T_c, is raised from 3 K for the as-grown crystals to 23 K by annealing at 550 ˚C for 2 weeks in a vacuum of ~10^{-4} Pa. The out-of-plane resistivity of the as-grown crystals remains metallic down to 20 K, while it becomes semiconductive below 160 K after the annealing.

Keywords : Bi-2201/ Single-crystal/ Floating Zone method/ Pb-Substitution/ Anisotropy

There are three superconducting phases in the Bi-Sr-Ca-Cu-O system the ideal formulas of which are $Bi_2Sr_2Ca_{n-1}CunO_{2n+4+\delta}$ (n = 1, 2 and 3). Among these, the Bi-2201 phase (n = 1) has the simplest structure with a single CuO_2 sheet in the fundamental unit, and its chemical stability and flexibility allowed to carry out detailed phase diagrammatic studies, various chemical substitutions, and also single crystal growth. Physically this phase has been considered useful to study the normal state properties over a wide temperature range because of its low T_c.

Of particular interest to us are the remarkable changes in structural and superconducting properties resulting from the addition of another element, Pb. Ikeda et al. [2] reported a wide monophasic range of $0 \le x \le 0.5$ and $0.1 \le y \le 0.5$ for $Bi_{2-x+y}Pb_xSr_{2-y}Cu_{1+y/4}O_z$ and showed, in particular, that the structural modulation disappears in a narrow region near the Pb-solubility limit of x = 0.4 at y = 0.125. The Pb-for-Bi substitution tended to increase the carrier density, and preparation in an Ar stream of 1 atm was needed to induce superconductivity (T_c = 14 K) from the high Pb content of x = 0.4.

The present work started aiming at the growth of crystals by floating zone method for various metallic compositions within the monophasic region mentioned above. In particular, it was thought interesting to obtain crystals in the modulation-free region because interpretation of experimental results like photoelectron spectroscopic data related to the band structure will be simplified. It should be noted here that Pb content in the previously reported crystals was rather low (x ~ 0.1 [3]). Here we report the growth of large plate-like crystals with the highest Pb content ever reported, which are modulation-free, and also the results of conductivity measurements.

Starting materials, which were Bi_2O_3, PbO, $SrCO_3$, and CuO, were weighed at an appropriate ratio, mixed in an agate mortar, pressed into pellets, and heated at temperatures from 720 ˚C to 840 ˚C over a period of 4 - 5 days in total with several intermittent grindings. The obtained powder was then isostatically pressed into a pair of rods of 6 mm in diameter and 60 mm in length and sintered

SOLID STATE CHEMISTRY — Artificial Lattice Compounds —

Scope of research

Syntheses of oxide thin films by reactive evaporation and ceramics by solid state reaction and their characterizations are studied. The main subjects are: preparation and characterization of ultrathin films of high-T_c superconductors: investigation of growth mechanism of thin films by in situ reflection high-energy electron diffraction: phase diagram of Bi_2O_3-SrO-CaO-CuO system: growth and characterization of single crystals of Bi-Sr-Ca-Cu-O system: preparation and observation of dielectric properties of ferroelectric thin films: growth and characterization of single crystals of $(Sr,Ca)_{14}Cu_{24}O_{41}$: scanning tunneling microscope observation of surface structures and electronic states of metallic oxide thin films

Instructor
IKEDA, Yasunori

Instructor
TERASHIMA, Takahito
(D Sc)

Students:
NIINAE, Toshinobu (DC)
FURUBAYASHI, Yutaka (MC)
KAWANO, Katsuya (MC)

Figure 1. Cleaved piece of single crystal.

subsequently at 840 ˚C for 24 h in air. A molten zone was formed between the pair of rods by infrared irradiation, and the zone was passed through the feed rod at a rate of 5 to 0.3 mm/h. During this growth process the two rods were counter-rotated at 30 rpm. The atmosphere was the air. Single crystals were taken mechanically from the grown ingot.

We could successfully obtain large high-quality single crystals from the initial composition of $Bi_{1.74}Pb_{0.38}Sr_{1.88}CuO_{6+\delta}$. The single crystal flake with large and plane surface parallel to the *ab* plane is shown in Fig. 1. The composition of the crystals was determined by fluorescence X-ray analysis to be $Bi_{1.80}Pb_{0.38}Sr_{2.01}CuO_{6+\delta}$.

The electron diffraction observation revealed that the structural modulation was absent as expected from the high Pb content. The four circle X-ray diffraction measurements showed the orthorhombic structure with lattice parameters of a = 5.300(3) Å, b = 5.392(3) Å, c = 24.603(5) Å, and V = 703.2 Å^3.

Typical temperature dependences of the in-plane resistivity, ρ_{ab}, and the out-of-plane resistivity, ρ_c, are shown in Figs. 2(a) and 2(b), respectively. T_c was 3 K for the as-grown crystal, while it was raised to 23 K by annealing at 550 ˚C for 2 weeks in a vacuum of ~10^{-4} Pa. This is along an experimentally observed tendency for both the 2201 and 2212 phases that annealing in vacuum reduces oxygen content in the double $BiO_{1+\delta}$ layers and thereby raises T_c. As shown in Fig. 2(b), ρ_c remains metallic down to near T_c for crystals annealed for relatively short times. Experimentally, Pb-free 2201 crystals have a typical ρ_c of 1 Ωcm at room temperature and its T - dependence remains semiconductive down to T_c [4]. It is known that substitution of La^{3+} for Sr^{2+} also reduces the carrier density and raises T_c [5]. The La-substituted crystals show one-order higher ρ_c at room temperature, and the semiconductive temperature dependence, $|d\rho_c / dT|$, is enhanced [5]. On the other hand, according to Wang et al. [3], a Pb-substituted crystal with $x \sim 0.1$ exhibits metallic behavior down to 80 K, below which ρ_c upturns. In contrast with these cases, an almost complete metallic T-dependence of ρ_c was observed for our as-grown crystals. It is now clear that the present heavy Pb-for-Bi substitution did increase the carrier density to the highest degree ever reported for single crystals.

From the proximity in ionic radius between Pb^{2+} and Bi^{3+} we assume that it is Pb^{2+} rather than Pb^{4+} that substitutes

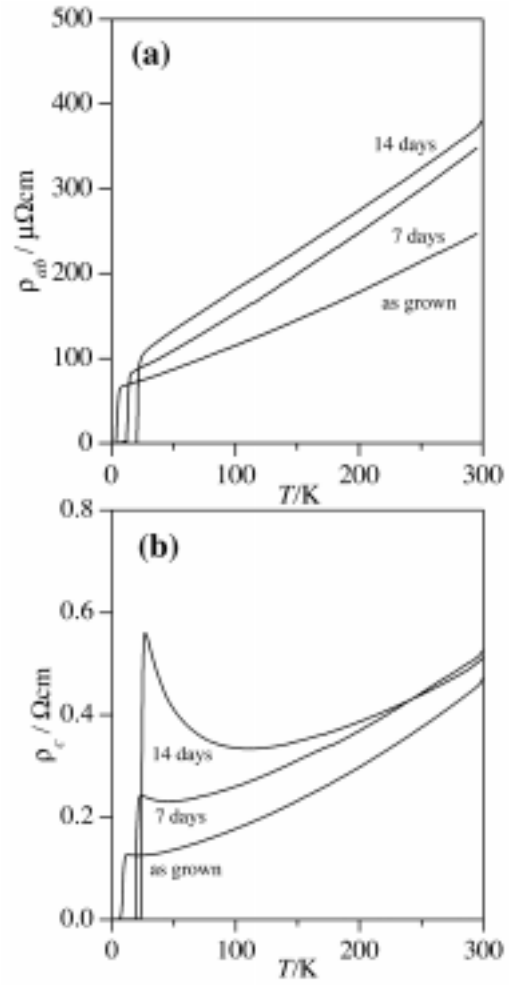

Figure 2. Temperature dependence of the in-plane resistivity (a) and the out-of-plane resistivity (b) of the as-grown and annealed crystals.

for Bi^{3+}. The (Bi, Pb)-O layers become atomically flat in modulation-free crystals as first reported by Ikeda et al. [2]. The flatness should increase the (Bi^{3+}, Pb^{2+}) 6*s* - O^{2-} 2*p* overlap and, thereby, lower the out-of-plane resistivity. We thus conclude that the Pb^{2+}-for-Bi^{3+} substitution makes the (Bi, Pb)-O layers more conductive. In addition to the flatness effects mentioned above, there is another factor which should be taken into consideration. If the energy difference between the Pb^{2+} 6*s* and the O^{2-} 2*p* orbitals is smaller than the difference between the Bi^{3+} 6*s* and the O^{2-} 2*p* orbitals, the relevant electronic band might become even more broadened. A detailed band structure calculation is desirable.

References

1. I. Chong, T. Terashima, Y. Bando, M. Takano, Y. Matsuda, T. Nagaoka and K. Kumagai, Physica C, 290, 57-62 (1997).
2. Y. Ikeda, Z. Hiroi, H. Ito, S. Shimomura, M. Takano and Y. Bando, Physica C 165 (1990) 189-198.
3. N. L. Wang, C. Geibel and F. Steglich, Physica C 260, 305-312 (1996) .
4. X. H. Hou, W. J. Zhu, J. Q. Li, J. W. Xiong, F. Wu, Y. Z. Huang and Z. X. Zhao, Phys. Rev. B 50, 496 (1994).
5. T. Ito, H. Takagi, S. Ishibashi, T. Ido and S. Uchida, Nature 350, 596-598 (1991) .

High Critical Current Density in the High-T_c Superconductor: Generation of Efficient Pinning Centers

Zenji Hiroi, Iksu Chong, Masaki Azuma, and Mikio Takano

We have found novel flux pinning centers in high-T_c oxide superconductor $Bi_2Sr_2CaCu_2O_8$ with T_c = 80 K that dramatically increase the critical current density (J_c). Single crystals with a large amount of Pb substituting for Bi were grown by the floating zone method, and their magnetic properties and microstructures have been studied by means of SQUID magnetometery and electron microscopy. J_c increases remarkably beyond a critical Pb content of ~0.4 per formula unit, where characteristic two-phase microstructures are revealed by high-resolution electron microscopy: The "single" crystals consist of alternating thin (several tens of nanometers) lamellar plates of two phases with the (010) interface; one with lower Pb content (~0.4) and a modulated structure and the other with higher Pb content (~0.6) and a modulation-free structure.

Keywords: Copper oxide superconductor/ $Bi_2Sr_2CaCu_2O_8$/ Pb substitution/ Microstructure

High temperature copper oxide superconductors (HTSCs) exhibit an unusual magnetic field - temperature (H - T) phase diagram which is quite different from that of conventional superconductors [1]. The major origin is strongly two-dimensional characters of HTSCs, as well as short coherence lengths and elevated critical temperatures (T_c's), which substantially change the vortex state in magnetic fields perpendicular to the CuO_2 layers; vortex lines become ill-defined and transform into pancake vortices confined within the CuO_2 layers which couple only weakly between the layers. Then, the role of thermal fluctuation on the dynamics of vortices is enormously enhanced, and flux flow and flux-lattice melting occurs in a wide temperature range below T_c, resulting in a finite resistivity. From the viewpoint of practical applications it is particularly important to increase J_c.

Among the many HTSCs studied up to date, $Bi_2Sr_2CaCu_2O_8$ (Bi-2212) has been considered to be one of the most promising materials to be used as wires for cables and magnets because of its chemical stability and flexibility in manufacturing processing: the melt-texture growth technique has sufficiently improved superconducting coupling between polycrystalline grains, which is another factor limiting the actual J_c value, and enabled to produce wires with relatively high J_c values below 20 K. However, one serious problem is that J_c decreases drastically above 20 K in magnetic fields. This arises from the breakdown of the zero-resistive state due to thermally activated flux flow. Suppression of the flux flow is particularly serious for this compound because of

SOLID STATE CHEMISTRY — Multicomponent Materials —

Scope of research

Novel inorganic materials that have new, useful or exotic features such as superconductivity, ferromagnetism and quantum spin ground state are synthesized by novel methods. Recent topics are:

- *High-T_c superconducting copper oxides with higher T_c or J_c.*
- *Perovskite-based compounds with unusual magnetic and electronic properties.*
- *Low-dimensional spin system showing dramatic quantum effects.*

Prof
TAKANO, Mikio
(D Sc)

Assoc Prof
HIROI, Zenji
(D Sc)

Instr
AZUMA, Masaki
(D Sc)

Students:
KOBAYASHI, Naoya (DC)
POULSEN, Jakob (DC)
KAWASAKI, Shuji (DC)
YAMADA, Takahiro (DC)
MATSUNAGA, Takanobu (MC)
IIDA, Mamoru (MC)
OKUMURA, Makoto (MC)
NABESHIMA, Yasuki (MC)
SAITO, Takashi (MC)
TAMADA, Takayuki (MC)
TOGANO, Hiroki (MC)

Research Fellow:
CHONG, Iksu

its inherent 2D anisotropy. There is no doubt that large-scale applications would be accelerated by finding an appropriate solution to overcome this obstacle.

A key to increase J_c is to generate efficient pinning centers in crystals. Recent studies using heavy ion irradiation have clearly exemplified that aligned columnar defects serve as flux pinning centers. However, these methods are rather formidable and not useful in practical material processing. We believe that an alternative breakthrough to generate efficient pinning centers in a more practical and useful way is necessary for future large-scale applications.

We have studied the single crystal growth of Bi-2212 and found that the partial replacement of Bi by a large amount of Pb remarkably affects the magnetic properties of Bi-2212 [2]. Single crystals of Pb-substituted Bi-2212 were grown from starting compositions $Bi_{2.2-x}Pb_xSr_{1.8}CaCu_2O_{8+\delta}$ (x = 0, 0.4, 0.6, 0.7, 0.8) by the conventional floating zone (FZ) method with an infra-red heating furnace. The atmosphere used was 20 % O_2 / 80 % N_2, and the growth rate was 0.5 mm h^{-1}. Plate-like crystals of dimensions 1.0 × 1.0 × (0.03 ~ 0.04) mm^3 were cleaved from each rod and used for magnetization measurements. A remarkable enhancement in J_c was found for large Pb content of $x \geq 0.6$. In addition, a characteristic lamellar structure was observed by means of high-resolution electron microscopy (HREM) only in crystals with $x \geq 0.6$. Figure 1 presents the HREM images of a typical fragment from the x = 0.7 crystal, where is seen a well-ordered zebra pattern composed of two kinds of lamellar plates; α-phase plates with Pb poor composition (~ 0.4 per formula unit) as examined by EDX microanalysis and a modulated structure (periodicity of 11 ~ 12*b*) and β-phase plates with Pb rich composition (~ 0.6) and a modulation-free structure. Each plate has a thickness of several tens of nanometer, and the interface is always perpendicular to the *b* axis. It is noted that structural modulations in the α-phase domains is considerably disordered, compared with those seen in uniform (Bi,Pb)-2212 crystals with less nominal Pb content. The lamellar microstructures found in the present study reminds us of eutectics and eutectoids cooled unidirectionally. They usually form either alternating lamellar plates or rods embedded in a matrix. Many examples have been known for metallic systems, while recently a large number of oxide-oxide eutectics have also been studied. As for cupric oxides, Revcolevschi et al. prepared an aligned eutectic structure made of $La_{2-x}Sr_xCuO_4$ and CuO by a FZ technique. The lamellar morphology observed in our study is quite similar to those found in Pb-Sn, NiO-ZrO_2, and Fe(C)-Fe_3C.

The improvement in J_c in the present heavily Pb-doped Bi-2212 single crystals must be due to an automatic, unintended generation of efficient pinning centers. The observed specific two-phase microstructures must be related to it. Since the interface always crosses the CuO_2 planes, the present microscopic two-phase structures must suppress the thermal fluctuation of pancake vortices more efficiently than randomly distributed point defects.

REFERENCES

1. Blatter G, Feigel'man MV, Geshkenbein VB, Larkin AI, Vinokur VM, Rev Mod Phys, **66**, 1125 (1994) .

2. Chong I, Hiroi Z, Izumi M, Shimoyama J, Nakayama Y, Kishio K, Terashima T, Bando Y, and Takano M, SCIENCE, **276**, 770 (1997).

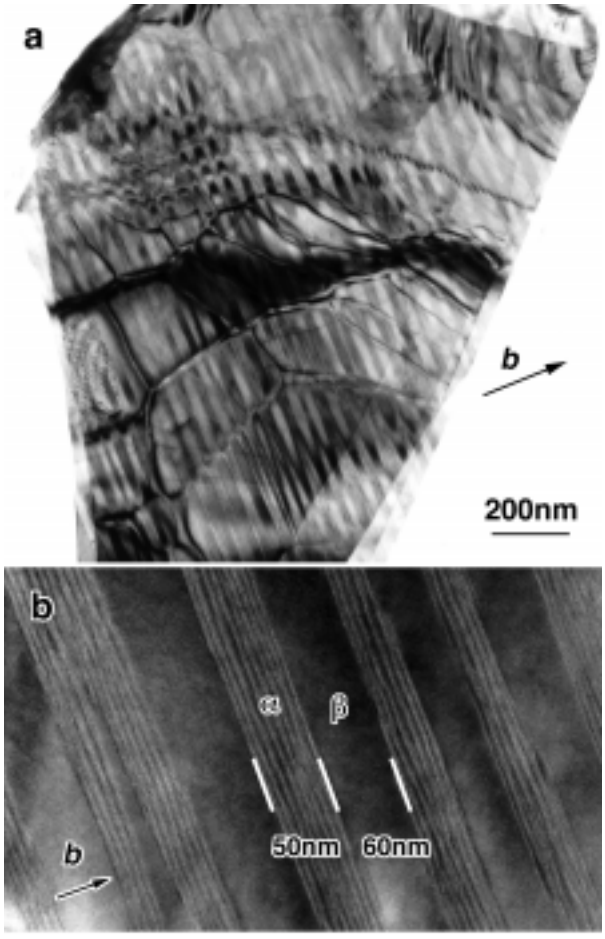

Figure 1. Electron micrographs showing typical microstructures of the x = 0.7 crystal. The incident electron beam was parallel to the [101] direction so that the *b* axis was perpendicular to the incident beam. The zebra pattern seen in (a) is due to alternating stacking of two kinds of lamellas along the *b* axis, resulting from phase separation at high temperature. The dense fringes seen in the α domains in (b) visualize the structural modulations.

Electrical Properties of Transparent Doped Titania Films by Sol-Gel Method

Hong Lin, Takashi Uchino, Hiromitsu Kozuka and Toshinobu Yoko

Transparent semiconductive TiO_2 films co-doped with Ru and Ta (Nb), and Co and Nb (Sb) were prepared on SiO_2 glass substrates by the sol-gel method using $Ti(OC_3H_7^i)_4$ solutions. The solution preparation condition, solution composition, dopant content and heat-treatment temperature all severely affected the electrical resistivity of the resultant films. TiO_2 films co-doped with Ru and Ta (Nb) showed n-type conductivity, while those co-doped with Co and Nb (Sb) showed p-type conductivity. It seems that the obtained films can be utilized for assembling all-solid-state TiO_2-based pn type solar cell.

Keywords : Transparent semiconductive films / Sol-gel method / Titania films / Electrical resistivity / pn type solar cell

Solar energy is believed to be an essential energy source of the next century. A pn type solar cell with all-solid-state TiO_2-based films seems to have many benefits for effective utilization of the solar energy because the ultra violet and visible light of solar light would be adsorbed by n-type TiO_2 and p-type TiO_2, respectively. Here, transparent semiconductor electrodes with high conductivity are requested. We prepared TiO_2 films co-doped with Ru and Ta (Nb), and Co and Nb (Sb) by sol-gel method, aiming at making n- and p-type transparent semiconductive films, respectively. The effects of solution composition, solution preparation condition, dopant content and heat-treatment temperature on the electrical resistivity of sol-gel derived films were studied. The conduction mechanisms of doped TiO_2 films were also discussed.

Transparent semiconductive n-type TiO_2 films were prepared by co-doping Ru and Ta (Nb). Titanium tetraisopropoxide ($Ti(OC_3H_7^i)_4$), $RuCl_3 \cdot xH_2O$, $TaCl_5$ ($NbCl_5$), C_2H_5OH, 36.5% HCl (60% HNO_3 or diethanolamine (DEA)) and H_2O were used as starting materials.

Transparent semiconductive p-type TiO_2 films were obtained by co-doping Co and Nb (Sb). $Ti(OC_3H_7^i)_4$, $CoCl_2$, $NbCl_5$ ($SbCl_5$), C_2H_5OH, acetylacetone (AcAc), (36.5% HCl) and H_2O were used to form $Ti_{3(1-x)}Co_xM_{2x}O_6$ (x = 0.3, M = Nb or Sb) solid solutions.

The gel films were dip-coated on SiO_2 glass substrates at a constant rate of 1 cm/min, heat-treated in air at 400°C-900°C for 10 min. Repeating the above procedure 3 times gave approximately 120 nm-thick films.

D.C. electrical resistivity was measured in air at room temperature for n-type TiO_2 films and during cooling from high temperature to room temperature for p-type TiO_2 films with two electrodes method.

The obtained n-type TiO_2 films were uniform and transparent in all the preperation conditions employed, and their crystalline phases were anatase when HCl or

SOLID STATE CHEMISTRY -Amorphous Materials-

Scope of research

Inorganic amorphous materials with various functions are the targets of research in this laboratory. (1) To obtain a clear view of "what is glass" and the bases for designing functional glasses, we investigate the structure of glasses using X-ray and neutron diffraction analysis, high resolution MAS-NMR, and ab initio MO calculation. (2) To develop materials of high optical nonlinearity, we search heavy metal oxide-based glasses and transition metal oxide thin films, and evaluate the nonlinear optical properties by Z-scan methods. (3) Using sol-gel method, synthesis and microstructure control are carried out on various functional oxide thin films.

Prof
YOKO, Toshinobu
(D Eng)

Assoc Prof
KOZUKA, Hiromitsu
(D Eng)

Instr
UCHINO, Takashi
(D Eng)

Instr
LIN, Hong
(D Eng)

Guest Research Associates:
JIN, Jisun (D Eng)
ZHAO, Gaoling (D Eng)

Students:
SAKIDA, Shinichi (DC)
TAKAISHI, Daigo (DC)
HATTORI, Takeshi (MC)
TOKUDA, Youmei (MC)
NIIDA, Haruki (MC)
TATSUMI, Masao (MC)
MIYAWAKI, Seikyo (MC)
KAJITA, Daisuke (UG)
KITAGAWA, Yukio (UG)
TAI, Hiroaki (UG)

HNO_3 was used as a catalyst. The resistivity of the films decreased in the order of DEA > HNO_3 > HCl additives. Refluxing the dopant solutions prior to mixing with $Ti(OC_3H_7^i)_4$ solution led to the decrease of the film resistivity. This was probably caused by the alkoxylation of $RuCl_3$ and $TaCl_5$ under refluxing, promoting the formation of solid solution.

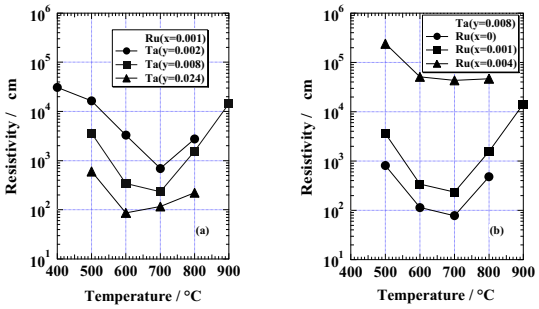

Figure 1. (a) Electrical resistivity of the titania films with a fixed content of Ru (x = 0.001) and various contents of Ta (y = 0 - 0.024). (b) Electrical resistivity of titania films derived with various Ru contents (x = 0 - 0.004) and a fixed Ta content (y = 0.008).

Figure 1 shows that the resistivity decreased with increasing Ta content and increased with increasing Ru content. This indicates that Ti^{3+} species, which are formed by Ta-doping via charge compensation, are the main donors responsible for the conduction in the present anatase samples (see Figure 2). Moreover, most of the films showed resistivity minima at a heat-treatment temperature of 700°C. This is due to the change of Ti^{3+} concentration by the Ta incorporation and the oxidation and reduction reactions during the heat-treatment. The lowest resistivity of $10^1 \sim 10^2$ Ω cm was attained.

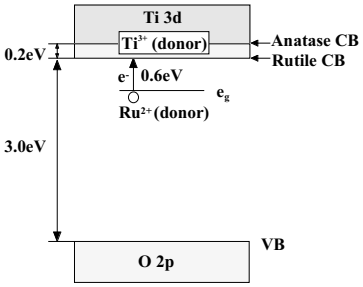

Figure 2. Schematic energy level diagram for Ti^{3+} and Ru^{2+} in anatase and rutile TiO_2.

The obtained p-type TiO_2 films were also uniform and transparent when AcAc was used, while samples heat-treated at 800°C became opaque when HCl was added. Rutile phases appeared when the films were heat-treated at 700°C. Films co-doped with Co and Sb changed their crystalline phases from amorphous directly to rutile with increasing heat-treatment temperature. Contrarily, films co-doped with Co and Nb showed phase transition from anatase to rutile on heating. The crystallinity of films co-doped with Co and Nb was slightly better than that of films co-doped with Co and Sb.

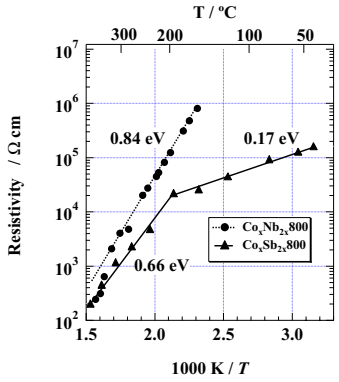

Figure 3. Variation of logarithmic resistivity with reciprocal temperature in K for $Ti_{3(1-x)}Co_xM_{2x}O_6$ (M = Sb or Nb) films heat-treated at 800°C. The inserted numericals in eV are activiation energies.

Figure 3 shows that logarithmic resistivity of films co-doped with Co and Nb was directly proportional to the reciprocal absolute temperature. On the other hand, the slopes for films co-doped with Co and Sb were different below and above 200°-220°C, indicating that there are at least two conduction mechanisms with different activation energies. The phenomenon should be closely related to the valence state of Sb ions, causing the formation of different acceptor levels. Moreover, Co ion in $Ti_{3(1-x)}Co_xM_{2x}O_6$ may be present as Co^{2+} in high spin state, acting as an acceptor for electrons from the valence band of TiO_2. (see Figure 4).

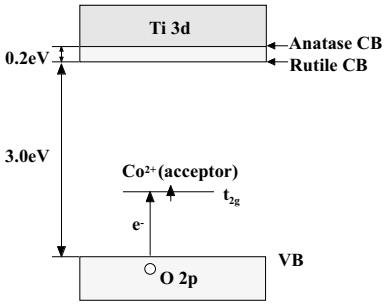

Figure 4. Schematic energy level diagram for high spin Co^{2+} in titania.

The above obtained transparent n- and p-type TiO_2-based semiconductors are promising materials for designing a pn type solar cell.

References

1. Triggs P and Levy F, *Phys. Stat. Sol.* (b), **129**, 363 (1985).
2. Belloch J M., Isasi J, Lopez M L , Veiga M L and Pico C, *Mater. Res. Bull.*, **29(8)**, 861-9 (1994).
3. Lin H, Kumon S, Kozuka H and Yoko T, *Thin Solid Films*, in press.

Nonlinear Viscoelasticity of Amorphous Polymers in the Vincinity of the Glass Transition Temperature.

Tadashi Inoue, Hiroshi Watanabe, and Kunihiro Osaki

Nonlinear viscoelasticity of atactic polystyrene around the glass transition was studied by means of constant rate elongation. The strain-induced birefringence and the stress were simultaneously measured and then the stress was separated into two components (Rubbery and Glassy components) by using the modified stress-optical rule. Behavior of the R component, having the molecular origin of chain orientation, was essentially linearly viscoelastic. On the other hand, the G component, originated by rotational orientation of chain units, showed remarkable thinning phenomena, which is commonly observed for glassy materials. Thus, the separation of stress for polymeric material simplifies phenomenological interpretation of nonlinear viscoelasticity of polymers near the glass transition zone.

Keywords : Glass transition/ Stress-optical Rule/ Viscoelasticity/ Amorphous polymer/ Rheo-optics/ Rheology/ Polystyrene

The glass transition phenomena are widely observed in various polymeric systems. In the vicinity of the glass transition temperature, the modulus typically varies from the glassy modulus(ca.10^9Pa) to the rubbery modulus(ca. 10^6Pa). Most widely accepted interpretation for the glass transition is "freezing of molecular motions", that is, competition between molecular relaxation time scale and experimental time scale. However, the molecular motion responsible to the glass transition is not fully specified.

We have previously found a new method [1] for decomposing the stress (modulus) into two components having different molecular origins. This method is based on the modified stress-optical rule: The rule says that the stress, $\sigma(t)$ and birefringence, $\Delta n(t)$, are composed of two components (denoted by subscripts R and G) and that proportionality holds valid for each component.

$$\sigma(t)=\sigma_R(t)+\sigma_G(t) \quad (1)$$

$$\Delta n(t)= C_R\sigma_R(t)+ C_G\sigma_G(t) \quad (2)$$

Here C_i is the proportionality coefficient called the stress-optical ratio for the component i. Eqs. 1 and 2 can be solved for $\sigma_R(t)$ and $\sigma_G(t)$. Systematic studies on various polymers revealed that the R component is related with the chain orientation and the G component is with rotational orientation of a structural unit around main chain axis. In the rubbery state the contribution of $\sigma_G(t)$ can be ignored.

Recently, we applied this method to constant elongation experiments of polystyrene around the glass transition temperature.[2] Figure 1 shows representative data

FUNDAMENTAL MATERIAL PROPERTIES — Molecular Rheology —

Scope of research

The molecular origin of various rheological properties of materials is studied. Depending on time and temperature, homogeneous polymeric materials exhibit typical features of glass, rubber, and viscous fluids while heterogeneous polymeric systems exhibit plasticity in addition to these features. For a basic understanding of the features, the molecular motion and structures of various scales are studied for polymeric systems in deformed state. Measurements are performed of rheological properties with various rheometers, of isochronal molecular orientation with flow birefringence, and of autocorrelation of the orientation with dynamic dielectric spectroscopy.

Prof
OSAKI, Kunihiro
(D Eng)

Assoc Prof
WATANABE, Hiroshi
(D Sc)

Instr
INOUE, Tadashi
(D Eng)

Techn
OKADA, Shinichi

Students:
SATO, Tomohiro (DC)
ABE, Shuichi (MC)
ONOGI, Takayuki (MC)
KUWADA, Syozo (MC)
MATSUMIYA, Yumi (MC)

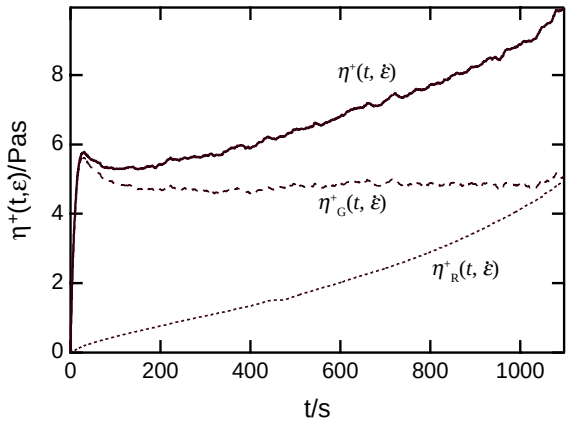

Figure 1. Stress growth during constant rate elongation of polystyrene at 100°C with $\dot{\varepsilon}$=0.001s^{-1}

for stress growth at 100°C with rate of strain, $\dot{\varepsilon}$=0.001s^{-1}. Here the tensile stress is reduced by rate of strain, $\eta^+(t, \dot{\varepsilon})=\sigma(t)/\dot{\varepsilon}$. The stress increases vary rapidly on start-up of deformation, shows a maximum, and then increases again with time. This type of stress growth cannot be described with linear viscoelastic theory for the small strain regime.

Dotted and broken lines in Figure 1 shows the result of decomposition of the stress into the two components. The R component, $\eta^+_R(t, \dot{\varepsilon})=\sigma(t)_R/\dot{\varepsilon}$, increased monotonically with time. We found that $\eta^+_R(t, \dot{\varepsilon})$ was in accord with linear viscoelastic theory. This means that the response of R component does not change in a wide range of strain examined.

On the hand, $\eta^+_G(t, \dot{\varepsilon})$ increases vary rapidly and then decreases and apparently reaches a steady state at long times. We may define the steady state viscosity, $\eta_{EG}(\dot{\varepsilon})$. The result quite resembles the features of the ordinary entangled polymer systems under shear flow, although the two phenomena have different molecular origins.

Similar results were obtained at different rates of strain and different temperatures. Figure 2 shows $\dot{\varepsilon}$ dependence of $\eta_{EG}(\dot{\varepsilon})$. Here, in order to compare the data at different temperatures, the data are reduced to 115°C with the method of reduced variables: $\eta_{EG}a_{TG}^{-1}$ is plotted against $a_{TG}\dot{\varepsilon}$, where a_{TG} is the shift factor for the G component determined by dynamic measurement. The data at different temperatures lie on a single curve. This result in turn suggests that the method of reduced variables works well for the G component even in the nonlinear viscoelastic region around the glass transition zone.

For the shear viscosity of polymer melts in the terminal flow zone, the non-Newtonian thinning is observed at rates $\dot{\gamma}>\tau^{-1}$ where τ is the longest relaxation time. In addition, viscosity is close to $|\eta^*(\omega)|_{\dot{\gamma}=\omega}$, measured in the linear regime(Cox-Melz rule). In contrast, Figure 2 demonstrates that η_{EG} has much stronger rate dependence than

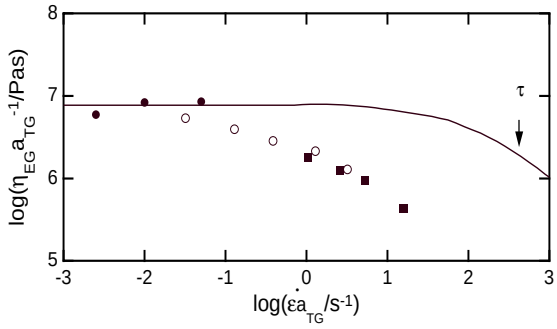

Figure 2. Rate dependence of viscosity for the G component. Line in the figure indicates $|\eta_{EG}^*(\omega)|_{\dot{\varepsilon}=\omega}$.

$|\eta_{EG}^*(\omega)|_{\dot{\varepsilon}=\omega}$. The rate where thinning starts is about 300 times smaller than that for $|\eta_{EG}^*(\omega)|_{\dot{\varepsilon}=\omega}$. It is well-known that the shear thinning of viscosity of polymer melts is associated with the strong strain dependence of the shear relaxation modulus. The very strong rate dependence of η_{EG} may be related to the very strong strain dependence of the Young's relaxation modulus.

As demonstrated in Figure 1, the separation of stress into the two components simplifies the phenomenological interpretation of viscoelasticity around the glass transition zone. The remarkable nonlinear viscoelasticity around the glass transition zone can be related with the strong rate dependence of the G component. We also emphasize that σ_G is a well-behaving viscoelastic quantity, for which the viscosity exhibits strong but smooth thinning and the method of reduced variables works well; see Figure 2.

Finally, we point out that viscoelastic behavior of the G component quite resembles that of inorganic glasses. η_E of these materials show a very similar shear thinning phenomenon when $\dot{\varepsilon}$ exceeds a certain $\dot{\varepsilon}$, a few hundredth of τ^{-1}.[3] Such a similarity strongly suggests a universal relaxation mechanism for glass forming materials, a cooperative relaxation mechanism which is insensitive to details of molecular structures.

Acknowledgment

This work was supported in part by the Grant-in-Aid for Scientific Research from the Ministry of Education, Science, Sports and Culture of Japan.

References

1. Inoue T, Okamoto M and Osaki K, *Macromolecules*, **24**, 5670-5675(1991).
2. Inoue T, Ryu DS and Osaki K, *Macromolecules*, in press.
3. Simmons JH, Mohr RK, Montrose CJ, *J. Appl.Phys*, **53**,4075-4080(1982).

Hierarchic Structure of Poly(vinyl alcohol) Gels

Toshiji Kanaya, Hiroki Takeshita, Yuichi Nishikoji, Masatoshi Ohkura, Koji Nishida and Keisuke Kaji

We studied the structure and its formation process of poly(vinyl alcohol) gels formed in a mixture of deuterated dimethyl sulfoxide (DMSO-d_6) and heavy water at 25 °C, using various kinds of scattering techniques such as wide-, medium-, small- and ultra small-angle neutron scattering and light scattering to cover a wide *Q*-range of 10^{-4} to 10 Å^{-1}, corresponding to a real space of 0.63 to 63000 Å. On the basis of the results, we will discuss the hierarchic structure of PVA gels, which is basically determined by competition between the rate of liquid-liquid phase separation and the rate of crystallization or formation of cross-linking points.

Keywords : Spinodal Decomposition / Phase Separation / Light Scattering (LS) / Ultra Small-Angle Neutron Scattering (U-SANS) / Small-Angle Neutron Scattering (SANS) / Wide-Angle Neutron Scattering (WANS)

Extensive studies on polymer gels have been performed from various points of view because a wide variety of polymer gels can provide various interesting features. One of the most interesting gel-forming polymers is poly(vinyl alcohol) (PVA), which can form gels on cooling in various solvents including water.

In the previous studies, we determined the sol-gel diagram and observed the turbidity of the PVA gels in a mixture of DMSO and water (60/40 v/v) as a function of temperature and PVA concentration [1, 2]. These macroscopic observations implied that the liquid-liquid phase separation plays an important role in the formation of the structure of the gels, suggesting that the studies of mesoscopic structure in μm scale as well as microspcopic structure in nm scale are very important to understand the properties of the gels.

In this paper, we report the results of structural studies of a PVA gel formed in a mixture of DMSO and water (60/40 v/v) at 23°C using wide-angle neutron scattering (WANS), small-angle neutron scattering (SANS), ultra small-angle neutron scattering (U-SANS) and light scattering techniques covering a very wide *Q* range from 10^{-4} to 10 Å^{-1} where $Q=4\pi\sin\Theta/\lambda$, 2Θ and λ being scattering angle and wavelength of neutrons.

Wide-Angle Neutron Scattering measurements [3]. PVA is one of typical crystalline polymers, and hence the cross-linking points or junction points in the gels are believed to be crystallites though it has never been directly confirmed. First of all, we conducted WANS measurements on the PVA gel in the *Q* range of 0.8 to 10 Å^{-1}. In this experiment, we employed a deuterated PVA to reduce the incoherent scattering background. In the scattering curve shown in Figure 1, a strong peak is

FUNDAMENTAL MATERIAL PROPERTIES – Polymer Materials Science –

Scope of research

The structure and molecular motion of polymer substances are studied using mainly scattering methods such as neutron, X-ray and light with the intention of solving fundamentally important problems in polymer science. The main projects are: the mechanism of structural development in crystalline polymers from the glassy or molten state to spherulites; the dynamics in disordered polymer materials including low-energy excitation or excess heat capacity at low temperatures, glass transition and local segmental motions; formation process and structure of polymer gels; the structure and molecular motion of polyelectrolyte solutions; the structure of polymer liquid crystals.

Prof
KAJI, Keisuke
(D Eng)

Assoc Prof
KANAYA, Toshiji
(D Eng)

Instr
NISHIDA, Koji

Students
TAKESHITA, Hiroki (DC)
MATSUBA, Go (MC)
NISHIKOJI, Yuichi (MC)
OGAMI, Akinobu (MC)
SHIBATA, Manabu (MC)
HAMAJIMA, Hirokazu (UG)
YAMAMOTO, Hiroyoshi (UG)
YAMASHITA, Ryoji (UG)

Research Fellow
TSUKUSHI, Itaru

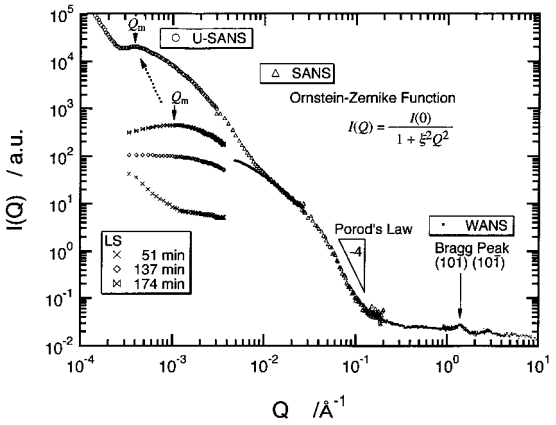

Figure 1. Scattering intensity $I(Q)$ of the PVA gel in DMSO-d_6/D_2O (60/40 v/v) with Cp = 5 g/dL, which was constructed by combining $I(Q)$'s measured by various scattering methods.

observed at Q=1.39 Å^{-1} which corresponds to the Bragg diffractions from (101) and (10$\bar{1}$) planes of PVA crystals, confirming that there exist crystallites in the PVA gel. It was also shown that the Bragg peak disappears at about 75°C when the temperature increases. This temperature agrees with the melting temperature of the PVA gel, suggesting that the cross-linking points of the gel are crystallites.

Small-Angle Neutron Scattering measurements [3, 4]. SANS measurements were made on the PVA gel in the Q range from 0.003 to 0.2 Å^{-1}. In the Q range above about 0.05Å^{-1}, the scattering intensity $I(Q)$ decreases with increasing Q according to the -4th power law (the Porod's law),

$$I(Q) \sim Q^{-4} \qquad (1)$$

indicating that the surfaces of the crystallites are very smooth. On the other hand, the scattering intensity $I(Q)$ in the Q range below 0.045 Å^{-1}can be described by the Ornstein-Zernike (OZ) formula

$$I(Q) = \frac{I(0)}{(1 + \xi^2 Q^2)} \qquad (2)$$

where ξ is a correlation length and $I(0)$ is the scattering intensity at Q=0. The values of ξ in the gel is about 180 Å, which corresponds to the distance between the nearest neighboring crystallites. The scattering intensity $I(Q)$ of the opaque PVA gel deviates from the OZ formula and shows an upturn below about 0.008 Å^{-1} while the transparent gel, which was obtained by quenching the homogeneous solution at 100 °C to -40 °C, obeys the OZ formula in the low Q range down to 0.003 Å^{-1}. This indicates that the opaque gels have a larger heterogeneity than the network structure. It is easily expected that this heterogeneity arises from the structure due to phase separation.

Light scattering measurements [4]. In order to get direct evidences for the phase separation, time-resolved light scattering (LS) measurements were carried out on the PVA gel after quenching to 25°C from 100 °C. The scattering intensity $I(Q)$ shows a maximum at about Q = 1.1 x 10-3 Å^{-1}, which does not change during the measurements. On the other hand, the peak intensity I_m at Q_m increases according to an exponential law in the early stage. These facts suggests that the phase separation or spinodal decomposition certainly occurs in the PVA solution. The characteristic length scale in the early stage of the phase separation is calculated to be 0.57 μm through the relation $2\pi/Q_m$.

U-SANS measurements. In the late stage of the phase separation, the PVA gel is so opaque that it is impossible to perform LS measurements on them. We therefore conducted U-SANS measurements to see the structure of the opaque PVA gel. As shown in Figure 1, the observed scattering intensity $I(Q)$ shows a broad maximum at Q = 0.35 x10^{-3} Å^{-1}, giving a characteristic length of 1.8 μm. This value is 3.2 times larger than that evaluated in the early stage, suggesting that the structural growth further proceeds even in the late stage against the elasticity of the gel network.

As was shown in this report, the PVA gel has a hierarchic structure in a very wide spatial scale from several Å to several μm and this structure is certainly related to the interesting properties of the PVA gel. Finally a schematic sketch of the hierarchic structure of the PVA gel is given in Figure 2.

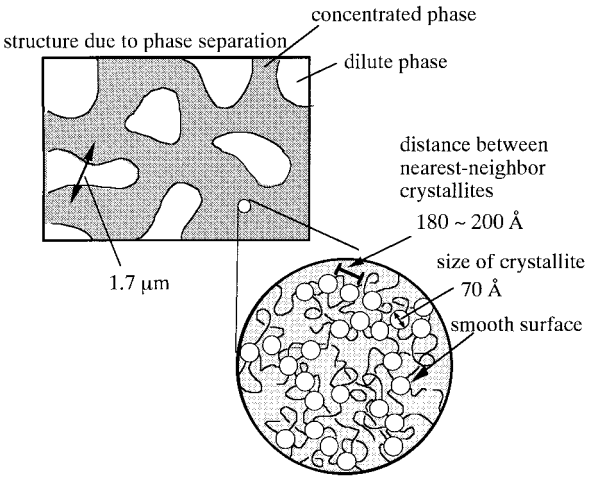

Figure 2. Schematic sketch of a PVA gel in DMSO-d_6/D_2O (60/40 v/v) with Cp = 5 g/dL elucidated in this work.

References

1. M. Ohkura, T. Kanaya and K. Kaji, *Polymer* **33**, 3689 (1992).
2. M. Ohkura, T. Kanaya and K. Kaji, *Polymer* **33**, 5044 (1992).
3. T. Kanaya, M. Ohkura, K. Kaji, M. Furusaka and M. Misawa, *Macromolecules* **27**, 5069 (1994).
4. T. Kanaya, M. Ohkura, H. Takeshita, K. Kaji, M. Furusaka, H. Yamaoka and G. D. Wignall, *Macromolecules* **28**, 3168 (1995).

Solid-State ^{13}C and ^{1}H NMR Analyses of Hydrogen Bonding and the Conformation of Poly(vinyl alcohol)

Kenji Masuda, Hironori Kaji, and Fumitaka Horii

CP/MAS ^{13}C NMR analyses have been made for different frozen solutions of poly(vinyl alcohol) (PVA) samples with different tacticities. The CH resonance lines of the frozen PVA solutions split in different ways significantly depending on the tacticities and the solvents. These CH resonance lines are well resolved into 9 constituent lines whose chemical shifts are estimated by assuming the downfield shifts due to intramolecular hydrogen bonding and the upfield shifts induced by the *γ-gauche* effect. Furthermore, the relative intensities of the lines for atactic PVA samples are successfully interpreted by the statistical treatment assuming the statistical formation of the intramolecular hydrogen bond and the random distribution of the *trans* and *gauche* conformations. Separate ^{1}H CRAMPS analyses have also revealed the existence of the OH groups free from hydrogen bonding together with hydrogen-bonded OH groups in PVA films.

Keywords: CP/MAS ^{13}C NMR / ^{1}H CRAMPS / Poly(vinyl alcohol) / Hydrogen bonding / Conformation

When hydrogen bonding with the oxgen-oxgen distance less than about 0.27 nm is formed, ^{13}C chemical shifts significantly shift downfield for carbons associated with such hydrogen bonding. For solid poly(vinyl alcohol) (PVA) samples with different tacticities, the CH resonance line splits into three lines (lines I, II, and III) in CP/MAS ^{13}C NMR spectra [1]. These lines are assigned to the CH carbons associated with the formation of two, one, and no intramolecular hydrogen bond(s) in the triad sequences at least for the crystalline component. By analyzing the relative intensities of the lines, we have already clarified features of hydrogen bonding for different PVA samples [1,2]. In this report, a similar analysis is applied to frozen PVA solutions, where conformational effects should be also considered. The first detection of the OH groups free from hydrogen bonding by ^{1}H CRAMPS is also briefly reported for PVA films.

The triad tacticities of PVA samples used in this work are as follows: HI-PVA (*mm* = 0.79, *mr* = 0.19, *rr* = 0.02), MI-PVA (*mm* = 0.66, *mr* = 0.28, *rr* = 0.06), LI-PVA (*mm* = 0.50, *mr* = 0.39, *rr* = 0.11).

CP/MAS ^{13}C NMR spectra were measured on a JEOL GSX-200 spectrometer operating under 4.7 T. ^{1}H CRAMPS spectra were obtained on a Chemagnetics CMX-400 spectrometer operating under 9.4 T by using the BR-24 multiple pulse sequence [3].

Figure 1 shows CP/MAS ^{13}C NMR spectra of frozen DMSO-d_6 solutions of PVA samples with different tacticities, which were measured at -50˚C [4]. For reference, the spectrum of the crystalline component for A-PVA films prepared from 10 wt% DMSO solution is also shown in this figure. The broken lines indicate ^{13}C chemical shifts of lines I, II, and III in the crystalline state. In

FUNDAMENTAL MATERIAL PROPERTIES — Molecular Dynamic Characteristics—

The Research activities in this subdivision cover structural studies and molecular motion analyses of polymers and related low molecular weight compounds in the crystalline, glassy, liquid crystalline, solution, and frozen solution states by high-resolution solid-state NMR, dynamic light scattering, electron microscopy, X-ray diffractometry, and so on, in order to obtain basic theories for the development of high-performance polymer materials. The processes of biosynthesis, crystallization, and higher-ordered structure formation are also studied for bacterial cellulose.

Prof
HORII
Fumitaka
(D Eng)

Assoc Prof
TSUNASHIMA
Yoshisuke
(D Eng)

Instr
KAJI
Hironori
(D Eng)

Assoc Instr
HIRAI
Asako
(D Eng)

Techn
OHMINE
Kyoko

Guest Scholar:
HU, Shaohua (Assoc Prof, D Eng)
MAS, Rosemal (Assoc Prof, Ph.D)
Students:
ISHIDA, Hiroyuki (DC)
KAWANISHI, Hiroyuki (DC)
KUWABARA, Kazuhiro (DC)
OHIRA, Yasumasa (DC)
MASUDA, Kenji (MC)
TAI, Toshihiro (MC)
HATTORI, Kimihiko (MC)
OHTSU, Takafumi (MC)
TAJIRI, Kouji (MC)
ISOMURA, Takenori (UG)
MIYAO, Manabu (UG)
NOMURA, Ryosuke (UG)
TAN, Quynh (RS)
ZHENG, Jianming (RS)

the frozen A-PVA/DMSO-d_6 solution, the CH resonance line clearly splits into two lines and these two lines have the same chemical shifts as lines II and III. In the frozen LI-PVA solution, however, the CH resonance line does not split clearly. In the frozen MI-PVA and HI-PVA solutions appears only a single line whose chemical shift is in disagreement with that of either line II or III. It has also been found that CP/MAS ^{13}C NMR spectra of frozen PVA aqueous solutions are significantly different from the spectrum of the crystalline component of PVA films.

The CH resonance lines of frozen PVA solutions, whose line splitting greatly depends on the solvents and tacticities as described above, can be well resolved into 9 constituent lines. These lines have different chemical shifts estimated by assuming the downfield shifts due to intramolecular hydrogen bonding and the upfield shifts induced by the *γ-gauche* effect [5]. Furthermore, the relative intensities of the respective constituent lines are successfully interpreted by the statistical treatment assuming the statistical formation of the intramolecular hydrogen bonds for the two appropriately successive OH groups and the random distribution of the *trans* and *gauche* conformations along the PVA chains. The probabilities for the *trans* conformation and the intramolecular hydrogen bond are also determined through this analysis for the atactic PVA samples. In contrast, such a statistical analysis cannot be applied to the cases of frozen solutions for PVA samples with higher isotacticity, suggesting the preferable formation of some specific conformations.

Similar statistical analyses have been also conducted for the crystalline and noncrystalline components of A-PVA films. In particular, the contribution of the *gauche* conformation can be well considered for the non-crystalline component as in the cases of the frozen solutions. The features of the crystalline and non-crystalline states of different PVA samples will be interpreted in terms of the probabilities of the intramolecular hydrogen bond and the *trans* conformation.

Figure 2 shows ^{1}H CRAMPS spectra of three types of A-PVA films; (a) A-PVA films, (b) OH-group deuterated films (A-PVA-d_1), (c) main-chain deuterated A-PVA (A-PVA-d_3). We have already been assigned three main resonance lines to OH, CH, and CH_2 protons in the order of increasing field [6]. Here, the OH line is markedly broader than the other two lines, probably reflecting the wide distribution of hydrogen bonding. However, the relative integrated intensity of the OH, CH, and CH_2 lines is not in accord with the composition ratio 1:1:2, because the intensity of the OH line is much low. In this figure, the results obtained by the lineshape analysis are also shown, in which a Gaussian curve is assumed for each line. It is found that an additional contribution indicated as OH_f should be introduced at 2.8 ppm to obtain best fitting. Moreover, the total intensity of the OH and OH_f lines well agrees with that of the CH line. In sample A-PVA-d_1, the OH_f line is greatly reduced in intensity together with the decrease of the OH line. From these experimental results, it is concluded that the OH_f line should be assigned to the OH protons free from hydrogen bonding.

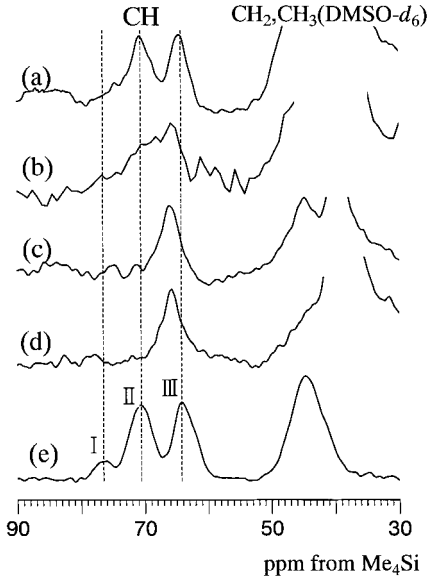

Figure 1. CP/MAS ^{13}C NMR spectra of frozen DMSO-d_6 solutions of PVA samples with different tacticities, measured at -50˚C: (a) A-PVA, (b) LI-PVA, (c) MI-PVA, (d) HI-PVA, (e) crystalline component of A-PVA films.

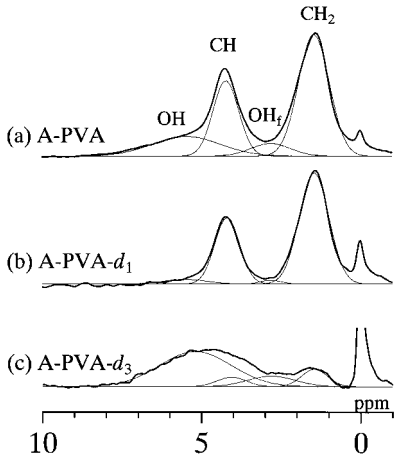

Figure 2. ^{1}H CRAMPS spectra of three types of A-PVA films, measured at room temperature.

As is described above, solid-state ^{13}C and ^{1}H NMR spectroscopies are found to be useful in characterizing hydrogen bonding and the conformation in different states of PVA.

References

1. Horii, F. *et al*., *Polymer* **1992**, *33*, 2299.
2. Hu, S. *et al*., *Polymer* **1994**, *35*, 2516.
3. Burum, D. *et al*., *J. Chem. Phys*. **1979**, *71*, 944.
4. Tonelli, A. E. *NMR Spectroscopy and Polymer Microstructure*; VCH: New York, 1989.
5. Horii, F. *et al*., *Macromolecules* **1997**, *30*, 2519.
6. Horii, F. *et al*., *Macromolecules* **1996**, *29*, 3330.

Controlled Graft Polymerization on Silicon Substrate by the Combined Use of the Langmuir-Blodgett and Atom Transfer Radical Polymerization Techniques

Muhammad Ejaz, Shinpei Yamamoto, Kohji Ohno, Yoshinobu Tsujii, Takeshi Fukuda and Takeaki Miyamoto

The atom transfer radical polymerization technique using the copper/ligand complexes was applied to the graft polymerization of methyl methacrylate on the Si wafer on which the monolayer of the initiator, 2-(4-chlorosulfonylphenyl) ethyl trimethoxysilane, was immobilized by the Langmuir-Blodgett technique. Atomic force microscopic and ellipsometric studies revealed that the polymerization with an additional initiator afforded a homogeneous graft layer, the thickness of which increased proportionally to the number-average molecular weight of the narrow-polydispersity homopolymers produced in the solution. This suggests that the graft polymerization is successfully controlled by the Cu/ligand complexes in the same way as the solution polymerization.

Keywords: Surface modification / Monolayer / Immobilization / Controlled radical polymerization / Graft layer / Ellipsometry

Recently much interest has been directed towards new ways to modify surfaces of solid substrates for potential applicability. Graft polymerization starting with the initiating sites fixed on the surface is one of the most effective and versatile methods for such surface modification. However, it is usually very difficult to control molecular weight, molecular weight distribution, and surface density of graft chains. We attempted to precisely control all these three parameters by the combined use of two independent techniques: one is the Langmuir-Blodgett (LB) technique to provide a well organized set of initiating sites on the substrate, and the other is the atom transfer radical polymerization (ATRP) technique using copper(Cu) /ligand(L) complexes[1] to achieve a controlled graft polymerization. ATRP is one of the several techniques of controlled/"living" radical polymerization that has been attracting much attention as a new route to well-defined polymers with low polydispersities.[2]

In this work, we have examined the graft polymerization of methyl methacrylate (MMA) by ATRP on an initiator-fixed substrate. 2-(4-Chlorosulfonylphenyl) ethyl trimethoxysilane (CTS) was used as an initiator which can be immobilized on an oxidized silicon substrate; the Cl atom of a chlorosulfonyl group (-SO_2Cl) is easily abstracted by the Cu/L complex, and the produced -SO_2* radical initiates the radical polymerization.

Immobilization of Initiator

Figure 1 schematically illustrates the immobilization

ORGANIC MATERIALS CHEMISTRY — Polymeric Materials —

Scope of research

Basic studies have been conducted for better understandings of the structure/property or structure/function relations of polymeric materials and for development of novel functional polymers. Among those have been the studies on (1) the syntheses and properties of cellulose- and oligosaccharide-based functional polymers, e.g., bio-degradable polymers, liquid crystals and polymers of well-defined structure having pendant oligosaccharides, (2) the structure of polymer gels, ultrathin films and polymer alloys, and (3) the syntheses of new types of block and graft copolymers and fullerene(C_{60})-including polymers.

Prof MIYAMOTO, Takeaki (D Eng)

Assoc Prof FUKUDA, Takeshi (D Eng)

Instr TSUJII, Yoshinobu (D Eng)

Instr MINODA, Masahiko (D Eng)

Assoc Instr DONKAI, Nobuo (D Eng)

Students:
IDE, Nobuhiro (DC)
TAKARAGI, Akira (DC)
OHNO, Kohji (DC)
OKAMURA, Haruyuki (DC)
YAMADA, Kenji (DC)
YAMAMOTO, Shinpei (DC)
GOTO, Atsushi (MC)
IMIYA, Chie (MC)
MIYAZONO, Kouki (MC)
MUHAMMAD, Ejaz (MC)
IZU, Yasumasa (MC)
YAMAMOTO, Shuichi (MC)
MARUMOTO, Yasuhiro (UG)
MIYAZAKI, Masayuki (UG)
MIURA, Shigenori (UG)
KITAGAWA, Hiroshi (RF)
LIU, Haiqing (RF)

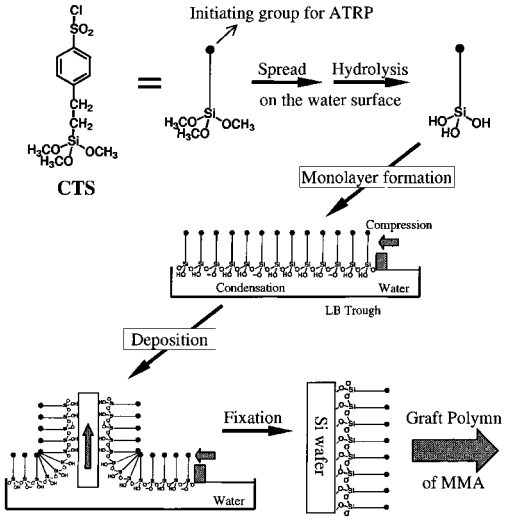

Figure 1 Schematic illustration of the immobilization process of the initiator by the LB technique.

process of the initiating groups. CTS was spread from a chloroform solution on the clean water surface in a Langmuir trough, where methoxysilyl groups (≡Si-OCH_3) of CTS were presumably hydrolyzed to silanol groups (≡Si-OH). The surface pressure (π) – occupied area (A) isotherm of CTS suggests the formation of a monolayer on the water surface. When π was kept 10 mN/m at which the isotherm gave the steepest rise, the occupied area decreased by about 10%, approaching a constant value. This initial decrease in A might be due to the polycondensation between silanol groups formed by the hydrolysis of CTS on the water surface.

After the surface monolayer was annealed for 30 min at π = 10 mN/m, it was transferred by the lifting-up method onto the oxidized silicon substrate. The transfer ratio, defined as the difference in the water surface area before and after the deposition divided by the substrate surface area, was approximately unity, indicating successful deposition and the formation of a Z-type monolayer film. Thermal treatment of thus obtained substrate at 110 °C for 20 min was carried out to promote the reaction of unreacted silanol groups of CTS with silanol groups on the silicon substrate, forming covalent bonds between the CTS film and the substrate. The atomic force microscopic (AFM) observation suggests that homogeneous immobilization of CTS has been achieved.

Controlled Graft Polymerization

The graft polymerization on the initiator-fixed substrate was carried out for various periods at 90 °C in a degassed diphenyl ether solution of CuBr, 4,4'-di-n-heptyl-2,2'-bipyridine (ligand), MMA, and an additional initiator, *p*-toluenesulfonyl chloride (TsCl). The polymerization without TsCl gave free homopolymers with high polydispersities (M_w/M_n > 3) like the conventional radical polymerization. This is presumably because the

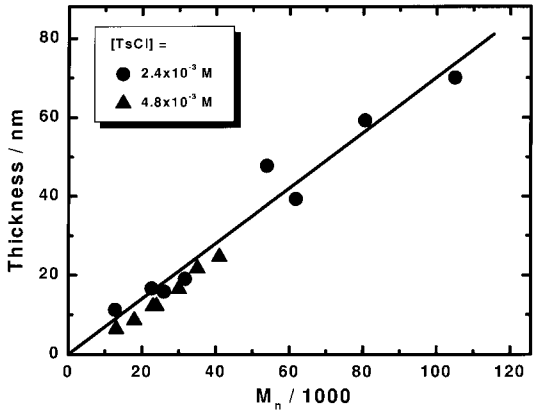

Figure 2 Relationship between graft-layer thickness and M_n of free homopolymers produced in solution.

concentration of initiator in the solution was much too low to control the polymerization. In fact, addition of an appropriate amount of TsCl as a free initiator in solution brought about well-controlled polymerization; the free homopolymers had relatively low polydispersities and the M_n values were proportional to the monomer conversion with the slope which is very close to the theoretical values defined by the feed concentration of TsCl. This indicates that the number of polymer chains is kept constant during the polymerization and hence transfer and termination reactions are negligible.

The AFM observation revealed that a homogeneous polymer layer was formed on the substrate. We confirmed by repeatedly rinsing the substrate with chloroform that the polymer chains were not physically adsorbed but chemically anchored onto the substrate. Ellipsometric study revealed that the thickness of the grafted layer increased with time, and the polymerization with a lower concentration of TsCl gave a thicker layer with the same polymerization time. Since the molecular weight of the polymer grafted on the substrate should be somehow correlated to that of the homopolymer produced in the solution, the graft layer thickness was plotted against the M_n values of the homopolymer in the solution (Figure 2). A proportional relationship was obtained between them, and the slope of the line was independent of the concentration of TsCl. This strongly suggests that the M_n of the graft polymer is almost equal or at least proportional to that of the homopolymer and the graft density is constant during the course of polymerization. Thus, it was concluded that the graft polymerization is controlled by the Cu/ligand complexes in the same way as the solution polymeirzation.

REFERENCES

[1] Wang, J. S. et al. *J. Am. Chem. Soc.* **1995**, *117*, 5614.

[2] a) Geroges, M. K. et al. *Trends Polym. Sci.* **1994**, *2*, 66; b) Matyjaszewski, K. et al. *J. Phys. Org. Chem.* **1995**, *8*, 306; c) Sawamoto, M. et al. *Trends Polym. Sci.* **1996**, *4*, 371.

Hydrocarbon Molecules with Novel Structure: the First Fullerene Derivative Having a Fulvene-Type π-System and Polycyclic Aromatics Having σ-π Conjugation

Koichi Komatsu, Tohru Nishinaga, Yasujiro Murata, and Akira Matsuura

A spacious π-conjugated carbanion such as fluorenyl anion was found to add to fullerene C_{60} with high positional selectivity to afford the first tetrakisadduct of C_{60} having a fulvene-type π-electronic system on its spherical surface. This derivative reacts with various carbon nucleophiles at the fulvene's "exocyclic" sp^2 carbon to give the corresponding cyclopentadienide ion. Also synthesized were the polycyclic aromatic hydrocarbons fully annelated with a rigid bicyclic framework, i.e. bicyclo[2.2.2]octene. These planar polycyclic systems are characterized by the high oxidizability affording stable cation radicals and dications.

Keywords: C_{60} / π-conjugation / electrochemistry / [4+2] cycloaddition / carbanion / cation radical

1. The First Tetrakisadduct of Fullerene C_{60} Having a Fulvene-Type π-System on the Spherical Surface [1].

Fulvene (**1**) is a polarized cross-conjugated π-system, which reacts with nucleophiles selectively at the exocyclic sp^2 carbon to generate a cyclopentadienide ion. It is of great interest to construct such a π-system on the spherical surface of the fullerene molecule.

The reaction of C_{60} with an excess amount of potassium fluorenide (3 equiv) in THF for 72 h under argon (*but without rigorous exclusion of air*) afforded tetrakis(9-fluorenyl)adduct **2** as a black powder in 40% yield. The results of X-ray crystallography of **2** (Figure 1) clearly indicated that the four sp^2 carbons (C-1 – C-4) of

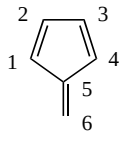

1

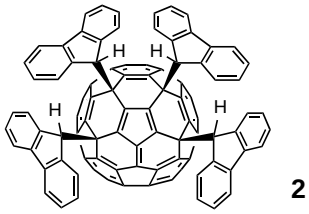

2

the fulvene structure are isolated from the outer rim π-conjugated system by four sp^3 carbons each bearing a fluorenyl group and that there is considerable bond alternation comparable to that in the previously reported planar fulvene derivatives.

Compound **2** reacts with various carbon nucleophiles selectively at the C-6 carbon to give stable cyclopenta-

ORGANIC MATERIALS CHEMISTRY —High-Pressure Organic Chemistry—

Scope of Research

Fundamental studies are being made for creation of new functional materials with novel structures and properties and for utilization of high pressure in organic synthesis. The major subjects are: synthetic and structural studies on novel cyclic π-systems; chemical transformation of fullerene C_{60}; utilization of carbon monoxide and dioxide for organic synthesis under the transition-metal catalysis.


Prof KOMATSU Koichi (D Eng)


Instr MORI Sadayuki (D Eng)


Instr KUDO Kiyoshi (D Eng)


Instr NISHINAGA Tohru (D Eng)


Techn YASUMOTO Mitsuo


Assoc Instr TANAKA Toru

Guest Res Assoc
STAHR, Helmut
Students
MURATA, Yasujiro (DC)
MATSUURA, Akira (MC)
NAKAYAMA, Hideaki (MC)
IZUKAWA, Yoshiteru (MC)
TAKAHASHI, Masayo (MC)
FUJIWARA, Koichi (MC)
KATO, Noriyuki (UG)
HIRATA, Kazuhisa (UG)
WAKAMIYA, Atsushi (UG)

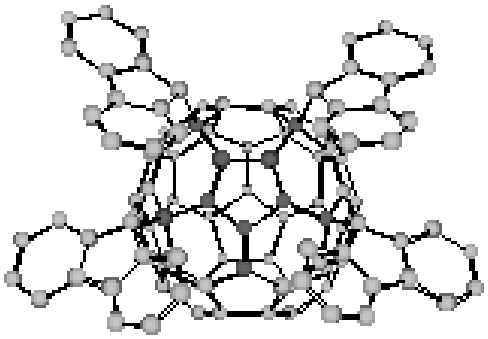

Figure 1. Molecular structure of **2** determined by Dr. M. Shiro of Rigaku Corp. The fulvenyl carbons and sp^3 carbons on the C_{60} cage are darkened for comprehensibility.

dienide ions. Of particular interest is the pentakis(9-fluorenyl)adduct **3**, which has the C_5 symmetric structure with the five spacious fluorenyl groups arrayed in a propeller-like arrangement (Figure 2). This anion undergoes a reversible one-electron oxidation to give a stable radical as shown by cyclic voltammetry and ESR experiments.

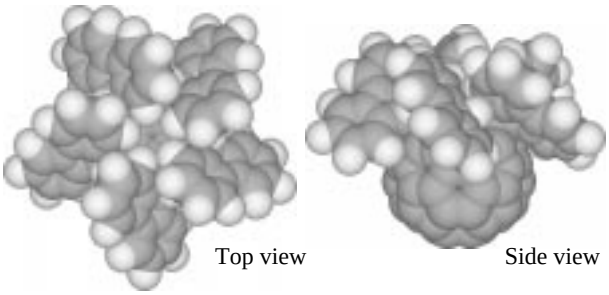

Figure 2. Space-filling representation of the AM1-optimized structure of **3**.

2. Synthesis, Structure, and Oxidizability of Polycyclic Aromatic Hydrocarbons Surrounded by Rigid Bicyclic Frameworks [2, 3].

In our previous studies, annelation with rigid bicyclic frameworks such as bicyclo[2.2.2]octene (abbreviated as BCO) was shown to be effective in stabilization of the positively charged, cyclic π-conjugated systems [4]. It is assumed that the rigidly held σ-bonds in the BCO unit exert not only the inductive effect but the σ-π conjugative (C-C conjugative) effect so that the HOMO levels of the π-system are raised.

Thus, the BCO dimer **4** exhibited high reactivity as a diene to give various [4+2] cycloadducts, which can be transformed, for example, into representative polycyclic benzenoid aromatics with 14 and 12 π-electrons, anthracene **5** and biphenylene **6**, as shown in Scheme 1.

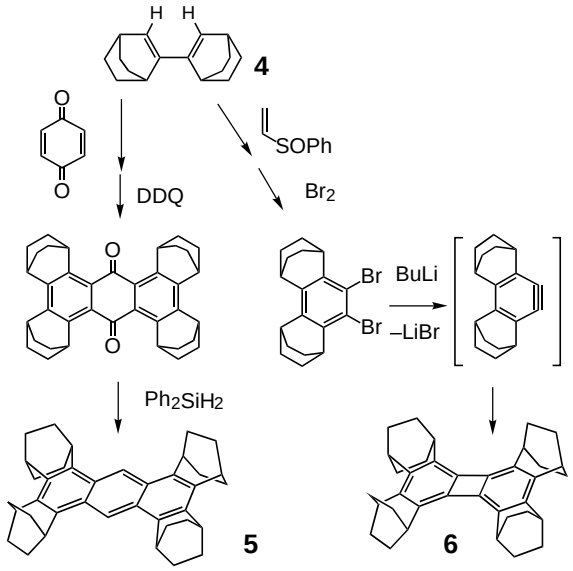

Scheme 1

In accord with the expectation, hydrocarbons **5** and **6** were characterized by the remarkably low oxidation potentials to generate the stable cation radicals ($E_{1/2}$ +0.21 and +0.33 V vs Fc/Fc^+) and less stable dications (E_{pa} +0.87 and +1.03 V). Chemical oxidation with $NO^+BF_4^-$ afforded the stable cation radical $\mathbf{5}^{+\cdot}$ (red-violet) and $\mathbf{6}^{+\cdot}$ (blue-violet) as the BF_4^- salts, the dichloromethane solutions of which exhibited the triplet and 9-line ESR spectra respectively.

The chemical two-electron oxidation of anthracene **5** readily proceeded by the use of SbF_5 to give the blue-colored solution of dication $\mathbf{5}^{2+}$, which was identified by both ^1H and ^{13}C NMR measurements. Elevation of the HOMO level of **5** was also demonstrated by its high reactivity as diene in the [4+2] reaction with various dienophiles affording the dibenzobarrelene derivatives **7** (Scheme 2). Studies are now under way to investigate the unique electronic properties of **7** and to extend this methodology for the synthesis of the corresponding triptycene derivative.

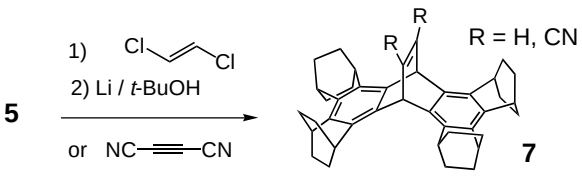

Scheme 2

References

1. Murata Y, Shiro M and Komatsu K, *J. Am. Chem. Soc*., **119**, 8117 (1997).
2. Matsuura A, Nishinaga T and Komatsu K, *Tetrahedron Lett*., **38**, 3427 (1997).
3. Matsuura A, Nishinaga T and Komatsu K, *Tetrahedron Lett*., **38**, 4125 (1997).
4. Komatsu K, *J. Synth. Org. Chem., Jpn*., **54**, 868 (1996).

Toward Silicon-Catenated Silole Polymers, Poly(1,1-silole)s: Syntheses and Structures of Oligo(1,1-silole)s

Shigehiro Yamaguchi, Ren-Zhi Jin, and Kohei Tamao

A series of 1,1-difunctionalized siloles have been synthesized from 1,1-diaminosiloles, which have been prepared via the intramolecular reductive cyclization of diaminobis(phenylethynyl)silane. With the 1,1-difunctionalized siloles in hand, oligo(1,1-silole)s, silole oligomers catenated through silicons, have been synthesized as model compounds of poly(1,1-silole)s. UV absorption spectra of the oligosiloles have been determined, in which tersilole and quatersilole have unique absorption maxima around 280-290 nm.

Keywords: Silole / Poly(1,1-silole) / Oligo(1,1-silole) / σ*–π* Conjugation / Polysilane / Intramolecular reductive cyclization / UV absorption spectra

Poly(1,1-silole)s, silole (silacyclopentadiene) polymers catenated through the ring-silicons, constitute a new class of polysilanes with σ*–π* conjugation, as shown in Figure 1. In the silole ring itself, there is a significant low-lying LUMO energy level due to the σ*–π* conjugation arising from the interaction of the σ* orbital of the two exocyclic σ bonds on silicon with the π* orbital of the *cisoid*-butadiene moiety [1]. This type of orbital interaction would also take place in the polymeric system, as schematically shown in Figure 1. Thus, σ*–π* conjugation between the σ* orbital delocalized over the polysilane main chain and the π*-orbital localized on the *cisoid*-butadiene moiety in every silole ring would lower the LUMO level. Poly(1,1-silole)s are thus interesting target molecules to synthesize, while only a few silole dimers have been synthesized to date. Reported herein are our recent results toward the still veiled poly(1,1-silole)s.

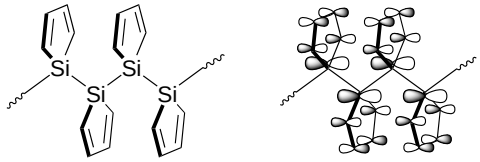

Figure 1. Schematic drawings of Poly(1,1-silole) and σ*–π* conjugation in the LUMO.

1. A New Synthetic Route to 1,1-Difunctionalized Siloles [2]

For the synthesis of poly(1,1-silole)s, 1,1-functionalized siloles, especially 1,1-dichlorosiloles, are an important class of compounds as starting materials. However, their synthetic methodologies have been rather limited. We have now developed a new general

SYNTHETIC ORGANIC CHEMISTRY –Synthetic Design–

Scope of research

(1) Synthesis, structural studies, and synthetic applications of organosilicon compounds, such as pentacoordinate silicon compounds, functionalized silyl anions, and functionalized oligosilanes. (2) Design and synthesis of novel π-conjugated polymers containing silacyclopentadiene (silole) rings, based on new cyclization reactions and carbon-carbon bond formations mediated by the main group and transition metals. (3) Chiral transformations and asymmetric synthesis via organosulfur and selenium compounds, especially via chiral episulfoniun and episelenonium ions.

Prof TAMAO, Kohei (D Eng)

Assoc Prof TOSHIMITSU, Akio (D Eng)

Instr KAWACHI, Atsushi (D Eng)

Instr YAMAGUCHI, Shigehiro (D Eng)

KATKEVICS, Martins (Guest Res Scholar); JIN, Ren-Zhi (Guest Scholar); ASAHARA, Masahiro (DC); TANAKA, Yoko (DC); AKIYAMA, Seiji (DC); ISHII, Hiroyuki (MC); TERADA, Masayoshi (MC); ITAMI, Yujiro (MC); ENDO, Tomonori (MC); MITSUDO, Koichi (UG); GOTO, Tomoyuki (UG); SAEKI, Tomoyuki (UG); SANO, Atsushi (UG)

synthetic route to 1,1-functionalized siloles using 1,1-diaminosiloles as key compounds.

Our method is based on the intramolecular reductive cyclization of bis(phenylethynyl)silanes, which we have recently developed [3]. Thus, bis(diethylamino)bis(phenylethynyl)silane was added dropwise into an excess amount of lithium naphthalenide (4 molar amount) at –78 °C to form 2,5-dilithio-1,1-diaminosilole cleanly. The dilithiosilole was successfully trapped with dimethyl sulfate to form 2,5-dimethyl-1,1-diaminosilole in good yield. A series of 1,1-difunctionalized siloles having alkoxy, Cl, and F functionalities were prepared by the conventional functional group transformation from 1,1-diaminosiloles (Scheme 1). The present methodology is also applicable to the synthesis of 1-monofunctionalized siloles.

Scheme 1

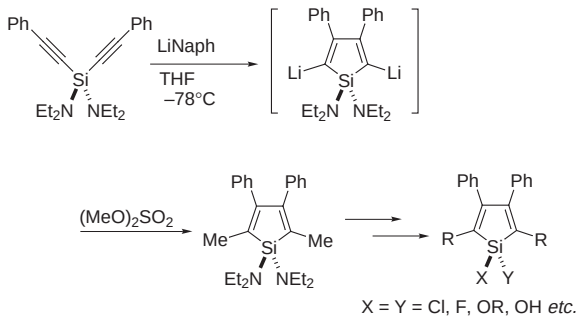

2. Oligo(1,1-silole)s as Models of Poly(1,1-silole)s [4]

With the silicon-chlorinated siloles **5** and **6** in hand, we have succeeded in the preparation of a series of oligo(1,1-silole)s from dimer **2** to tetramer **4** (Chart 1). Thus, silole trimer, tersilole **3**, has been obtained by the coupling of monochlorosilole **5** with silole dianion **7**, which was cleanly prepared from 1,1-dichlorosilole **6** with Li in THF. Quatersilole **4** has also been obtained by a similar coupling reaction. Thus, 1,1-dichlorosilole **6** was reduced with 3 molar amount of Na, resulting in the formation of a mixture of the bisilole dianion **8** and the silole dianion **7**. The mixture was treated with 1.5 molar amount of 1-chlorosilole to afford quatersilole **4** and tersilole **3** in 20% and 8% yields, respectively. These are the first examples of oligo(1,1-silole)s catenating more than three silole rings.

UV absorption data are summarized in Table 1, in which the data of the perphenyl- and permethyl-trisilanes and tetrasilanes are also given for comparison. The monosilole **1** has two absorption bands around 250 nm and 310 nm, assignable to the π–π* transitions of the

Chart 1

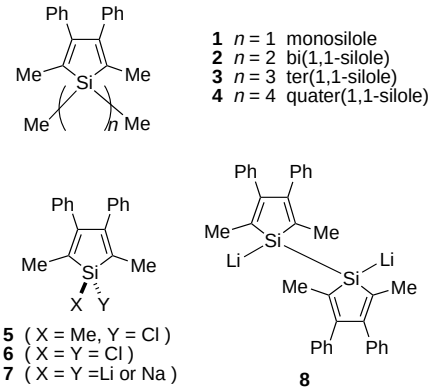

phenyl and silole moieties, respectively. In comparison with the monosilole **1**, the oligosiloles **2**-**4** show distinct spectra, where the absorption of the silole moieties is hidden by broad bands. Remarkably, tersilole **3** and quatersilole **4** have unique absorptions at around 280 and 290 nm, respectively. These absorption maxima are 50-60 nm longer than those of the permethyl oligosilanes. In comparison with the perphenyl counterparts, **3** has a 20 nm longer λ_{max} and **4** has a comparable λ_{max}. As mentioned previously, the unique absorptions of the oligo(1,1-silole)s would have arisen from the orbital interactions.

Table 1. UV Spectral Data for Oligo(1,1-silole)s[a]

compound	λ_{max} / nm	logε
monosilole **1**	307	3.22
bisilole **2**	255	4.42
tersilole **3**	279	4.60
quatersilole **4**	289	4.59
$Ph(Ph_2Si)_3Ph$[b]	255	4.51
$Ph(Ph_2Si)_4Ph$[c]	288	4.36
$Me(Me_2Si)_3Me$[d]	216	3.96
$Me(Me_2Si)_4Me$[d]	235	4.17

[a] In chloroform. [b] Gilman H, Atwell W. H, Sen P. K, and Smith C. L, *J. Organomet. Chem.*, **4**, 163 (1964). [c] Gilman H, and Atwell W. H, *J. Organomet. Chem.*, **4**, 176 (1964). [d] Gilman H, Atwell W. H, and Schwebke G. L, *J. Organomet. Chem.*, **2**, 369 (1964).

1. Yamaguchi S, and Tamao K, *Bull. Chem. Soc. Jpn.* **69**, 2327 (1996).
2. Yamaguchi S, Jin R.-Z, Tamao K, and Shiro M, *Organometallics*, **16**, 2230 (1997).
3. Tamao K, Yamaguchi S, and Shiro M, *J. Am. Chem. Soc.*, **116**, 11715 (1994).
4. Yamaguchi S, Jin R.-Z, Tamao K, and Shiro M, *Organometallics*, **16**, 2486 (1997).

Kinetic Resolution of Racemic Alchols by a New Nuclephilic Catalyst

Takeo Kawabata, Minoru Nagato, Kiyosei Takasu and Kaoru Fuji

A new nucleophilic catalyst **1** promotes the kinetic resolution of racemic alcohols through enantioselective acylation at ambient temperature. The Key feature of **1** involves an induced fit intermediate due to the π-π interaction, although **1** exists in the open conformation in the ground state.

Keywards : Kinetic resolution/ Acylation/ Nucleophilic catalyst/ Diol

Enzymatic kinetic resolution of racemic alcohols through acylation or de-acylation has been extensively studied and established as one of the most effective methods for the preparation of optically active alcohols. Non-enzymatic alternatives in this field have also been developed recently. Use of stoichiometric amounts of chiral acylating agents effected the kinetic resolution of racemic alcohols with high stereoselectivity.[1] On the other hand, the corresponding catalytic process is still in the developmental stage. We report here development and properties of a new nucleophilic catalyst **1**.[2]

In designing the catalyst, we focused on how strict stereocontrol could be realized without retarding its catalytic activity. We chose 4-pyrrolidinopyridine as a model of the active site because it is known to be the most effective catalyst for the acylation of alcohols. To achieve effective stereocontrol, a conventional strategy would involve the introduction of sterically demanding asymmetric center(s) near the active site (pyridine-nitrogen). However, this would lead to a dramatic reduction in the catalytic activity. To overcome the *selectivity-reactivity dilemma*, we designed catalyst **1** in which stereo-controlling chiral centers are located far

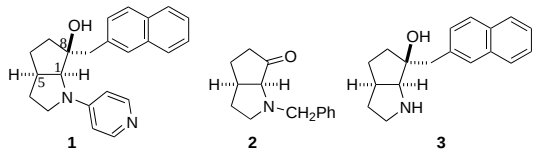

from the active site. This catalyst is expected to cause remote asymmetric induction through chirality transfer from the C(1) and C(8) chiral centers to the active site (*N*-acyliminium) in the reactive intermediate (Figure 1).

Catalyst **1** was prepared from a known racemic ketone **2**. Addition of 2-lithiomethylnaphthalene to **2** followed by hydrogenolysis gave **3** in 80% yield. Racemic **3** was resolved by recrystallization of the salt obtained with (-)-camphorsulfonic acid to give **3** in enantiomerically pure form. A pyridine moiety was introduced into **3** by the palladium-catalyzed coupling with 4-bromopyridine to

SYNTHETIC ORGANIC CHEMISTRY — Fine Organic Synthesis —

Scope of Research

The research interests of the laboratory include the development of new synthetic methodology, molecular recognition, and screening of antitumor natural products. Programs are active in the areas of use of chiral leaving groups for an asymmetric induction, desymmetrization of symmetrical compounds, asymmetric alkylation of carbonyl compounds based on “memory of chirality”, use of binaphthalenes in the asymmetric Wittig-type reactions, syntheses of molecular switch, and Taxus diterpenoids.

Professor FUJI, Kaoru (D Pharm Sc)

Assoc Prof TANAKA, Kiyoshi (D Pharm Sc)

Instructor KAWABATA, Takeo (D Pharm Sc)

Thechnician TERADA, Tomoko

Secretary
ISHIDA, Emi
Guest Research Associate
CHEN, Jijun; LAKSHMAIAH, Gingipalli; YANG, Xiaosheng
Students
FURUTA, Takumi (DC); SHANG, Muhong (DC); SUZUKI, Hideo (DC); TAKASU, Kiyosei (DC); TSUBAKI, Kazunori (DC); WATANABE, Toshiyuki (DC); HAMADA, Masaki (MC); KOYAMA, Naohisa (MC); MORIYAMA, Shoko (MC); NAGAE, Yoshikazu (MC); NURUZZAMAN, Mohammad (MC); OHNISHI, Hiroshi (MC); YAMAMOTO, Kensaku (MC); YOSHIDA, Masato (MC); HAYASHI, Noriyuki (UG); KAWAI, Seiji (UG); MAKIHARA, Masaru (UG); YOSHIDA, Hiroshi (UG)
Research Fellow
KINOSHITA, Naozumi; MOMOSE, Yashima
Research Student
OHTSUBO, Tadamune

give **1** in 84% yield. Using catalyst **1**, the kinetic resolution of racemic alcohols **4**-**8** was examined. Treatment of racemic **4a** (R=^{i}Pr) with 5 mol % of **1** and 0.7 mol equivalent of isobutyric anhydride in toluene at ambient temperature gave **9** and recovered **4a** in yields of 60% and 27%, respectively. The optical purity of recovered **4a** was 76% ee. With pivaloate **4b** (R=^{t}Bu), the enantioselectivity increased to 94% ee. When benzoate and substituted benzoates were used as substrates, a clear tendency was observed: the stronger the electron-donating ability of the aromatic ring, the higher the enantioselectivity of the reaction. The enantiomerically pure (>99% ee) alcohol **4c** (R=*p*-$Me_2NC_6H_4$) was recovered from the kinetic resolution of racemic **4c** with 5 mol % of **1** at 72% conversion. Even with 0.5 mol % of catalyst **1** (substrate : catalyst = 200 : 1), the optical purity of the recovered **4c** was 93% ee. The kinetic resolution of several racemic mono(*p*-

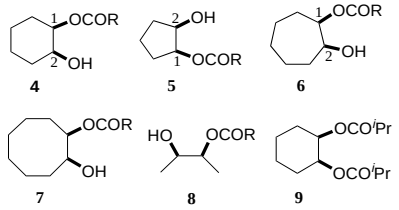

dimethylaminobenzoate) of diols was examined with 5 mol % of **1**. In both cyclic diol-monoesters **5**-**7** and the acyclic variant **8**, acylation proceeded enantioselectively to give the recovered alcohols with 92 ~ 97% ee at 70 ~ 77% conversion.

To obtain insight into the reaction mechanism, the ^{1}H NMR spectra of **1** and its *N*-acyliminium ion were measured in $CDCl_3$ at 20 °C (Figure 1). The observed NOE's suggest that the preferred conformation for **1** is an "open conformation"(**A**), in which the naphthalene ring and the pyridine ring lie apart from each other. Protons H^a and H^b are indistinguishable and appear at δ 8.01 ppm. Similarly, protons H^c and H^d appear at δ 6.37

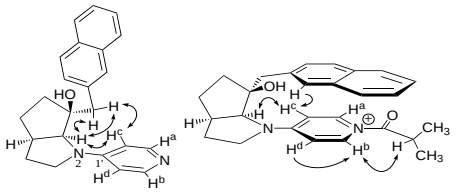

A (open conformation) **B** (closed conformation)

Figure 1. ^{1}H NMR study of **1** (**A**) and its acyliminium ion (**B**) in $CDCl_3$ at 20 °C. Arrows denote the observed NOE's. In **A**, protons H^a, H^b and H^c, H^d appear at δ 8.01 and 6.37 ppm, respectively. In **B**, protons H^a, H^b, H^c, and H^d appear independently at δ 7.45, 8.73, 5.69, and 6.87 ppm, respectively.

ppm. These observations indicate free rotation of the N(2)-C(1') bond and no significant interactions between the naphthalene ring and the pyridine ring. The *N*-acyliminium ion (**B**) is assumed to be the reactive intermediate in the catalytic cycle, and was alternatively formed by mixing **1** and isobutyryl chloride in a 1:1 ratio in $CDCl_3$. Protons H^a, H^b, H^c, and H^d appear independently at δ 7.45, 8.73, 5.69, and 6.87 ppm, respectively. The significant upfield shift (0.56~0.68 ppm) of H^a and H^c as well as the downfield shift (0.50~0.72 ppm) of H^b and H^d indicate π–π interaction between the naphthalene ring and the acylpyridinium moiety. We refer to this conformation as a "closed conformation". Informative NOE's were observed between H^b and the proton, $N^+COC\underline{H}(CH_3)_2$, which imply that the *si* face of the carbonyl group is blocked by the naphthalene ring and the *re* face is open for reaction with alcohols.

Catalyst **1** exists in an "open conformation" (**A**) in its ground state, which is free from steric interaction at the active site. Thus, a facile reaction takes place with acid anhydride. The resulting acylpyridinium intermediate (**B**) is stabilized by attractive π–π interaction between the electron-deficient acylpyridinium π-system and the electron-donating naphthalene ring. The "closed conformation" is suitable for controlling the π-facial reactivity of the *N*-acyliminium ion, which directs the enantioselectivity of the subsequent acylation of alcohols. The reorganization of the catalyst triggered by binding of the specific substrate (acid anhydride) is referred to as an "induced-fit" process, which is currently recognized as a key process in enzymatic catalysis. Since the enantioselectivity of the reaction increases in proportion to the electron-donating ability of the aromatic part of the substrates, it is suggested that the participation of additional π–π interaction between the 4-aminopyridinium π-system of **B** and the aromatic ring of the substrates. The π–π interaction involving the substrate-binding and -recognizing properties of catalyst **1** would regulate the direction of the substrate approach. The total catalytic process would result from co-operative and consecutive events at the active site (pyridine-nitrogen), the stereo-controlling site (naphthalene moiety), and the binding site (4-aminopyridinium π-system). Although the proposed mechanism is speculative, it is worth noting that catalyst **1** has similar properties as enzymes have acquired only after a long history of evolution.

In summary, we have developed a catalyst **1** for the kinetic resolution of racemic alcohols. The properties of **1** appear to approach some of the enzymatic functions with regard to mildness of the reaction conditions, enantioselectivity, and the reaction mechanism. Another distinctive feature of **1** is its catalyst design based on attractive interaction in non-organometallic species, which is in contrast to the conventional design of catalysts based on repulsive steric interaction in the coordination sphere of the central metal. Catalyst **1** is also expected to catalyze several other types of asymmetric reactions in addition to the kinetic resolution of alcohols such as peptide-bond formation, carbon-acylation, and lactonization.

References

1. a) Evans, D. A.; Anderson, J. C.; Taylor, M. K. *Tetrahedron Lett*. **1993**, *34*, 5563. b) Ishihara, K.; Kubota, M.; Yamamoto, H. *Synlett* **1994**, 611. c) Vedejs, E.; Chen, X. *J. Am. Chem. Soc*. **1996**, *118*, 1809.
2. Kawabata, T.; Nagato, M.; Takasu, K.; Fuji. K. *J. Am Chem. Soc*. **1997**, *118*, 3169.

Stereochemical Control of Yeast Reduction of α-Keto Esters in an Organic Solvent

Kaoru Nakamura, Shin-ichi Kondo, Nobuyoshi Nakajima, and Atsuyoshi Ohno

Yeast reduction of α-keto esters in water afforded the corresponding (*R*)-hydroxy ester while the antipodes were obtained in the reduction in benzene. To elucidate the mechanism for stereochemical control of yeast reduction, seven enzymes responsible for the reduction have been isolated from bakers' yeast and kinetic parameters for enzymatic reductions have been measured. It was found that the (*R*)-producing enzymes have smaller *K*ms than those of the (*S*)-producing enzymes. When the reaction is run in benzene, however, the produced α-hydroxy ester does not undergo further decomposition. The inhibition of enzymatic decomposition in an organic solvent is also accounted for by low concentration of α-hydroxy ester in aqueous phase surrounding the bakers' yeast.

Keywords: Stereochemical control / Microbial reduction / Organic solvent

Microbial reductions have widely been used to synthesize chiral alcohols because of their easiness in treatment and mild reaction conditions. Unfortunately, however, enantioselectivities of microbial reductions are not usually satisfactory, and it is necessary to improve low enantioselectivity of yeast reduction. We have been developed several methods to control stereochemistry of yeast reduction without changing microbes, *i.e.*, modification of substrate, addition of an inorganic salt, addition of an inhibitor to the specific enzyme, and thermal treatment. Here, we report that the use of an organic solvent affects largely the stereochemistry of yeast reduction of α-keto esters. For example, ethyl 2-oxohexanoate (**1d**) was reduced to (*S*)-ethyl 2-hydroxyhexanoate ((*S*)-**2d**) in 99% e.e. and to the antipode, (*R*)-**2d**, in 86% e.e. by the reaction in water and benzene, respectively. The same tendency was observed in the reduction of **1f**. Here, although both reactions in water and in benzene afford the same isomer, (*R*) products, enantioselectivity increases from 19% e.e. to 90% e.e. by changing the medium from water to benzene. Enantioselectivity of the reduction shifts to (*R*)-side in nonpolar organic solvent such as benzene or hexane compared to that in water.

To elucidate the mechanism the effect of organic solvent on stereochmical control of yeast reduction, enzymes were isolated from bakers' yeast and kinetic parameters of these α-keto ester reductases were measured. Five reductases (YKER-I, -IV, -V, -VI, and -VII) are found to be responsible to the reduction of **1d**.

BIOORGANIC CHEMISTRY – Bioorganic Reaction Theory –

Scope of research

Biochemical reactions are studied from the viewpoint for physical organic chemistry. Specifically, the reaction mechanism and stereochemistry of NAD-dependent oxidoreductases are explored. Stereospecific redox transformations mediated by certain biocatalysts such as microbes, enzymes, cultured tissues are also studied. The results will be applied to develop new organic reactions.


Prof OHNO, Atsuyoshi (D Sc)


Assoc Prof NAKAMURA, Kaoru (D Sc)


Instr SUGIYAMA, Takashi


Instr KAWAI, Yasushi (D Sc)


Assoc Instr YAMAZAKI, Norimasa (D Sc)


Techn HIRANO, Toshiko

Students

KINOSHITA, Masamichi (RF, D Sc)
KUNITOMO, Jun (DC)
HIDA, Kouichi (DC)
TAKENAKA, Keishi (DC)
INABA, Yoshikazu (DC)
MATSUDA, Tomoko (DC)
ISHIKAWA, Yoshiteru (MC)
FUJII, Mikio (MC)
MATSUO, Takashi (MC)
ITO Kenji (MC)
TAKEUCHI Minoru (MC)
HAYASHI Motoko (MC)
DAO, Duc Hai (RS)

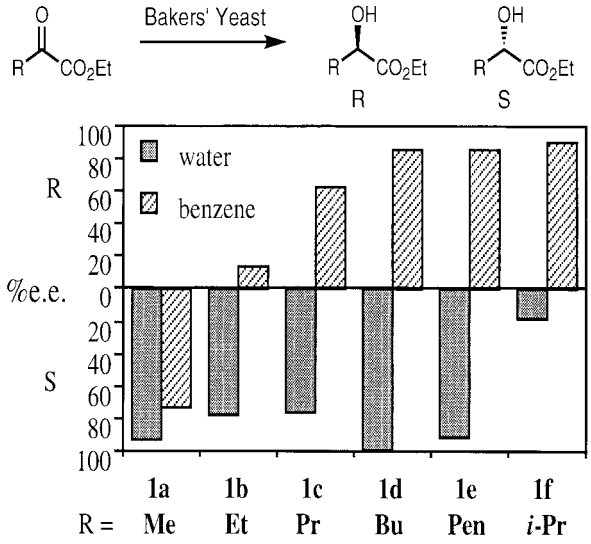

Figure 1. Enantioselectivity of bakers' yeast reduction of α-keto esters.

Among them, two enzymes (YKER-V and -VII) afforded (*S*)-**2d** and the other three enzymes (YKER I, -IV, and -VI) gave (*R*)-**2d**. Kinetic study reveals that YKER-IV and -VI have smaller *K*m (0.14 mM and 1.03 mM, respectively) than the other enzymes. Then, the reduction of **1d** in benzene is catalyzed mainly by YKER-IV and -VI affording (*R*)-**2d**, whereas the reduction in water is also contributed by YKER-V and -VII. Concentration of α-keto ester in yeast cell plays an important role for the stereochemistry of reduction in an organic solvent system. Since the substrate is more soluble in benzene than in water, the substrate concentration in the aqueous phase around yeast cell. Although stereoselectivity of the reduction in benzene is, thus, explainable quantitatively (e.e. of yeast reduction = 86% (*R*) and that of YKER-IV = 88% (*R*)) on the basis of enzyme activity, that in water can be reproduced only qualitatively: e.e. of yeast reduction (99% (*S*)) exceeds that of enzymatic reduction (31% (*S*) and 84% (*S*) for YKER-V (*K*m = 5.7 mM) and -VII (*K*m = 27 mM), respectively). The phenomenon can be accounted for by asymmetric decomposition of the (*R*)-product. During yeast reduction in water, certain α-hydroxy esters (**2c**, **2d**, and **2e**), the products, are decomposed under the catalysis of bakers' yeast. Thus, the (*R*)-α-hydroxy esters are decomposed preferentially remaining the antipodes unaffected. The asymmetric decomposition is one of the tricks for stereochemical control of yeast reduction of α-keto esters in water. For example, when racemic **2d** was incubated with bakers' yeast in water, the *R*-isomer disappeared after 2 h and only the *S*-counterpart was recovered. On the other hand, the enzymatic decomposition of (*R*)-**2d** was not observed when the reaction was run in benzene under the same conditions as those for the reduction in benzene. Suppress of asymmetric decomposition in benzene is also accounted for by the decrease in substrate concentration in the aqueous phase. Apparent *K*m for the decomposition was determined to be 2.2 mM by measuring initial rate of the decomposition of **2d** catalyzed by whole bakers' yeast cell in water. Since the concentration of **2d** in the aqueous phase is much smaller than *K*m for the decomposition, the rate of decomposition of the produced α-hydroxy esters dramatically depressed in benzene.

References

1. Nakamura K, Kondo S, Kawai Y, and Ohno A, *Tetrahedron Lett.*, **32**, 7075-7076 (1991).
2. Nakamura K, Kondo S, Kawai Y, and Ohno A, *Bull. Chem. Soc. Jpn.*, **66**, 2738-2743 (1993).
3. Nakamura K, Kondo S, Kawai Y, Nakajima N, and Ohno A, *Biosci. Biotech. Biochem.*, **58**, 2236-2240 (1994).
4. Nakamura K, Kondo S, Nakajima N, and Ohno A, *Tetrahedron*, **51**, 687-694 (1995).
5. Nakamura K, Kondo S, Kawai Y, Nakajima N, and Ohno A, *Biosci. Biotech, Biochem.*, **61**, 375-377 (1997).

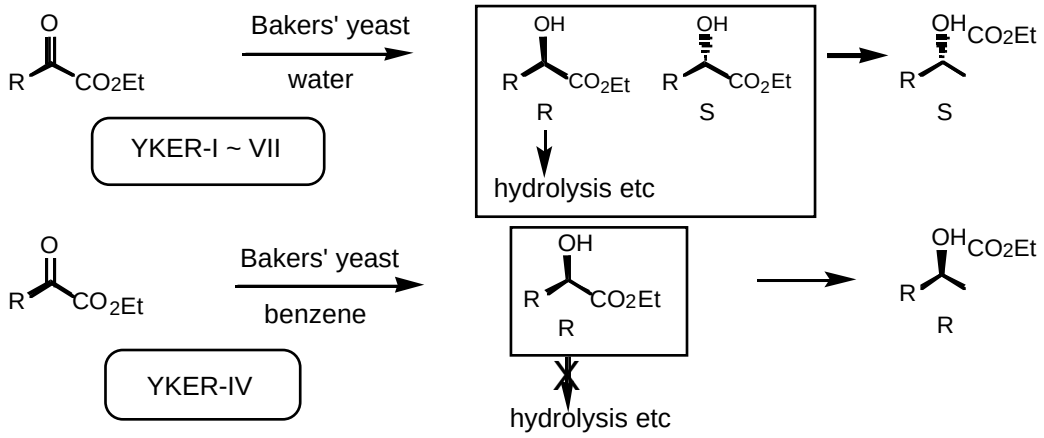

Arranging Functional Quarternary Structures of DNA Binding Peptides

Takashi Morii, Yasunori Aizawa, Yukio Sugiura

Our research seeks to use a combination of synthetic, organic biochemical and molecular biological approaches to study the principle of molecular recognition associated with biological macromolecules. We have focused mainly on the action of transcription factors, especially that of the basic leucine zipper proteins. The model systems described herein have been used to address the issues of protein-protein and protein-DNA recognitions in far greater detail than is possible with the native protein systems.

Key Words:Molecular recognition/ Cooperativity/ Host-guest complex/ Dimerization/ Oligomerization/ Leucine zipper protein

Transcription factors alone do not bind to DNA with enough specificity to discriminate a unique gene from the whole genomic DNA. This fact alone suggests that transcription is controlled by multi-protein complexes in which the sequence-specificity of DNA binding by each proteins is modulated by the combinatorial interactions between proteins themselves. Therefore, understanding the sequence-specific DNA binding by proteins requires a coherent elucidation of the mechanisms in which the protein-DNA interaction and protein-protein interaction complement one another to enhance the specificity of recognition.

Interestingly, nature uses the above proposed strategy to gain sequence-specific DNA binding, for transcription

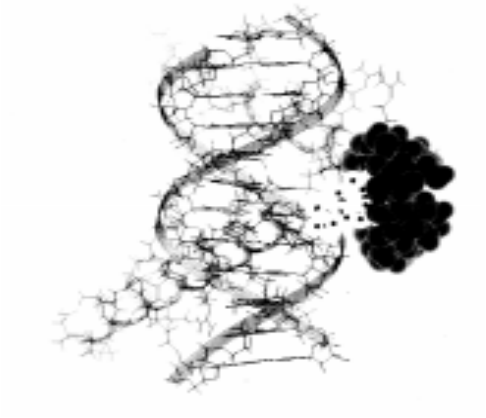

Figure 1. Possible DNA binding Structure of GCN4 basic region peptide dimer with β-cyclodextrin/adamantane dimerization module.

BIOORGANIC CHEMISTRY- Bioactive Chemistry-

Scope or research

The major goal of our laboratory is to elucidate the molecular basis of the activity of various bioactive substances by biochemical, physicochemical, and synthetic approaches. These include studies on the mechanism of sequence-specific DNA cleavage by antitumor or carcinogenic molecules, studies on the DNA recognition of zinc-finger proteins, studies on the cooperative mechanism of DNA binding by using peptide dimers, and model studies on the action of ion channels.

Prof
SUGIURA,Yukio
(D Pharm Sci)

Assoc Prof
FUTAKI, Shiro
(D Pharm Sci)

Instr
MORII, Takashi
(D Eng)

Assoc Instr
OKUNO, Yasushi

Students
AIZAWA, Yasunori (DC)
INOUE, Teruhiko (DC)
ARAKI, Michihiro (MC)
KAMIUCHI, Tatsuya (MC)
SASAKI, Daisuke (MC)
YOKONO, Masanori (MC)
HARA, Yuji (MC)
IMANISHI, Miki (MC)
MATSUSHITA, Keizo (MC)
SAEGUSA, Nana (MC)
SUZUKI, Kazuo (MC)
FUJITANI, Sumiaki (UG)
OMOTE, Masayuki (UG)
KAJI, Tamaki (UG)
MAEDA, Yoshitaka (UG)
MATSUOKA, Mieko (UG)
MIYAGAWA, Naoko (UG)

factors and bacterial repressors often operate as homo- or hetero-dimers, or as higher oligomers. The sequence-specific DNA binding of dimeric protein offers the simplest example for the recognition event including both the protein-DNA and the protein-protein interactions.

We have already developed some model systems that seek to understand the functional roles of dimerization on the sequence-specific DNA binding properties of dimeric proteins. The first model system applies a steric constraint on the two DNA contact regions of the dimeric peptides since formation of the well ordered dimer would determine the relative orientation of each monomer [1, 2, 3]. The position of the recognition helices relative to DNA is constrained by such a quaternary structure formation. Moreover, this positioning would also be dictated by the shape and size of the dimerization module.

DNA Binding Of Peptide Dimers With An Artificial Dimerization Module. Another role for the protein dimerization domain is to modulate the cooperativity of DNA binding by non-covalent protein-protein interactions. The protein-protein interaction plays a key role in both enhancing the selectivity of specific DNA binding and in increasing the sensitivity of equilibrium binding to changes in protein concentrations. To this end, an artificial dimerization module (**Figure 1**) was developed to prove at the atomic level the specific non-covalent interactions involved in protein dimerization. A guest-host inclusion complex comprising of β-cyclodextrin (Cd) and adamantane (Ad) provides a new method to associate oligopeptides in aqueous solution. We found that the GCN4 peptide modified at the C-terminus with an adamantyl group indeed dimerized with another peptide that had the β-cyclodextrin attached to the C-terminus. This peptide dimer further showed specific DNA binding to the native GCN4 site [4].

Sequence-Specific DNA Binding Of Peptide Hetero-Dimers. The hetero-dimerization of transcriptional factors has been shown to play an important role in the gene control events. However, a more tantalizing question would ask whether the heterodimers actually bind non-palindromic DNA sequences. We used the DNA binding regions of two different basic leucine zipper proteins that each recognize unique palindromic DNA sequence upon homodimer formation. Upon heterodimerization through the synthetic dimerization module, the resulting heterodimer recognizes a non-palindromic DNA sequence that consists of two distinct half-sites which correspond to the native protein binding sequences [5].

Cooperative DNA Binding Of Peptide Oligomers. We next ask whether our strategy of artificial dimerization module could extend to a cooperative DNA binding by peptide homo-oligomers [6]. An oligopeptide derived from the basic region of GCN4 was used as the "protein-DNA interaction" domain to address this question. GCN4 binding palindromic sequence without any cooperativity. However, when both β-cyclodexterin and adamantyl group are incorporated into the same peptide chain, binding of the peptide to the tandemly repeated half-site become cooperative. Interestingly, the peptide with both host and guest molecules shows reduced affinity towards the single half-site. The peptide with both host and guest molecules form an intramolecular inclusion complex. Stability of this cyclic peptide is a key factor in reducing the affinity of GAdCd peptides to the isolated half-site. The balance of intramolecular versus intermolecular interactions accounts for binding selectivity. The observed high-selectivity was accomplished by (i) the cooperative nature of DNA binding and by (ii) reducing the stability of the non-specific DNA binding complex. In this vain such strategies employing guest-host complex could be quite useful in designing novel sequence-specific DNA binding peptides.

References

1. T. Morii, M. Shimomura, S. Morimoto and I. Saito, *J. Am. Chem. Soc.* **1993**, *115*, 1150.
2. M. Okagami, M. Ueno, K. Makino, M. Shimomura, I. Saito, T. Morii and Y. Sugiura, *Bioorg. Med. Chem.* **1995**, *3*, 777.
3. T. Morii, Y. Saimei, M. Okagami, K. Makino, Y. Sugiura *J. Am. Chem. Soc*. **1997**, *119*, 3649-3655.
4. M. Ueno, A. Murakami, K. Makino and T, Morii, *J. Am. Chem. Soc*. **1993**, *115*, 12575.
5. M. Ueno, M. Sawada, K. Makino and T. Morii, *J. Am. Chem. Soc*. **1994**, *116*, 11137-11138.
6. T. Morii, J. Yamane, Y. Aizawa, K. Makino and Y. Sugiura, *J. Am. Chem. Soc*. **1996**, *118*, 10011-10017.

APOE Gene ε4 Allele Accelerates the Atrophy of the Inferior Temporal Lobe in Alzheimer's Disease

Seigo Tanaka and Kunihiro Ueda

The apolipoprotein E (*APOE*) gene ε4 allele is a genetic risk factor for late-onset familial and sporadic Alzheimer's disease (AD). The change in size of the whole brain or total ventricular system did not differ significantly among *APOE* genotypes. The patients with ε3/ε4 or ε4/ε4 genotype (ε4+ group), however, exhibited severe atrophy in the inferior temporal lobe, while those with ε3/ε3 genotype (ε4- group) showed mild atrophy. Regional cerebral blood flow (rCBF) in the cerebral cortex, particularly in the temporal lobe, was lower in the ε4+ group than in the ε4- group. These results indicate that possession, and thus expression, of the *APOE* ε4 allele preferentially affects the inferior temporal lobe, encompassing the hippocampus and amygdala, in AD patients.

Keywords : Apolipoprotein E / X-ray CT / MRI / Xe-133 SPECT / Hippocampus / Amygdala

Alzheimer's disease (AD) is the most prevalent neurodegenerative disorder in senescence presenting as progressive dementia. It is pathologically characterized by βA4 amyloid deposition in senile plaque cores and cerebral vessels. In our previous study on Japanese sporadic AD patients [1], we confirmed the association between apolipoprotein E (*APOE*) gene ε4 allele and late-onset AD. In the present study, we approached the issue of how *APOE* genotype affects the progression of the disease by analyzing AD brains with X-ray computed tomography (CT), magnetic resonance imaging (MRI) and Xe-133 single photon emission CT (SPECT) [2].

I. X-ray CT Findings and *APOE* Genotypes

We estimated the whole brain atrophy and ventricular dilatation by using X-ray CT. A comparison between control and AD revealed a significant difference in the size of the cerebral hemispheres and ventricular systems. However, there was no significant difference in these areas among AD subgroups of different *APOE* genotypes. A retrospective study revealed that the progress of cerebral atrophy along the clinical course was not significantly faster in patients with ε3/ε4 or ε4/ε4 genotype than in those with ε3/ε3 genotype. Thus the ε4 allele does not appear to accelerate atrophy of the brain as a whole in the course of the disease.

BIOORGANIC CHEMISTRY — Molecular Clinical Chemistry —

Scope of research

This laboratory was founded in 1994 with the aim of linking (bio)chemical research and clinical medicine. Thus, the scope of our research encompasses the structure, function and regulation of various biomolecules, the pathophysiological significance of bioreactions in relation to human diseases, and the application of molecular techniques to clinical diagnosis and therapy. Our current interest is focused on poly(ADP-ribosyl)ation, nuclear (de)localization of proteins in association with apoptosis, and the molecular etiology of Alzheimer's disease and related disorders.

Prof
UEDA, Kunihiro
(D Med Sc)

Assoc Prof
TANAKA, Seigo
(D Med Sci)

Instr
ADACHI, Yoshifumi
(D Med Sci)

Guest Scholar
BANASIK, Marek (D Med Sci)
Guest Rec Assoc
STROSZNAJDER, Robert (Ph D)
Students
MINAKUCHI, Masayoshi (DC)
MATOH, Naomi (DC)
SHO, Toh (DC)
TAKANO, Emiko (RF)
KITAGAWA, Koichiro (RF)
WILLIAMS, Tyler (RS)
TAKEHASHI, Masanori (RS)

II. MRI Findings and *APOE* Genotypes

We focused further analysis on the inferior temporal lobe, including the hippocampus and amygdala. This region is known to be severely affected in AD and responsible for memory impairment and cognitive decline. MRI allowed clear visualization of this region. As a distinct finding, AD patients with ε3/ε4 or ε4/ε4 genotype exhibited severe atrophy in this region, while those with ε3/ε3 showed milder atrophy (Figure 1). Atrophy of this region accompanied dilatation of the temporal horn of the lateral ventricle. The atrophic change in the inferior temporal lobe was more marked on the medial side, which encompasses the limbic system, such as the hippocampus and amygdala. We analyzed the association of the size of this region with *APOE* genotypes and found a difference among AD subgroups (Figure 2). These results indicate that the *APOE* ε4 allele promotes atrophic change in the brain preferentially in the inferior temporal lobe.

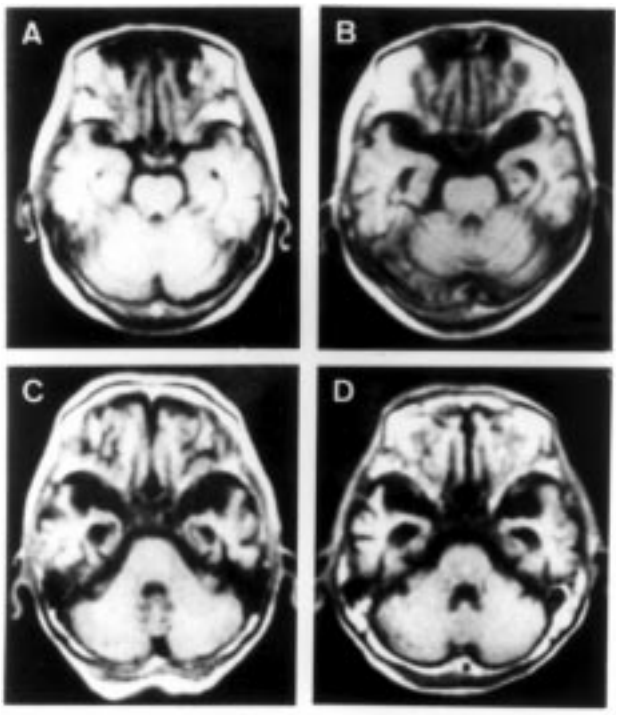

Figure 1. Findings of MRI at the level of the pons. No atrophy was observed in the inferior temporal lobe of the control subject (A). Patients with ε3/ε3 (B), ε3/ε4 (C) and ε4/ε4 (D) genotypes showed mild, moderate or severe atrophy, respectively.

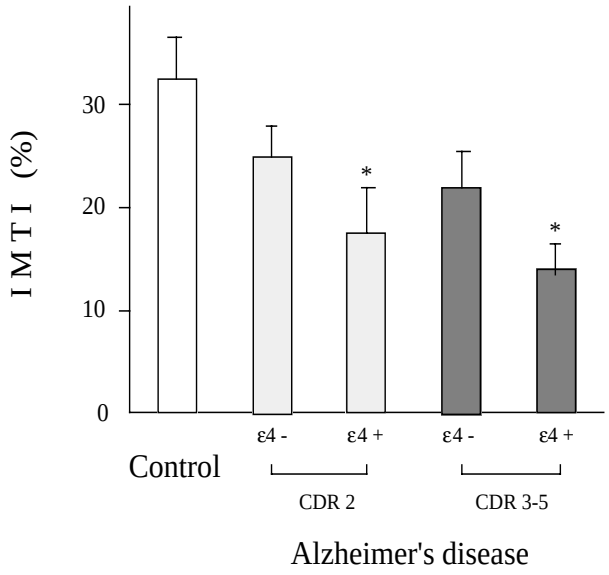

Figure 2. Infero-medial temporal index (IMTI) of control subjects and AD patients. The patients were classified into subgroups of CDR (Clinical Dementia Rating) 2 (moderate) and CDR 3-5 (severe) with *APOE* genotype, ε4- or ε4+.
* $p < 0.05$, as compared with the ε4- group (unpaired *t* test).

III. Xe-133 SPECT Findings and *APOE* Genotypes

In addition to the morphological analysis by X-ray CT and MRI, we assessed a functional change of AD brain by Xe-133 SPECT. The mean value of the regional cerebral blood flow (rCBF) was significantly lower in AD than in control in all cerebral regions except for the occipital lobe. Among the AD subgroups, the rCBF was lower in patients with ε3/ε4 or ε4/ε4 genotype than those with ε3/ε3; the difference was statistically significant in the temporal lobe. In view of the fact that rCBF reflects a functional activity of the brain, the reduction of rCBF indicates an impaired brain function. A reduction of rCBF might be caused by the deposition of vascular amyloid, which was reported to be severe in patients with the *APOE* ε4 allele.

References

1. Kawamata J, Tanaka S, et al., J. Neurol. Neurosurg. Psychiatry 57, 1414-1416 (1994)
2. Tanaka S, Kawamata J, et al., Dement. Geriatr. Cogn. Disord., in press.

Crystal Structure of Asparagine Synthetase Reveals a Close Evolutionary Relationship to Class II Aminoacyl-tRNA Synthetase

Toru Nakatsu, Hiroaki Kato, and Jun'ichi Oda

The crystal structure of *E. coli* asparagine synthetase has been determined by X-ray diffraction analysis at 2.5 Å resolution. The overall structure of the enzyme is remarkably similar to that of the catalytic domain of yeast aspartyl-tRNA synthetase despite low sequence similarity. These enzymes have a common reaction mechanism that implies the formation of aminoacyl-adenylate intermediate. The active site architecture and most of the catalytic residues are also conserved in both enzymes. These enzymes have probably evolved from a common ancestor even though their sequence similarities are small.

Keywords : X-ray crystallography/ Evolution/ Structural similarity/ Aspartyl-tRNA synthetase/ Amino acyl-adenylate intermediate/ Enzymatic reaction

Asparagine synthetase (AsnA) from *E. coli* catalyzes the synthesis of L-asparagine from L-aspartic acid and ATP in the presence of a magnesium ion using ammonia as a nitrogen source [1]. The crystal structure of the *E. coli* AsnA (amino acids 4 - 330) complexed with L-asparagine was determined by X-ray crystallography using multiple isomorphous derivatives at 2.5 Å resolution. The structure exists as a dimer of identical subunits. Each monomer consists of a core eight-stranded, mostly anti-parallel β-sheet that is flanked by two long and eight shorter α-helices. A small lobe composed of a three-stranded β-sheet (Fig. 1) completes the protein fold. L-Asparagine is bound in a rather open and solvent-exposed cleft located on the surface of the eight-stranded β-sheet.

The overall structure of *E. coli* AsnA is remarkably similar to the catalytic domain of yeast aspartyl-tRNA synthetase (AspRS) (Fig. 1). Their core structural elements (175 α-carbon atoms) can be superimposed with a root-mean-square distance of 1.9 Å. This value is similar with that derived from superinposition among class II aminoacyl-tRNA synthetases in which AspRS is involeved.

There is low sequence similarity between *E. coli* AsnA and the catalytic domain of yeast AspRS**,** however, their sequence comparison based on the crystal structure indicates that most of the structurally and catalytically important residues in AspRS are conserved over

MOLECULAR BIOFUNCTION — Functional Molecular Conversion —

Scope of research

Our research aims are to elucidate structure-function relationships of biocatalysts in combination with organic chemistry, molecular biology and X-ray crystallography, and to design and generate a novel biocatalysis for use as a tailor-made catalyst for organic reations. Major subjects are (1) Design and synthesis of transition-state analogue inhibitors of ATP-dependent synthetases, (2) Time-resolved X-ray crystallographic study of glutathione synthetase, (3) X-ray diffraction analysis of tropinone reductase II, luciferase and asparagine synthetase, (4) Design and preparation of catalytic antibodies for chemiluminescence, (5) Overexpression and purification of pyruvate phosphate dikinase from Maize, and (6) Characterization of an activation protein of Pseudomonas lipase.

Prof
ODA, Jun'ichi
(D Agr)

Assoc Prof
HIRATAKE, Jun
(D Agr)

Instr
KATO, Hiroaki
(D Agr)

Assoc Instr
NAKATSU, Toru
(D Agr)

SHIBATA, Hiroyuki (DC)
AOYAGI, Amane (DC)
KATOH, Makoto (DC)
SAWA, Masaaki (DC)
YAMASHITA, Atsuko (DC)
INOUE, Makoto(DC)
IRIE, Takayuki (MC)
OOKI, Yasushi (MC)
KOIZUMI, Mitsuteru (MC)
ENDO, Masaharu (MC)
FUJII, Ryota (MC)
NAKANISHI, Hidemitsu (MC)
TOKUTAKE, Nobuya
(RF, D Agr)

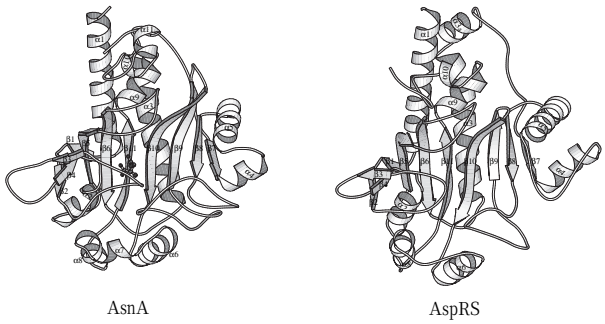

Figure 1. Ribbon diagram ofAsnA from *E. coli* and the catalytic domain of AspRS from *S. cerevisiae*. The ball and stick model in AsnA shows the ligand L-asparagine.

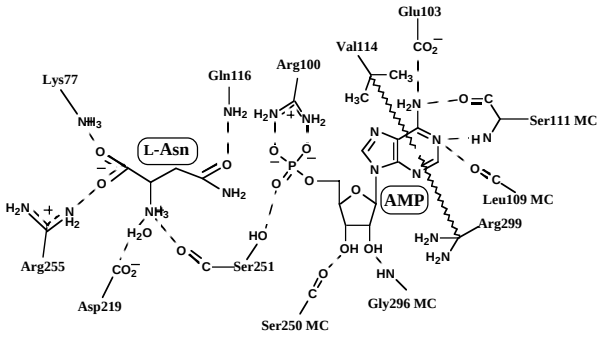

Figure 2. Schematic drawing of the interaction of the ligands and the residues of asparagine synthetase in the catalytic region. Dashed and waved lines correspond to polar and hydrophobic interactions, respectively.

the entire length of AsnA. A proline residue, Pro35, is conserved and seems to be important for subunit-subunit interaction in AsnA as well as in AspRS. There is a small cluster of conserved residues (GGGIG, 292—296). This sequence motif is a part of the highly conserved residues, called motif 3 in the class II aminoacyl-tRNA synthetases, allowing the formation of a cavity that can accommodate bound ATP [2]. In addition, the other conserved residues are also catalytically critical, and interact with the substrates ATP or L-aspartic acid in yeast AspRS. AspRS uses two conserved arginine residues, corresponding to Arg100 and Arg299 in AsnA, to coordinate the α- and γ-phosphates of ATP, respectively. The serine residue of AspRS, which interacts with the α-phosphate of ATP, is conserved as Ser251 in AsnA. Finally, the three AspRS residues which recognize L-aspartic acid by forming a network that interacts with its β-carboxylate group correspond with Lys77, Glu120 and Arg255 in AsnA.

To confirm the function of these conserved residues in the *E. coli* AsnA, the locations of its ligands, L-asparagine and AMP in the three dimensional structure were determined at 2.2 Å resolution (Fig. 2). The crystallographically observed positions of these conserved residues described above are superposable with the related side chains in AspRS. Indeed both enzymes are expected to proceed through the formation of an aminoacyl-adenylate intermediate in their reaction.

The largest differences between AsnA and AspRS were found in their recognition of the reactive carboxyl group and an amino group in the substrate L-aspartic acid (Fig. 3). In the ternary complex structure of *E. coli* AsnA, the amino group of Gln116 interacts with the β-carbonyl group of the bound L-asparagine while the side chain carboxyl group of Asp219 interacts with the amino group of the ligand through a water molecule. Thus, both residues are likely to facilitate the recognition of the substrate L-aspartic acid with a productive binding mode. Structural and mutagenic studies implicated that yeast

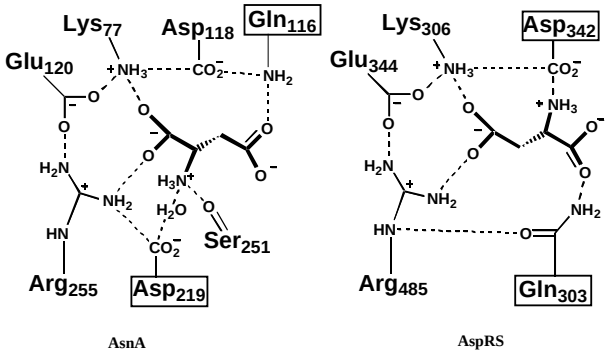

Figure 3. Schematic drawing of the substrate L-aspartic acid binding site of asparagine synthetase and aspartyl-tRNA synthetase.

AspRS utilizes the side chain carboxyl group of Asp342 and the amino group of Gln303 to interact with the amino group and α-carboxyl group of the substrate, respectively. Those glutamine or aspartic acid residues are found at different positions in their crystal structures, however, the role of the glutamine and aspartic acid residues in the substrate recognition are similar.

Crystal structure of *Thermus thermophilus* AspRS [3] has been solved and has provided the finding that it has an extra domain between the helices, aligned with helix 4 and 5 of *E. coli* AsnA, nevertheless the other part of the structure is superimposable with the yeast enzyme. The amino acid sequence of *E. coli* AsnA is less similar to that of *T. thermophilus* or *E. coli* AspRS than that of yeast one. In addition, amino acid sequence of archaean AspRS in the catalytic domain region is similar to the yeast enzyme than *E. coli* one, and there is no additional domain found in the *E. coli* enzyme. These evidence may suggest that this archaean AspRS could be a reliable candidate of the ancestor protein for AsnA.

References

(1) Meister A., *The Enzymes*, **10**, 561-580 (1974)
(2) Cavarelli J., *et al. EMBO J*. **13**, 327-337 (1994)
(3) Delalue M., *et al. J. Mol. Biol.* **234**, 965-974 (1993)

Cysteine Sulfinate Desulfinase, a NIFS-like Protein of *Escherichia coli* with Selenocysteine Lyase and Cysteine Desulfurase Activities: Gene Cloning, Purification and Characterization of a Novel Pyridoxal Enzyme

Nobuyoshi Esaki, Tatsuo Kurihara, Tohru Yoshimura, Kenji Soda, Hisaaki Mihara

Selenocysteine lyase (EC 4.4.1.16) exclusively decomposes selenocysteine to alanine and elemental selenium whereas cysteine desulfurase (NIFS protein) of *Azotobacter vinelandii* acts indiscriminately on both cysteine and selenocysteine to produce elemental sulfur and selenium respectively, and alanine. These proteins exhibit some sequence homology. The *Escherichia coli* genome contains three genes with sequence homology to *nif*S. We have cloned the gene mapped at 63.4 min in the chromosome, and have expressed, purified to homogeneity, and characterized the gene product. The enzyme comprises two identical subunits with 401 amino acid residues (*Mr* 43,238) and contains pyridoxal 5'-phosphate as a coenzyme. The enzyme catalyzes the removal of elemental sulfur and selenium atoms from L-cysteine, L-cystine, L-selenocysteine and L-selenocystine to produce L-alanine. Because L-cysteine sulfinic acid was desulfinated to form L-alanine as the preferred substrate, we have named this new enzyme cysteine sulfinate desulfinase. Mutant enzymes having alanine substituted for each of the four cysteinyl residues were all active. Cys358 corresponds to Cys325 of *A. vinelandii* NIFS, which is conserved among all NIFS-like proteins and catalytically essential is not required for cysteine sulfinate desulfinase. Thus, the enzyme is distinct from *A. vinelandii* NIFS in this respect.

Keywords : Cysteine sulfinate desulfinase/ NIFS/ Pyridoxal phosphate

We found selenocysteine lyase in mammals and bacteria, and purified the enzyme from pig liver (1) and *Citrobacter freundii* (2). The enzyme specifically decomposes L-selenocysteine into L-alanine and elemental selenium; L-cysteine is inert as a substrate. Zheng *et al.* (3) recently demonstrated the function of NIFS protein, which is required for the efficient construction of the Fe-S clusters of nitrogenase in a diazotrophic bacterium *Azotobacter vinelandii*. NIFS catalyzes the same type of reaction as selenocysteine lyase, but acts on both L-

MOLECULAR BIOFUNCTION - Molecular Microbial Science -

Scope of research

Structure and function of biocatalysis, in particular, pyridoxal enzymes, NAD enzymes, and enzymes acting on xenobiotic compounds are studied to elucidate the dynamic aspects of the fine mechanism for their catalysis in the light of recent advances in gene technology, protein engineering and crystallography. In addition, the metabolism and biofunction of selenium and some other trace elements are investigated. Development and application of new biomolecular functions of microorganisms are also studied to open the door to new fields of biotechnology. For example, molecular structures and functions of thermostable enzymes and their application are under investigation.

Prof ESAKI, Nobuyoshi (D Agr)

Assoc Prof YOSHIMURA, Tohru (D Agr)

Instr KURIHARA, Tatsuo (D Eng)

Technician GUTIERREZ, Aldo Francisco

Technician: GUTIERREZ, Aldo Francisco
Guest Research Associate: GALKIN, Andrey; SEONG, Dong-Ho; HONG, Seung-Pyo
Students: CHOO, Dong-Won (DC); KISHIMOTO, Kazuhisa (DC); LIU, Lidong (DC); PARK, Chung (DC); FUCHIKAMI, Yoshihiro (DC); LI, Yong-Fu (DC); MIHARA, Hisaaki (DC); WATANABE, Akira (DC); BAHK, Song-Chul (DC); ICHIYAMA, Susumu (DC); KULAKOVA, Ludmila (DC); UO, Takuma (DC); ENDO, Keiji (MC); NISHIHARA, Mitsuhiro (MC); HIRANO, Yuriko (MC); MAEDA, Masaki (MC); SHIOMI, Kazuo (MC); YOSHIMUNE, Kazuaki (MC); KATO, Shin-ichiro (MC); NISHIYAMA, Tozo (MC); TAKEDA, So (MC); UEDA, Momoko (MC); WATANABE, Tasuku (MC); WEI, Yun-Lin (RS); SUZUKI, Takeshi (RF)

cysteine and L-selenocysteine indiscriminately. The enzyme was named cysteine desulfurase, based on its inherent physiological role.

The nucleotide sequence of the whole *Escherichia coli* genome has been determined (4), and the bacterium appears to contain three *nif*S-like genes. One of the genes located at 57.3 min in the chromosome presumably encodes the NIFS-like protein purified by Flint (5). Not only the amino acid sequence but also the catalytic properties of the enzyme resemble those of *A. vinelandii* NIFS. We have found that the N-terminal amino acid sequence of pig liver selenocysteine lyase is similar to that of *A. vinelandii* NIFS (6). If we assume that *E. coli* contains selenocysteine lyase and that the enzyme resembles NIFS, one or both of the other two *nif*S-like genes may encode selenocysteine lyase(s). Alternatively, the genes may encode new enzymes participating in an unknown metabolism of sulfur or selenium amino acids. We have cloned the *nif*S-like gene mapped at 63.4 min by PCR with the *E. coli* JM109 chromosomal DNA as a template, and investigated the properties of the gene product.

The molecular weight of the homogeneous preparation of the gene product estimated by SDS-PAGE (about 43,000) agreed with the value calculated from the deduced amino acid sequence (43,238). The molecular weight of the purified protein in the native form was estimated to be about 97,000 by gel filtration.

The enzyme showed at pH 7.4 an absorption maximum at 420 nm. Reduction with sodium borohydride resulted in the disappearance of the absorption band at 420 nm with a concomitant increase in the absorbance at 335 nm. The reduced enzyme was catalytically inactive. These results show that the enzyme requires pyridoxal phosphate as a cofactor.

The enzyme resembles selenocysteine lyase and NIFS in that it removes elemental sulfur or selenium from L-cysteine or L-selenocysteine in the reaction. L-Cysteine sulfinic acid acted as the best substrate of the enzyme, and essentially the same amounts of L-alanine and sulfite were produced in the reaction. Maximum activity for the desulfination was found at around pH 8.2 in Tricine-NaOH. We named our new enzyme cysteine sulfinate desulfinase, because the enzyme showed the lowest K_m value and the highest k_{cat} and k_{cat}/K_m values for L-cysteine sulfinic acid .

NIFS has been classified into the same group as aminotransferases of class V (7) and subgroup IV (8), which include serine-pyruvate aminotransferase (EC 2.6.1.51) and phosphoserine aminotransferase (EC 2.6.1.52), on the basis of sequence homology analysis. We have found that NIFS family proteins are classified into two groups, I and II, according to their sequence similarities. Average sequence similarities of cysteine sulfinate desulfinase to Group I and II members were 23 and 37%, respectively.

NIFS of *A. vinelandii* participates in construction of the Fe-S clusters of not only nitrogenase, but also other iron-sulfur proteins such as SoxR and FNR. The NIFS-like enzyme of *E. coli* found by Flint (5) also provides apo dihydroxy-acid dehydratase with a [4Fe-4S] cluster to reconstitute the enzyme *in vitro*. NIFS and the NIFS-like protein from *E. coli*, which belong to Group I, have common characteristics: both contain essential cysteinyl residues at the active sites. The thiol group presumably attacks as a nucleophile the sulfur atom of the substrate, cysteine, to form the intermediate, enzyme-bound cysteinyl persulfide (3, 5). By contrast, no cysteinyl residue of cysteine sulfinate desulfinase is essential for catalysis. The cysteine sulfinate desulfinase-reaction is assumed to proceed through direct release of elemental selenium or sulfur atom from the substrate, selenocysteine or cysteine. It has been assumed that formation of the enzyme-bound cysteinyl persulfide is crucial to deliver sulfur atoms efficiently to iron-sulfur proteins. If this is the case, cysteine sulfinate desulfinase will not be related metabolically to the formation of Fe-S clusters, although sulfur atoms produced from cysteine by the enzyme are probably incorporated into iron-sulfur proteins with low efficiency. The fact that the K_m value of cysteine sulfinate desulfinase for cysteine is high also suggests that cysteine is not the physiological substrate of the enzyme. Whatever the physiological function of cysteine sulfinate desulfinase is, this is the first enzyme in Group II whose catalytic function has been clarified. Other proteins of this group probably have a similar catalytic function to cysteine sulfinate desulfinase. Cloning and expression of the Eco2 gene, the last *nif*S-like gene of *E. coli* mapped at 38.3 min in the chromosome, and characterization of the gene product, are now being studied.

References

1. Esaki, N., Nakamura, T., Tanaka, H., and Soda, K.: *J. Biol. Chem.*, **257**, 4386-4391 (1982)
2. Chocat, P., Esaki, N., Tanizawa, K., Nakamura, K., Tanaka, H., and Soda, K.: *J. Bacteriol.*, **163**, 669-676 (1985)
3. Zheng, L., White, R. H., Cash, V. L., and Dean, D. R:. *Biochemistry*, **33**, 4714-4720 (1994)
4. O'Brien, C.: *Nature*, **385**, 472-472 (1997)
5. Flint, D. H.: *J. Biol. Chem.*, **271**, 16068-16074 (1996)
6. Beynon, J., Ally, A., Cannon, M., Cannon, F., Jacobson, M., Cash, V., and Dean, D. R.: *J. Bacteriol.*, **169**, 4024-4029 (1987)
7. Grishin, N. V., Phillips, M. A., and Goldsmith, E. J.: *Protein Sci*, **4**, 1291-1304 (1995)
8. Mehta, P. K., and Christen, P.: *Eur. J. Biochem.*, **211**, 373-376 (1993)

Molecular Mechanism of Myosin Assembly

Tohru Akutagawa

Myosin of muscle (skeletal muscle, smooth muscle or cardiac muscle) has an intensive tendency to assemble with the axial staggers of 14.3 and 43 nm under the physiological conditions of ionic strength 0.05–0.20 M and pH 6–8. For the molecular mechanism of self-assembly by the myosin molecule, we first reported that the myosin molecule has a specific region which is responsible for the self-assembly. Later, Nyitray *et al*. showed that this region is located near the COOH terminus of the rod segment of the myosin molecule. The molecular mechanism of myosin assembly has been studied in more detail in order to elucidate how this region is related to axial stagger of 43 nm.

Key words ; Light meromyosin/ Axial stagger/ Solubility determining region

The myosin molecule of muscle cell is composed of two heavy chains and four light chains. Each heavy chain has an NH_2-terminal globular head with chain mass of ~95 kDa and a COOH-terminal long fibrous portion folded into an α-helix. The two α-helices wrap around each other to construct the α-helical coiled-coil known as the myosin tail or the myosin rod. It is well known that the myosin rod amino acid sequence is highly repetitive and has the characteristics of α-helical coiled-coil [1]. Myosin self-assembly results from interactions between the rods. Whether the myosin molecule prefers an assembled and polymerized form or a soluble form is strongly dependent on both ionic strength and pH [2]. The polymerized form of myosin *in vivo* is known as thick filament. The thick filament, together with the actin-containing thin filament, forms the smallest structural unit for tension generation in muscle [3]. In thick filament, myosin molecules assembled in a parallel arrangement are obliged to cause the axial staggers of 14.3 and 43 nm [4] at the rod segments of adjacent myosin molecules. Myosin heads projecting away from the thick filament surface can act as movable cross-bridges between the thick and thin filaments [5]. The axial spacings between heads on the filament surface are 14.3 and 43 nm, and these spacings result from the axial staggers between the rods.

McLachlan *et al*. reported excellent results on the molecular mechanism of myosin to explain how these axial staggers are caused between two parallel rods by an analysis of the amino acid sequence of the rod portion of a myosin heavy chain and by a computational analysis of electrostatic interactions between the two rods [1]. The important points of their conclusions are that the periodic charge distributions in the amino acid sequence of the rod are in good agreement with these axial staggers and that the electrostatic interactions between the rods play a crucial role in causing the axial staggers. However, what regions of the rod are crucial for the axial stagger of 43

MOLECULAR BIOLOGY AND INFORMATION – Biopolymer Structure –

Scope of research

Our research aims are to elucidate structure-function relationships of biological macromolecules, mainly proteins, by using physicochemical methods such as spectroscopic and X-ray diffraction methods. The following attempts have been mainly made in our laboratory for that purpose. (1) Peptide secondary or supersecondary structures in aqueous or hydrophobic environments are studied to get a principle of protein architecture, employing various spectroscopic methods. (2) X-ray diffraction studies on protein structures in crystal and in solution are carried out by crystallographic and/or small-angle X-ray scattering techniques to elucidate structure-function relationships of proteins. (3) Molecular mechanism for myosin assembly is studied by proteolytic method, electron microscopy, and computer analysis of the amino acid sequence.

Prof TAKAHASHI, Sho (D Sc)

Assoc Prof HATA, Yasuo (D Sc)

Instr HIRAGI, Yuzuru (D Sc)

Instr FUJII, Tomomi

Instr AKUTAGAWA, Tohru

Students:
MATSUMOTO, Tomoharu (DC)

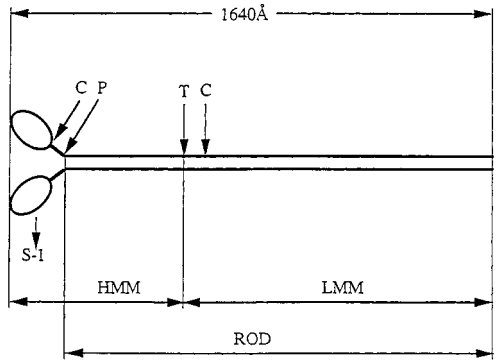

Figure 1. Model picture of myosin molecule. C→, T→, and P→ are chymotryptic, tryptic, and papainic cleavage sites, respectively. HMM is heavy meromyosin which is composed of the head and one-thirds of the rod in the myosin heavy chain, and LMM corresponds to the COOH-terminal two-thirds of the rod. The myosin head is called S-1.

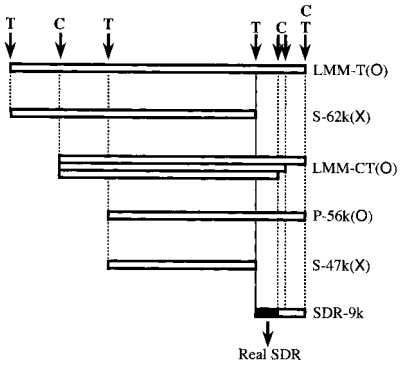

Figure 2. Positional relationships between proteolytic cleavage sites and fragments in LMM-T. The chain masses of fragments LMM-T S-62k, LMM-CT, P-56k, S-47k and SDR-9k were determined to be 70, 62, 62, 56, 47 and 9 kDa, respectively. The black portion in the figure shows the position of SDR. The symbols ((O) and ((×) show whether fragments can assemble with the axial stagger of 43 nm or not, respectively. The former fragments have SDR, but the latter lack it. Therefore, SDR is located near the COOH terminus of the myosin rod, and the existence of SDR in fragments is crucial for myosin assembly.

nm has not been clarified yet.

It is well known that myosin assembly occurs within the COOH-terminal two-thirds of the rod (light meromyosin or LMM). The LMM gene of rabbit leg muscle is cloned to give the LMM protein of the sequenced 676 amino acid residues [6]. However, LMMs obtained by proteolytic cleavage of myosin [7] have often been used for the study of LMM assembly, because the proteolytic method permits the isolation of different LMMs in length by selection of enzymes used [8]. LMMs produced by the proteolytic cleavage can also cause the axial staggers of 14.3 and 43 nm when they assembles by themselves, and produce LMM crystals [9]. It should be noted, however, that LMMs obtained by proteolytic cleavage are necessarily shorter than the recombinant LMM of 676 residues because LMM has some cleavage sites in the COOH-terminal portion. Akutagawa *et al*. first reported that the LMM molecule has a region which is responsible for the LMM assembly [8]. Later, Nyitray *et al*. showed that this region is located near the COOH terminus of the myosin rod [10], and called this region the solubility determining region (SDR). Their group and our group independently showed that the lack of this region induces the myosin molecule to cause neither the assembly nor the aggregation. SDR is probably related to molecular mechanism of the axial staggers of 14.3 and 43 nm because the myosin assembly accompanies these axial staggers.

Here we show that SDR is located near the COOH terminus of the LMM molecule by using LMM-T which was prepared by tryptic split of myosin. Fig. 1 shows a model picture of myosin molecule of skeletal muscle and a relationship between the segments in the myosin molecule. Fig. 2 shows the chain mass relationship among the fragments obtained from LMM-T by proteolytic cleavage using trypsin and chymotrypsin. Here LMM-CT is obtained by chymotryptic cleavage of LMM-T. SDR is obtained by enzymatic splits. As shown in Fig. 2, the chain mass of SDR-9k is determined to be 9 kDa corresponding to the difference of chain mass between the precipitated fragment P-56k and the soluble fragment S-47k. The real chain mass of SDR shown as the black region in Fig. 2 is smaller than 9 kDa, because LMM-CT contains a small number of LMMs which are able to assemble in spite of difference in COOH terminus. Characterization of the real SDR is essential to know the molecular mechanism for the axial stagger of 43 nm, because the charge distributions in SDR possibly contributes to electrostatic interactions between parallel two rods. The axial stagger of 43 nm can not be caused by the single SDR per one rod when this stagger is caused between two parallel rods by using SDR. Plural SDRs for each rod are required to induce the stagger between the two parallel rods. In order to elucidate whether an axial stagger determining region exists in the rod, we have recently isolated LMM whose length is thought to be shortest to cause the axial stagger of 43 nm, and are characterizing the shortest LMM.

Reference

1. McLachlan A D and Karn J, *Nature*, **279**, 226–231 (1982).
2. Davis J S, *Annu. Rev. Biophys.*, **17**, 217–239 (1988).
3. Huxley H E and Hanson J, *Nature*, **173**, 973–976 (1954).
4. Offer G and Elliot A, *Nature*, **271**, 325–329 (1978).
5. Huxley H E, *Scientific Industrial and Medical Aspect*, **1**, 71–95 (1979).
6. Maeda K, Sczakiel G and Wittinghofer A, *Eur. J. Biochem.*, **167**, 97–102 (1983).
7. Szent-Gyorgyi A G, *Arch. Biochem. Biophys.*, **42**, 305–320 (1953).
8. Akutagawa T and Ooi T, *J. Biochem. (Tokyo)*, **92**, 999–1007 (1982).
9. Yagi N, and Offer G W, *J. Mol Biol.*, **151**, 467–490 (1981).
10. Nyitray L, Mocz G, Szilagyi L and Balint M, *J. Biol. Chem.*, **258**, 13213–13220 (1983).

Structural Characterization of the *virB* Operon of the Hairy-root-inducing Plasmid pRiA4

Yajie Liang, Takashi Aoyama, and Atsuhiro Oka

The virulence (*vir*) loci of the hairy-root-inducing plasmid pRiA4 are essential for pathogenicity of its host *Agrobacterium rhizogenes* A4. We have now determined the nucleotide sequence of *virB* region (9,926 bp). It was found that the *virB* operon is composed of 11 genes (*virB1* to *virB11*), whose products mostly appear to be associated with the cell membrane. A novel structural characteristic is frequent overlapping between the translation termination and initiation codons of the adjacent genes This is indicative of fine tuning of relative translation frequencies for each VirB protein, supporting the view that VirB multisubunit complexes provide facilities for T-DNA transfer at the bacterial cell membrane.

Keywords: *Agrobacterium*/ Membrane protein/ Plant-microbe interaction/ Virulence regulon

The agropine-type hairy-root-inducing plasmid pRiA4 confers tumorigenic symptoms at wound sites on a wide variety of dicotyledonous plants upon infection by its host bacterium, *Agrobacterium rhizogenes* A4. Tumorigenesis is caused by the transfer of a defined DNA segment (T-DNA) on the plasmid from a bacterium into the plant nuclear genome and subsequent constitutive synthesis of plant phytohormones directed by the T-DNA. T-DNA transfer requires the 25 bp imperfect direct repeats at both extremities of T-DNA as *cis* factors, and the virulence (*vir*) loci outside of T-DNA as *trans* factors. The *vir* genes constitute the six transcriptional units, *virA*, *virB*, *virC*, *virD*, *virE*, and *virG*. Their expression is tightly regulated as a regulon by both the *virA* and *virG* gene products, being inducible by plant phenolic compounds such as acetosyringone. Nucleotide sequences of all of the *vir* loci, except the largest *virB* operon, have been determined by our laboratory, and compared with those of tumor-inducing plasmids harbored by *A. tumefaciens* (for reviews, see ref. 1 and 2). Here, we report the nucleotide sequence of the *virB* operon together with its flanking regions, thus completing sequencing of the entire *vir* loci of pRiA4.

The *vir* loci of pRiA4 have been identified with transposon (Tn*3*-HoHo1) insertion mutations that lead to defects in pathogenicity, and the *vir* gene organization examined from the similarity with that of the tumor-inducing plasmid pTiA6 by hybridization experiments. As a result, it has been found that pRiA4 *virB* is located in a region corresponding to the *Hin*dIII-10, -8 and -32b frag-

MOLECULAR BIOLOGY AND INFORMATION — Molecular Biology —

Scope of research

Attempts have been made to elucidate structure-function relationships of genetic materials and various gene products. The major subjects are mechanisms involved in signal transduction and regulation of gene expression responsive to environmental stimuli, differentiation and development of plant organs, and plant-microbe interaction. As of December 1997, study is being concentrated on the roles of homeo domain proteins, MADS box proteins, and DDK response regulators of higher plants in developmental and signal transduction processes.

Prof
OKA, Atsuhiro
(D Sc)

Assoc Prof
AOYAMA, Takashi
(D Sc)

Instr
GOTO, Koji
(D Sc)

Students:
TSUKUDA, Mayumi (DC)
HOMMA, Takashi (DC)
OHGISHI, Maki (DC)
SAKAI, Hiroe (DC)
LIANG Yajie (MC)
UEDA, Yumi (MC)
YANO, Hiroyuki (MC)
OHASHI, Yohei (MC)

ments. These three fragments were purified from a cosmid clone (pBANK1329) covering the DNA region from the *Hin*dIII-23b to *Hin*dIII-25 fragments (3), and then separately inserted into pUC18. With the resulting recombinant plasmids, progressive deletion derivatives were constructed by either ejecting appropriate restriction fragments or recloning smaller fragments. Each of the inserted DNA segments was sequenced from either side for both strands by an ABI Prism 377 DNA sequencer. In addition, adjacent restriction fragments actually being contiguous was confirmed by sequencing overlapping fragments with appropriate custom primers. By arranging overlapping sequences of both strands, the nucleotide sequence from the *Eco*RI site downstream of *virA* to the *Dra*I site upstream of *virG* was deduced (9,926 bp; see http://molbio.kuicr.kyoto-u.ac.jp/virb).

The occurrence of initiation and termination codons for protein synthesis in all possible reading frames suggests that the *virB* locus carries information to code for 11 polypeptides of 26.4 kDa, 12.3 kDa, 11.7 kDa, 87.7 kDa, 23.1 kDa, 31.8 kDa, 5.9 kDa, 26.2 kDa, 32.2 kDa, 40.3 kDa, and 38.2 kDa. Each of the presumed coding frames was named *virB1* to *virB11*, respectively, all of which were accompanied by a potential ribosome-binding sequence (4). The initiation codon for all *virB* genes except *virB1* was the conventional AUG codon. However, *virB1* appeared to use a rare initiation codon AUC. This was not a result of base substitution occurred during cloning experiments because direct sequencing of the corresponding region of pRiA4 DNA gave an identical result. The transcription start site is located 65 bp upstream of the *virB1* translation initiation site (5). There are helically phased vir box sequences essential for VirG binding and the promoter -10 region, though no typical promoter -35 region is present (5). These structural features strongly support all of *virB1* to *virB11* being actually structural genes and constituting an operon.

A novel structural characteristic of the *virB* operon is frequent overlappings of the translation termination codon of the preceding gene with the translation initiation codon of the following gene. Those from *virB1* to *virB4* overlap for 1 bp, and those from *virB8* to *virB10* do for 2 bp. Furthermore, in case of *virB7* and *virB8*, the coding region itself (11 bp) is overlapped with each other. Such kinds of overlapping for compacting have never been found in other *vir* operons.

Computer analyses of amino-acid sequences of each VirB suggest the presence of N-terminal signal sequences in VirB1, VirB5, VirB7, and VirB9, and of the transmembrane regions in VirB2, VirB3, VirB6, VirB8, VirB9, and VirB10. Since the smallest VirB7 protein contains a putative target sequence for signal peptidase II, the enzyme involved in lipoprotein recognition and processing, it appears to associate with lipid. Besides, VirB4 and VirB11 are presumed to be the ATP-binding proteins.

It is well known that *vir* regions of pRi and pTi are exchangeable without loss or alteration of the pathogenic specificity, and DNA fragments carrying *vir* of a given plasmid hybridize with those of other plasmids (3). Therefore, the pRiA4 *virB* operon should structurally be close to those of pTi's, as already shown for the other *vir* genes of pRiA4 (3). Indeed, both the gene organization in the pRiA4 *virB* operon and the amino-acid sequence of each VirB protein were exceedingly similar to those of pTi's at the nucleotide sequence level. The identities of amino-acid residues between pRiA4 and pTiC58 VirB's and between pRiA4 and pTiA6 VirB's occurred at 90%-95% and at 70%-92% residues, respectively. Also the overlapping feature is completely identical with that of pTiC58 and close to that of pTiA6. Conservation of the overlapping feature seems to reflect the control of translation initiation frequency relative to that of the preceding gene, providing the exact molar ratio of synthesized VirB proteins. This view supports the idea that VirB proteins make multisubunit complexes at the bacterial cell membrane, presumably giving facilities for the passage of T-DNA from a bacterium to a plant cell.

The similarity scores of VirB between pRiA4 and pTiC58 (compatible combination) are significantly higher than those between pTiA6 and pTiC58 (incompatible combination), whereas the similarity scores between pTiA6 and either pRiA4 or pTiC58 are comparable. These are consistent with the view that the *vir* regions of the three plasmids have evolved from a common ancestral *vir* gene set from which pTiA6 *vir* was initially separated. Since plasmids belonging to a single incompatibility group are usually more cognate to each other than those involved in different incompatibility groups, functional domains of pRi and pTi, at least those determining virulence on plants (*vir* and T-DNA) and autonomous replication and incompatibility (*ori*/*inc*), appear to have been shuffled during evolution of these plasmids.

References

1. Hooykaas PJJ, *Plant Mol. Biol.*, **13**, 327-336 (1989).
2. Oka A, *Tanpakushitsu-Kakusan-Kouso*, **40**, 1010-1021 (1995).
3. Hirayama T, Muranaka T, Ohkawa H, and Oka A, *Mol. Gen. Genet.*, **213**, 229-237 (1988).
4. Shine J and Dalgarno L, *Proc. Natl. Acad. Sci. USA*, **71**, 1342-1346 (1974).
5. Aoyama T, Takanami M, and Oka A, *Nucl. Acids Res.*, **17**, 8711-8725 (1989).

Developing Molecular Interaction Database and Searching for Similar Pathways

Shuichi Kawashima, Toshiaki Katayama and Minoru Kanehisa

We have developed a database named BRITE, which contains knowledge of interacting molecules and/or genes concering cell cycle and early development. Here, we report an overview of the database and the method of automatic search for functionally common sub-pathways between two biological pathways in BRITE.

keywords: Knowledge-base/ Cell cycle/ Development/ Graph theory/ WWW

All known biological processes in living organisms are maintained and carried out by various molecular/ genetic interactions. While a large amount of knowledge on metabolic and regulatory pathways that has been accumulated is quite valuable in theoretical or computational studies for understanding biological systems, the knowledge mainly exists in research papers or reviews which are unsuitable for computational analyses. Besides, the existing molecular biology databases such as GenBank, EMBL, SWISS-PROT, and PDB, focus on representing the information about DNA, RNA or protein molecules and do not fully represent molecular interactions. Thus, we have initiated efforts to collect the knowledge in a different format and construct a new database of molecular interactions. In view of the surprising functional similarities that have been found in pathways among various species, the knowledge-base such as BRITE would lead to a new research area for analysis of biological networks.

The knowledge-bases concerning metabolic pathways have already been developed, such as KEGG, EcoCyc, and WIT, and proved to play important roles in bioinformatics. We are constructing a new knowledge-base named BRITE [1] (Biomolecular Relations in Information Transmission and Expression) which focuses on regulatory pathways in various biological processes. BRITE is a flat-file collection of entries, where each entry contains a relation of two molecules. The data representation of molecular relations in BRITE is based on KEGG [2], where the concept of 'biological links' is represented as follows:

organism:gene1 -> organism:gene2

This scheme can also be regarded as the following:

organism:relation

This is the basic component of an entry in BRITE.

MOLECULAR BIOLOGY AND INFORMATION — Biological Information Science —

Scope of research

This laboratory aims at developing theoretical frameworks for understanding the information flow in biological systems in terms of genes, gene products, other biomolecules, and their interactions. Towerd that end of a new deductive database is being organized for known molecular and genetic pathways in living organisms, and computational technologies are being developed for retrieval, inference and analysis. Other studies include: functional and structural prediction of proteins from sequence information and development of sequnece analysis tools.

Prof
KANEHISA, Minoru
(D Sc)

Instr
GOTO, Susumu
(D Eng)

Instr
OGATA, Hiroyuki

Students:
TOMII, Kentaro (DC)
SUZUKI, Kenji (DC)
KIHARA, Daisuke (DC)
KAWASHIMA, Shuichi (DC)
PARK, Keun-joon (DC)
HATTORI, Masahiro (DC)
BONO, Hidemasa (DC)
IGARASHI, Yoshinobu (MC)
KATAYAMA, Toshiaki (MC)
TAKAZAWA, Fumi (MC)
TANIGUCHI, Takeaki (MC)
NAKAO, Mitsuteru (MC)

Research Fellow:
SATO, Kazushige (RF)
SUGIYAMA, Yukiteru (D Agr)

Each entry in the BRITE database contains the ENTRY and DEFINITION lines at the top. The ENTRY line holds a unique identifier and the summary of each entry is described in the DEFINITION line. The core section is RELATION, which describes the molecular interaction in the form of a binary relation. The RELATION section consists of three items: FROM for the regulating molecule, TO for the regulated molecule, and MESSAGE for the relation between two molecules, such as 'transcriptionally activate/repress', 'phosphorylate', and 'bind'. BRITE does not store detailed information of molecules that appear in the entry, but provides links to other existing databases for such information, including GENES, GenBank, and SWISS-PROT. The cross-reference information to other databases is described in the FACTORS section. The bibliographic information of references associated with the entry is described in the REFERENCE section with links to Medline.

Originally, molecular interaction data concerning only cell cycle controls were accumulated in BRITE. Now we collect data concerning developmental pathways as well. At present BRITE contains data about cell cycles of *S. cerevisiae*, *S. pombe* and *H. sapiens* and early developments of *D. melanogaster* and *X. laevis*. The amount of data in BRITE is shown in Table 1.

The BRITE database is available through the GenomeNet WWW service at the following address:

http://www.genome.ad.jp/brite/brite.html

We provide two facilities for data retrieval. One is retrieving an entry through the clickable map. The user can easily retrieve entries by clicking on a molecule or an interaction on the graphical pathway maps implemented in WWW. The other is by keyword search using the DBGET system. DBGET is the integrated database retrieval system with two basic commands, bfind and bget, to search and extract entries from a wide range of molecular biology database. The keyword search using bfind command is made against the DEFINITION line in BRITE. The result of the search is a list of entry names found, from which an entry can be selected to view the content. When the user already knows the entry identifier, it can be retrieved simply by using bget command. If the user has the amino acid sequence data for the molecular interaction of interest, a homology search can be performed against the BRITE database using the sequence as a query. This is especially useful when searching similar interactions and similar pathways in different species or in different biological processes.

Table 1. The number of entrys in BRITE

	Organism	Number of entries
Cell cycle	*S. cerevisiae*	64
	S. pombe	65
	H. sapiens	102
Development	*D. melanogaster*	80
	X. laevis	15

In order to automatically find functionally similar sub-pathways in the maps of BRITE we have developed a method similar to the one utilized for recognizing common structural fragments among chemical compounds [3]. By regarding each molecule and relation in a map as a vertex and edge, respectively, a pathway in BRITE is represented as a graph. Because the method introduces relations among all molecules irrespective of whether they exist or not in the database, the graph representing a pathway is defined as an edge-weighted complete graph. Then we construct a docking graph from two edge-weighted complete graphs. Searching for an edge-weighted maximal common subgraph for two complete graphs is equivalent to searching for a clique (complete subgraph of graph) in this docking graph.

Acknowledgments

This work was supported in part by a Grant-in-Aid for Scientific Research on Priority Areas 'Genome Science' from the Ministry of Education, Science, Sports and Culture in Japan. The computation time was provided by the Supercomputer Laboratory, Institute for Chemical Research, Kyoto University.

References

1. Tsukamoto N and Kanehisa M, Proc. Genome Informatics Workshop 1995, 158-159 (1995).
2. Kanehisa M, Trends Biochem. Sci., 22, 442-444 (1997)
3. Takahashi Y, Maeda S and Sasaki S, Anal. Chim. Acta, 200, 363-377 (1987).

Development of Compact Proton Synchrotron Dedicated for Cancer Therapy

Akira Noda, Yoshihisa Iwashita, Akio Morita, Toshiyuki Shirai, Makoto Inoue, Kazuo Hiramoto*, Jun-ichi Hirota, Masahiro Tadokoro** and Masatsugu Nishi***

A compact proton synchrotron has been developed to be dedicated for cancer therapy. A combined function lattice and an untuned RF cavity have been adopted to realize compactness of needed cost and operation manpower. With the present design, the control of the synchrotron is also expected to become very easy for daily operation.

Keywords : Proton Cancer Therapy/ Combined Function Synchrotron/ Untuned RF Cavity / Solid State Amplifier/ Multifeed Coupling

Recently radiation cancer therapy has been paid attention from the point of view of *quality of life of the patient*, because it is superior to preserve the shape and function of the human body in addition to its merit of fairly mild load to the patient. Further charged particle therapy has such a merit as can concentrate the dose to the tumor due to the presence of Bragg-peak.

In our country, University of Tsukuba has been treating patients by proton therapy and realized a remarkable results especially in liver cancer. National Institute of Radiological Sciences has started treatment with carbon beam since 1994. In addition, East Hospital of National Cancer Center is now constructing a proton therapy facility and Hyogo prefecture is constructing cancer therapy facility with use of both proton and carbon beams. The number of patients to be treated by these facilities, however, is rather limited. Every facility can only treat 1000 patients per year at maximum and usually such number is much smaller. This limits the wide use of the benefits of charged particle therapy, because more than 30,000 patients per year need such therapy even if we only

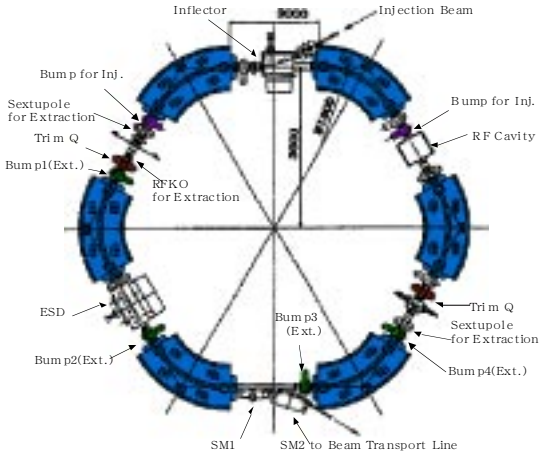

Figure 1. Lattice of the combined function proton synchrotron dedicated for cancer therapy.

NUCLEAR SCIENCE RESEARCH FACILITY — Particle and Photon Beams —

Scope of research

Particle and photon beams generated with accelerators and their instrumentations both for fundamental research and practical applications are studied. The following subjects are being studied: Beam dynamics related to space charge force in accelerators: Beam handling during the injection and extraction processes of the accelerator ring:radiation mechanism of photon by electrons in the magnetic field:Interactions in the few-nucleon systems: R&D to realize a compact proton synchrotron dedicated for cancer therapy: Control of the shape of beam distribution with use of nonlinear magnetic field: and Irradiation of materials with particle and photon beams.

Prof
NODA, Akira
(D Sc)

Assoc Prof
KAKIGI, Shigeru
(D Sc)

Instr
SHIRAI, Toshiyuki

Techn
TONGUU, Hiromu

Lecturer(part-time):
YAMADA, Satoru(Head; H.E. Acc. Div., National Institute of Radiological Sciences)
Students:
IKEGAMI, Masanori (DC)
KANDO, Masaki(DC)
SUGIMURA, Takashi(DC)
KIHARA, Takahiro (DC)
FUJIEDA, Miho (DC)
URAKABE, Eriko (MC)
MORITA, Akio (MC)
NISHI, Masatsugu(RF, D Eng)

** Power &Industrial Systems R&D Division, Hitachi Ltd., **Hitachi Works, Hitachi Ltd.*
This work is supported by a Grant-in-Aid for scientific Research from Ministry of Education, Science, Sports and Culture of Japan.

Figure 2. Fabricated untuned cavity.

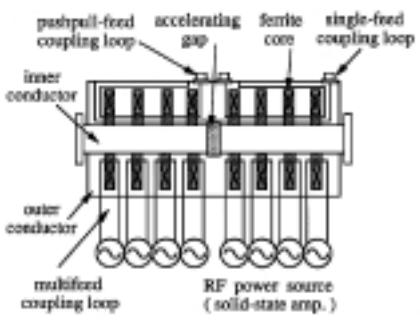

Figure 3. Schematic diagram of the fabricated untuned cavity. The cavity consists of two quater-wavelength coaxial resonators with a single accelerating gap.

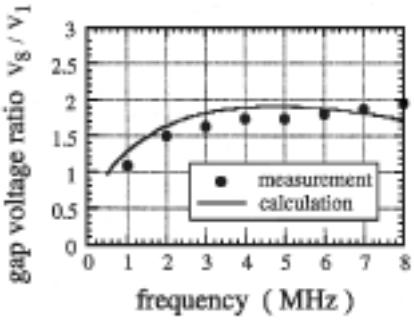

Fig.4. Frequency dependence of the gap voltage relation between multifeed coupling (V_8) and single-feed coupling(V_1).

consider the area west to Kinki district. From this point, it is required to establish a good reference design of a commercially available compact proton synchrotron which has a size acceptable for a hospital having the role as the center of each prefecture. We are proposing a combined-function proton synchrotron illustrated in Fig.1[1].

The required acceleration voltage per turn in a synchrotron is proportional to the product of time derivative of magnetic field strength, the circumference and the radius of curvature. For the presented compact proton synchrotron, only a few hundreds volts are needed as the accelerating voltage. Such a low voltage can be generated with an untuned cavity as shown in Fig.2 with a solid state amplifier, whose output impeadance is 50Ω[2]. The untuned cavity does not require complicated bias-winding for the resonant frequency tuning. In order to reduce the power reflection at the power feeder of the untuned cavity and increase the efficiency of power utilization, a new power feeding method called multifeed coupling has been invented, which is illustrated in Fig. 3[3]. By this feeding method, the power utilization efficiency is increased and thus the realized voltage at the accelerating gap has been increased as shown in Fig. 4 compared with the conventional method.

The other merit of combined function lattice is that the magnet current tracking control between power supplies for dipole and quadrupole magnets is not needed and the operation becomes very easy once a good design has been established. Because a combined function lattice has less adjustability, the magnet should be designed carefully before fabrication. This is the main reason that this type has not yet widely applied for medically dedicated machine. In order to demonstrate a good design, we are constructing a model magnet for the combined function synchrotron. Based on the magnetic field calculation with use of the three-dimensional code TOSCA, a real size magnet for the combined function lattice shown in Fig. 1

Figure 5. Configuration of the combined-function magnet. Its three dimensional magnetic field distribution is calculated with the computer code TOSCA.

is fabricated. In the iron pole, several slots are located as illustrated in Fig. 5 so as to realize good field property in the wide excitation range by equalizing the magnetic flux density in the iron pole[4]. The betatron tunes are evaluated for various excitation levels utilizing the calculated field distribution by TOSCA as shown in Fig.6. It is expected that lower order resonances up to sixth order can be well kept away from the operating point.

References

1. A. Noda et al., Proc. of the 11th Symp. on Accelerator Science and Technology, 314 (1997)

2. K. Saito et al., Nucl. Instrum. & Meth. **A401**, 133(1997)

3. Y. Iwashita, Jpn. J. Appl. Phys. **36**, L727 (1997)

4. M. Tadokoro et al., Proc. of PAC 1997, Vancouver,

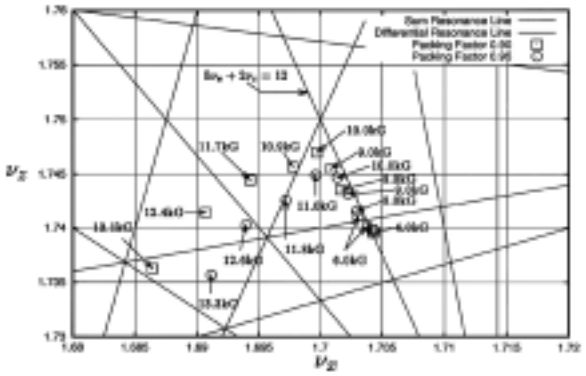

Figure 6. Operating points for various excitation levels estimated from three dimensional field calculation.

Study of RFQ Accelerating Structures Based on Multi-conductor Resonators

Valeri Kapin, Makoto Inoue, Yoshihisa Iwashita and Akira Noda

An analytical method which treats the radio-frequency quadrupole (RFQ) accelerating structures based on 4-rod configuration of electrodes has been developed. A new electric-field potential function in RFQ-channel with 4-rod configuration of the electrodes has been formulated for analytical study of effects of the intrinsic field distortion. Modifications of 4-rod RFQ structure and a new multiple-beam RFQ structure have been suggested.

Keywords : Linear accelerator (linac)/ Beam dynamics/ Resonance/ Resonator/ Multiple-beam RFQ

Radio-frequency quadrupole (RFQ) accelerating structures based on 4-rod configuration of electrodes are widely used in linear accelerators. We have developed a theoretical model of the RFQ resonators with 4-rod configurations [1-5]. It advances a conceptual design study of both beam dynamics and resonance structure in the 4-rod RFQ or multi-rod RFQ system.

The general concept of the 4-rod RFQ structures is shown in Fig.1. The 4-rod RFQ resonator consists of four longitudinal electrodes connected with a tank by transverse conducting stems. The resonator is simulated as a set of four conductor shielded transmission lines (4CSTL) connected in a cascade manner by coupling network (see Fig. 2). It was shown [1,3], that any field in a 4-rod RFQ resonator is expressed as a superposition of four normal modes propagating in the 4CSTL. Figure 3 shows the E-line patterns of four normal modes.

Qualitative analysis of 4-rod RFQ resonators has been done [3]. The examples to reconstruct the RFQ

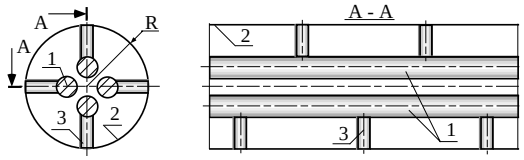

Figure 1. General concept of the 4-rod RFQ structure: 1 is a quadrupole electrode; 2 is a tank; 3 is a transverse stem.

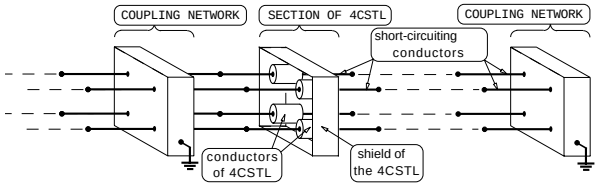

Figure 2. Block diagram of the equivalent circuit of an RFQ resonator having a 4-rod configuration of the electrodes.

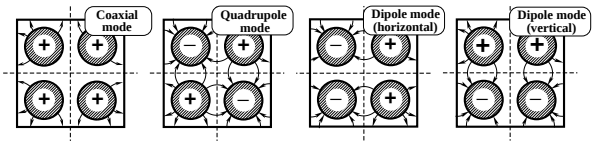

Figure 3. The E-line patterns of normal modes.

NUCLEAR SCIENCE RESEARCH FACILITY — Beams and Fundamental Reaction —

Scope of research

Particle beams, accelerators and their applications are studied. Structure and reactions of fundamental substances are investigated through the interations between beams and materials such as nuclear scattering. Tunable lasers are also applied to investigate the structure of unstable nuclei far from stability and to search for as yet unknown cosmological dark-matter particles in the Universe.

Prof
INOUE, Makoto
(D Sc)

Assoc Prof
MATSUKI, Seishi
(D Sc)

Instr
IWASHITA, Yoshihisa
(D Sc)

Instr
OKAMOTO, Hiromi
(D Sc)

Guest Research Associate
KAPIN, Valeri (D Sc)

Students:
YOSHIMURA, Tadahiko (DC)
TADA, Masaru (DC)
KISHIMOTO, Yasuhiro (DC)
AO, Hiroyuki (DC)
SHIBATA, Masahiro (MC)

fields from the results of the normal mode analysis have been presented in [2, 3]. They are in good agreement with numerical calculations done with MAFIA code.

Formulas for the resonance frequency, flatness of the longitudinal voltage distribution in RFQ-channel, RF power, Q-value and the specific shunt impedance have been obtained. They are in agreement with MAFIA calculations and experimental data.

A new formulation [5] for an electric-field potential function in RFQ-channel with 4-rod configuration of the electrodes has been developed for analytical study of effects of the intrinsic field distortion. The electric-field potential function is expanded into four components corresponding to four normal modes. With this function, an analytical study of beam dynamics for typical RFQ-channels with the free-space wavelength λ of 2 m has been made in case of the periodical accelerating structure (see Fig.4). Dependence of beam oscillations on the length of the resonator period l_p has been analyzed including distorted fields. At a long period of the resonator ($l_p/\lambda > 0.1$), resonances of beam oscillations have been found. It has been confirmed by numerical simulations. Under the resonance condition with the field distortion of 5%, the beam transmission degrades from 95% to 60% (see Fig.5).

Two modifications of 4-rod RFQ structure (with incorporated quarter-wavelength matching section and with frequency variation) has been proposed on the base of the normal mode technique [2].

There are applications, which require MeV-range broad beams, e.g. heating of plasmas in confinement devices and ion implantation. The broad-beams are formed as multiple-beams consisting of an array of identical beamlets. The beamlets should be packed very closely. We have concluded that a simple extention of the usual design principle from a single-channel RFQ to a multiple-beam RFQ (MB-RFQ) reduces a packing factor considerably, since adjacent RFQ electrodes can not be interconnected at any point.

To preserve a high packing of beamlets, a new MB-RFQ accelerating structure arranged as a matrix-array of the electrodes has been suggested [4] (see Fig.6). This structure is based on a new combination of normal modes and allows discrete connections of adjacent electrodes. The beam dynamics in RFQ-channels is modified. Beams perform “slalom” motions, utilizing intrinsic transverse oscillations. Figure 7 shows the example of the beam-structure and the electrode profiles in the X0Z-plane. The analysis of this system is in progress.

This work is supported in part by the Grant-in-Aid for JSPS Fellows from the Ministry of Education, Science, Sports and Culture of Japan.

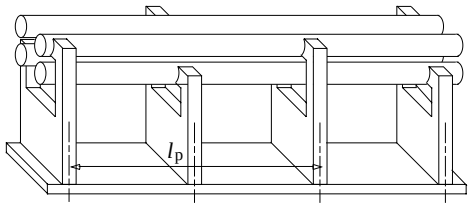

Figure 4. Schematic diagram of the periodic 4-rod RFQ.

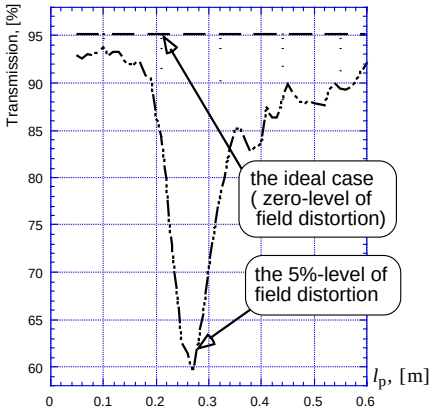

Figure 5. Transmission efficiency as a function of the structure period l_p.

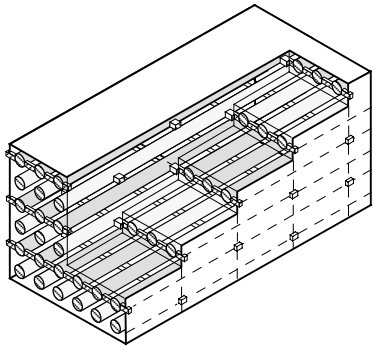

Figure 6. MB-RFQ resonator with a 6x6 matrix array of the RFQ-electrodes.

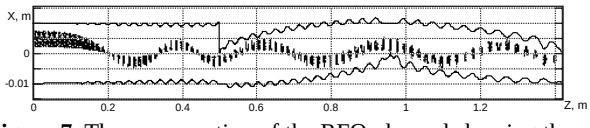

Figure 7. The cross-section of the RFQ-channel showing the beam structure and the electrode profiles.

References

1. V.Kapin, *Proc. of the Fourth European Particle Accelerator Conf.*, World Sci. Publ. Co. Pte. Ltd., 2191-2193 (1994).
2. V.Kapin, M.Inoue, Y.Iwashita and A.Noda, *Proc. of the XVII Int. Linac Conf.*, KEK, Japan, 254-256 (1994).
3. V.Kapin, M.Inoue, Y.Iwashita and A.Noda, *Bull. Inst. Chem. Res.*, Kyoto Univ., **73**, No.1, 50-77 (1995).
4. V. Kapin, A. Noda, Y. Iwashita and M. Inoue, *Proc. of the XVIII Int. Linear Accelerator Conf.*, CERN, Geneva,722-724 (1996).
5. V. Kapin, *Jpn. J. Appl. Phys.*, **36**, Part 1, No.4A, 2415-2427 (1997).

DBGET/LinkDB: A Way of Solution to Integrate Diverged Biological Databases

Wataru Fujibuchi

To extract and utilize information from various forms of biological databases together with your own database are labor-intensive for resarchers. We present here an integrated database retrieval system DBGET/LinkDB, which is the backbone of the Japnese GenomeNet service, to manage those tasks. DBGET is used to search and extract entries from a wide range of molecular biology databases, while LinkDB is used to compute links between entries in different dtabases. It is designed to be a network distributed database system with an open architecture, which is suitable for incorporating local databases or establishing a server environment. The WWW version of DBGET/LinkDB is integrated with other search tools, such as BLAST, FASTA and MOTIF to conduct further retrievals instantly. Moreover, LinkDB can search biological links to get more abstract links of biological objects, and it is the first step toward computerization of logical reasoning process of biological data.

Keywords : Biological Database/ Database Integration/ GenomeNet Service/ DBGET/LinkDB/ Link Computation/ Biological Link

In order to effectively make use of the information in the network of molecular biology databases, it is essential to develop an integrated database retrieval system. The key interst in integrating different source of data is the types of data coupling. Loosely coupled approach has been successful where different databases are linked at the level of entries, rather than the fields that form an entry.

The DBGET/LinkDB has the following characteristics:

• Distributed database: DBGET is organized and accessible through a network configuration systm. Database can exist in different servers, but from the user's point of view they all exist in a single DBGET server.

• Simple architecture: DBGET/LinkDB emphasizes the manipulation of flat file databases at the level of entries. By keeping the search capabilities of individual fields at a minimal level, the updating of DBGET databases requires minimal indexing, which is suited for rapid daily updates of a number of databases.

• Open architecture: The user can set up his/her own DBGET world by integrating the local databases with the databases on the DBGET server. It is also possible to down load public databses from GenomeNet to the user's closed environment. Moreover, LinkDB contains links to other databases outside of DBGET.

RESEARCH FACILITY OF NUCLEIC ACIDS

Scope of research

The following is the current major activities of this facility.
With emphasis on regulatory mechanisms of gene expression in higher organisms, the research activity has been focused on analysis of signal structures at the regulatory regions of transcriptional initiation and of molecular mechanisms involved in post-transcriptional modification by the use of eukaryotic systems appropriate for analysis. As of December 1994, studies are concentrated on the molecular mechanism of RNA editing in mitochondria of kinetoplastids.

Assoc Prof
SUGISAKI, Hiroyuki
(D Sc)

Instr
FUJIBUCHI, Wataru

Techn
YASUDA, Keiko

• Different interfaces: The simplest way to access DBGET is to use the Web interface, but by installing the special client program NetDBget, the DBGET commands can be entered at the UNIX command level.

DBGET does not convert the original files but use them as they are. In order to accomplish rapid access and search of entries, a small number of auxiliary files are created by the indexing program *seqnew* during the update procedure as shown in Table 1.

Table 1: The list of auxiliary files created by *seqnew*.

filename	*file type*	*contents*
db.pag	dbm	hash by entry and accession
db.acc	flat	primary and secondary accession
db.tit	flat	title or definition field of entry
db.tit.pag	dbm	hash by db.tit
db.ref	flat	references in entry
db.auf	flat	authors in entry
db.lnk+.pag	dbm	hash by entry for original links
db.lnk-.pag	dbm	hash by entry for reverse links

LinkDB contains the original links provided by each database and the indirect and reverse links that are computed. They are defined in the *link table*, and the route of computing indirect links is predefined in the *route table*.

At present, 17 databases and links to Medline database are supported in DBGET/LinkDB. As shown in Table 2, all the major databases are daily or weekly updated. PATHWAY, LIGAND and GENES are the products of the KEGG project, where PATHWAY is the database of metabolic pathways and regulatory pathways, LIGNAD is a composite database of ENZYME and COMPOUND, and GENES is a collection of gene catalogs for a number of oraganisms.

Table 2: The DBGET database on GenomeNet service..

Group of Databases	*Database Names*
nucleic acid sequences	*GenBank, *EMBL
protein sequences	*SWISS-PROT, PIR, PRF, *PDBSTR
3D structures	*PDB
sequence motifs	PROSITE, EPD, TRANSFAC
enzyme reactions	*LIGAND
metabolic pathways	*PATHWAY
amino acid mutations	PMD
amino acid indices	AAindex
genetic diseases	*OMIM
literature	LITDB
genes and genomes	*GENES

Those marked by asterisks are daily or weekly updated.

Once an entry is retrieved in the WWW mode of DBGET, all links from this entry can be obtained by clicking on the entry name, which causes the search against LinkDB. Figure 1 shows one of the Web interfaces at GenomeNet to access DBGET/LinkDB, wihch illustrates the supported databases and the original links among them.

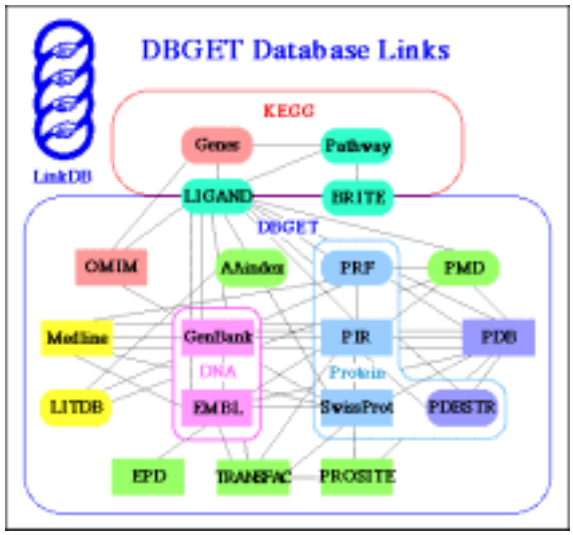

Figure 1. A framework diagram of LinkDB, a database of cross-links between molecular biology databases.

LinkDB started as a collecction of factual links only. Recently similarity links were added but they are not yet integrated with factual links for computing indirect and reverse links. Biological links are being identified by the KEGG project. They are stored as cross-references in the GENES databases that can be treated in a similar way as factual links.

Acknowledgment

This work was supported in part by the Grant-in-Aid for Scientific Research on the Priority Area 'Genome Informatics' from the Ministry of Education, Science, Sports and Culture of Japan. The computation time was provided by the Supercomputer Laboratory, Institute for Chemical Research, Kyoto University.

References

1. Fujibuchi W, Goto S, Migimatsu H, Uhicyama I, Ogiwara A, Akiyama Y and Kanehisa M, *Proc. Pacific Symposium on Biocomputing '98*, 683-694 (1997).
2. Kanehisa M, Fickett JW and Goad WB, *Nucl. Acids Res.*, **12**, 149-158 (1984).
3. Akiyama Y, Goto S, Uchiyama I and Kanehisa M, *MIMBD '95: Second Meeting on the Interconnection of Molecular Biology Databases* (1995).
4. Goto S, Akiyama Y and Kanehisa M, *MIMBD '95: Second Meeting on the Interconnection of Molecular Biology Databases* (1995).
5. Kanehisa M, *Trends Biochem. Sci.*, **22**, 442-444 (1997).

LABORATORIES OF VISITING PROFESSORS

SOLID STATE CHEMISTRY — Structure Analysis —

Vis Prof
KOMATSU, Takayuki
(D Eng)

Professor
KOMATSU, Takayuki
Department of Chemistry, Faculty of Engineering, Nagaoka University of Technology and Science (1603-1 Kamitomioka-cho, Nagaoka 940-21)

Lecture at *ICR*
Structure of TeO_2-Based Glasses
Transparent TeO_2-Based Glass-ceramics
Nonlinear Optical Preperties
Relaxation of Glass Structure

Vis Assoc Prof
TAKAGI, Hidenori
(D Eng)

Associate Professor
TAKAGI, Hidenori
Institute for Solid State Physics, University of Tokyo (Roppongi 7-22-1, Minato-ku, Tokyo 106)

Lectures at *ICR*
Transport Properties IV and V
Disorder Induced Metal-Insulator Transitition IV and V
Metal-Insulator Transitition in $YBa_2Cu_4O_8$

FUNDAMENTAL MATERIAL PROPERTIES — Composite Material Properties —

Vis Prof
MICHIHIKO, Tanaka
(D Eng)

Vis Assoc Prof
FUJIKI, Michiya
(D Eng)

Professor
TANAKA, Michihiko (D Eng)
Director, Information Systems Division
Toray Industries Inc.
Lectures at *ICR*
Application of Functional Polymers
- Membranes for Artificial Kidney, Ultrafiltration and Reverse Osmosis
- Polymers for Contact Lens

Recent Progress of Synthetic Fibers
Recent Progress of Engineering Plastics
Specialty Fibers
- Graphite Fibers
- Optical Fibers
- Polystyrene Based Functional Fibers

Associate Professor
FUJIKI, Michiya (D Eng)
Senior Research Scientist, Supervisor, NTT Basic Research Laboratories
(Wakamiya 3-1, Morinosato, Atsugi-shi, Kanagawa 243-01)
Lectures at *ICR*
(1) Recent Progress in Polysilane Chemistry.
(2) One-Dimensional Self-Assemblies of Optically Inactive and Optically Active Phthalocyanine Derivatives: Molecular Design, Structure and Properties.
(3) Inversion of Helicity of Optically Active Synthetic and Biological Polymers.

SYNTHETIC ORGANIC CHEMISTRY —Synthetic Theory —

Vis Prof
NAKATA, Tadashi
(D Pharm Sci)

Vis Assoc Prof
YAMADA, Haruo
(D Eng)

Professor
NAKATA, Tadashi (D Pharm Sci)
The Institute of Physical and Chemical Research (RIKEN) (Wako-shi, Saitama 351-01)
Lectures at *ICR*
Synthesis of Biologically Active Marine Natural Products. Total Synthesis of Preswinpholide A.
Synthesis of Biologically Active Marine Natural Products. Total Synthesis of Mycalamide A.

Associate Professor
YAMADA, Haruo (D Eng)
Department of Chemical Engineering, Tokyo Institute of Technology (Meguro, Tokyo 152)
Lecture at *ICR*
Organic Synthesis Utilizing Theoretical Calculations. From Conformational Analysis to Transition State Modeling. Part 1.
Organic Synthesis Utilizing Theoretical Calculations. From Conformational Analysis to Transition State Modeling. Part 2.
Synthesis of Oligosaccalides by One-Pot Glycosidation

PUBLICATIONS

STATES AND STRUCTURES

I. Atomic and Molecular Physics

Mukoyama T, Nakamatsu H, Adachi H: Chemical Effect on X-ray Fluorescence Yields for Carbon, *International Journal of PIXE*, **6**, 3&4 , 447-452 (1997)

Toksie K, Sarkadi L, and Mukoyama T: Model calculation of the electron capture to the continuum paeak at neutral particle impact, *J. Phys.* **B**: *At. Mol. Opt. Phys.* **30**, 123-129 (1997).

Yamaguci K and Mukoyama T: Calculations of discrete and continuum wave functions for atoms using wavelets, *Nucl. Instr. and Meth. in Phys. Res.* **B124**, 361-364 (1997).

Ito Y, Mukoyama T, Vlaicu A M, Tochio T, Takahashi M, Emura S, and Azuma Y: Multielectron transitions in photoabsorption spectra above the Xe L edges, in Abst. of Contributed Papers of *Twentieth Internat. Conf. on the Physics of Electronic and Atomic Collisions*, Vienna, 23-29 July, 1997, ed. by F. Aumayr, G. Betz, and H. P. Winter, P. MO 034.

Mukoyama T and Lin C -D:Inner-shell ionization of atoms by charged particles in the distortion approximation, *"Application of Accelerators in Research and Industry"*, ed. by J. L. Duggan and I. L. Morgan (AIP Press, New York, 1997) 101-104.

Mukoyama T, Kaji H, Taniguchi K, and Adachi H: Theoretical estimation of the chemical effect on K X-ray intensity ratios for 4d elements, *X-Ray Spectrometry* **26**, 269-271 (1997).

Emura S, Ito Y, Takahashi M, and Mukoyama T: Thresholds f x-ray absorption structure in Zn between the 500 ~ 1000 eV energy region above K edge, *Photon Factory Activity Report* #**14**,159 (1997).

Ito Y, Vlaicu A M, Tochio T, Mukoyama T, Takahashi M, Emura S, and Azuma Y: X-ray absorption features from double-electron excitations above Xe L edges, *Photon Factory Activity Report* #**14**,160 (1997).

Sekino T, Nakata Y, Hitotsu Y, Emura S, Ito Y, Tanaka A and Sakamoto H: Structure analysis of Ti - Ni amorphous alloys, *Photon Factory Activity Report* #**14**,171 (1997).

Tochio T, Ito Y, Mukoyama T, Takahashi M and Emura S: Multielectron excitations above the Xenon L edges, *J.Phys.*, **C2**,1263-1264 (1997).

Takahashi T, Ishida A, Emura S, Osawa D, Yamaguchi K, Ito Y and Mukoyama T: Multielectron excitations in x-ray absorption spectra of KOH, *J.Phys.*, **C2**, 1265-1266 (1997).

Ohsawa D,Katano R, Ito Y,Isozumi Y: A simple crystal spectrometer for low-energy photons emitteed from radioactive sources, Part II, *Nucl. Instr.and Methods.* **A390** 183-190 (1997).

Kurakado M, Ohsawa D, Katano R,Ito S,Isozumi Y: Futher developments of series-connected superconducting tunnel junctionto radiation detection, *Review of Scientific Instruments*, **68**(10) 3685-3696 (1997)

Ueda K, Shimizu Y, Chiba H, Okunishi M, Ohmori K, West J.B, Sato Y, Hayashi T, Nakamatsu H and Mukoyama T: Correlation between Core-Hole Polarization and Localized Bond Rupture Probed by Anisotropy in the Photofragmentation of F 1s Excited SF_6, *Phys. Rev. Lett.*, **79**, 3371-3374 (1997).

Ikeda T, Kobayashi H, Ohmura Y, Nakamatsu H and Mukoyama T: Electronic Structure of Alkaline-Earth Fluorides Studied by Model Clusters. II. Auger-Free Luminescence, *J. Phys. Soc. Jpn.*, **6**, 1079-1087 (1997).

Hirata M, Monjyushiro H, Sekine R, Onoe J, H. Nakamatsu, Mukoyama T, Adachi H and Takeuchi K: Valence Elecronic Structure of Uranyl Nitrate $UO_2(NO_3)_2 \cdot H_2O$, *J. Electron Spectrosc.*, **83**, 59-64 (1997).

Ikeda T, Kobayashi H, Ohmura Y, Nakamatsu H and Mukoyama T: Electronic Structure of Alkaline-Earth Fluorides Studied by Model Clusters. I. Ground State, *J. Phys. Soc. Jpn.*, **66**, 1074-1078 (1997).

Onoe J, Nakamatsu H, Mukoyama T, Sekine R, Adachi H and Takeuchi K: Structure and Bond Nature of the UF_5 Monomer, *Inorg. Chem.*, **36**,1934-1938 (1997).

Adachi K, Sekine R and Nakamatsu H: Electronic states of CaB_6 and YB_6H (in Japanese), *Bull. Soc. Discrete Variational* $X\alpha$ **10**, 126-130 (1997).

Bastug T, Nakamatsu H, Onoe J, Takeuchi K and Mukoyama T: Relativisitc DV-Xa calculations for the potential energy surface of the UF_5 molecule (in Japanese), *Bull. Soc. Discrete Variational* $X\alpha$ **10**, 35-39 (1997).

Nakamatsu H: Report on visiting Ellis' laboratory (in Japanese), *Bull. Soc. Discrete Variational* $X\alpha$ **10**, 58-62 (1997).

Hirata M, Sekine R, Onoe J, H. Nakamatsu, Mukoyama and Tachimori S: Electronic structure of actinide-nitrite system (in Japanese), *Bull. Soc. Discrete Variational* $X\alpha$ **10**, 118-121 (1997).

Kurihara M, Hirata M, Sekine R, Onoe J, H. Nakamatsu, Mukoyama and Adachi H: Eletronic structure of uranium (2) (in Japanese), *Bull. Soc. Discrete Variational* $X\alpha$ **10**, 136-140 (1997).

II. Crystal Information Analysis

Kobayashi T, Furukawa C, Ogawa T and Isoda S: Structures of Germanium- and Silicon-phthalocyanine Thin Films; Polymorphism and Isomorphism, *J. Porphyrine and Phthalocyanines*, **1**, 297-305 (1997).

Ogawa T, Isoda S and Kobayashi T: Structure Analysis of C_{60} Low-Temperature Phase by Electron Crystallography with Cryo-TEM, *Acta Cryst.*, **B53**, 831-837 (1997).

Irie S, Hoshino A, Kuwamoto K, Isoda S, Miles M J and Kobayashi T: Point-on-Line Coincidence in Epitaxial Growth of $CuPcCl_{16}$ on Graphite, *Appl. Surf. Science*, **113/114**, 310-315 (1997).

Sano Y, Inoue H, Kajiwara K, Hiragi Y and Isoda S: Structural Analysis of A-Protein of Cucumber Green Mottle Mosaic Virus and Tabacco Mosaic Virus by Synchrotron Small-Angle X-ray Scattering, *J. Protein Chemistry*, **16**, 151-159 (1997).

Irie S, Isoda S, Kobayashi T, Ozaki H and Mazaki Y: Photopolymerization of Alkyldiyne Monolayer, *Technical Report of IEICE*, **OME97-59**, 5-10 (1997) (in Japanese).

Fujiwara E, Omoto K and Fujimoto H: Theoretical Study of Strong Basicity in Aromatic Diamines, *J. Org. Chem.*, **62**, 7234-7238 (1997).

Tosaka M, Hamada N, Tsuji M, Kohjiya S, Ogawa T, Isoda S and Kobayashi T: Crystallization of Syndiotactic Polypropylene in β-Form. 1: Positional Identification of Stacking Faults in the

Solution-grown Single Crystals, *Macromolecules*, **30**, 4132-4136 (1997).

Isoda S and Kobayashi T: Phthalocyanine, Chemistry and Functions, IPC Press, 63-78 (1997) (in Japanese).

Ogawa T, Moriguchi S, Isoda S and Kobayashi T: Electron Crystallography with a New High Voltage Electron Microscope, *Proc. Swiss-Jpn. Joint Forum on Elec. Microsc. in Mat*., 31-34, Zurich, Swiss, (1997).

Kim D G, Karasawa T, Komatsu T and Kobayashi T: Exciton Transition in Size-Distributed BiI_3 Microcrystallites Embedded in CdI_2 Crystals, *J.Phys.Soc.Jpn*., **65**, 3371-3378 (1997).

Kobayashi T: Molecular Images and Stacking Fault of an Organic Complex Prepared by Chemical Reaction on a Solid Surface, ed. *Nihon Denshi-Kenbikyou-Gakkai*, 96-97, Gakusai-Kikaku, (1997) (in Japanese).

Knippelmeyer R, Wahlbring P and Kohl H: Relativistic Ionization Cross Section for Use in Microanalysis, *Ultramicroscopy*, **68**, 25-41 (1997).

Kobayashi T: Direct Observation of Atom Arrangement in an Organic Molecule, ed. *Nihon Dennshi-Kennbikyou-Gakkai*, 94-95, Gakusai-Kikaku, (1997) (in Japanese).

III. Polymer Condensed States Analysis

Kohjiya S: Overview - Can Metallocene Polyolefins be Developed to a Novel Elastomers**?**, *J. Soc. Rubber Ind., Jpn.*, **70**, 62-68 (1997) (in Japanese).

Ikeda Y, Tanaka A, Kohjiya S: Effect of Catalyst on *in situ* Silica Reinforcement of Styrene-Butadiene Rubber Vulcanizate by the Sol-Gel Reaction of Tetraethoxysilane, *J. Mater. Chem*., **7**, 455-458 (1997).

Takino H, Iwama S, Yamada Y, Kohjiya S: Effect of Processing Additives on Carbon Black Dispersion and Grip Property of High-Performance Tire Tread Compound, *Rubber Chem. Technol.*, **70**, 15-24 (1997).

Sugiya M, Terakawa K, Miyamoto Y, Tomono S, Kohjiya S, Ikeda Y: Dynamic Mechanical Properties and Morphology of Silica-Reinforced Butadiene Rubber by the Sol-Gel Process, *Kautsh. Gummi Kunst.*, **50**, 538-543 (1997).

Kohjiya S, Hashim A S: Chemistry of Epoxydized Natural Rubber with Amine Compounds, *Proc. Int. Workshop on Green Polymers - Reevaluation of Natural Polymers*, (Ed. Hendayani T, et al.), 109-134 (1997).

Ikeda Y, Masui H, Syoji S, Sakashita T, Matoba Y, Kohjiya S: Comb-shaped High Molecular Weight Polyether Consisting of Oxyethylene Units for Polymer Solid Electrolyte, *Polym. Int.*, **43**, 269-273 (1997).

Ikeda Y, Kohjiya S: *In Situ* Formed Silica Particles in Rubber Vulcanizate by the Sol-Gel Method, *Polymer*, **38**, 4417-4423 (1997).

Ikeda Y, Tanaka A, Kohjiya S: Reinforcement of Styrene-Butadiene Rubber Vulcanizate by *in situ* Silica Prepared by the Sol-Gel Reaction of Tetraethoxysilane, *J. Mater. Chem*., **7**, 1497-1503 (1997).

Urayama K, Kohjiya S: Uniaxial Elongation of Deswollen Polydimethylsiloxane Networks with Supercoiled Structure, *Polymer*, **38**, 955-962 (1997).

Kidera A, Higashira T, Ikeda Y, Urayama K, Kohjiya S: GPC Analysis of Polymer Network Formation: 2. Bifunctional PPG Prepolymer/Crosslinker System, *Polym. Bull.*, **38**, 461-468 (1997).

Ikeda Y, Yonezawa T, Urayama K, Kohjiya S: Thermal and I.R.-Dichroic Properties of Side-Chain Type Liquid-Crystalline Elastomers, *Polymer*, **38**, 3229-3235 (1997).

Urayama K and Tsuji M (Partial Collaboration): in *Dictionary of Rubber Technology*, (Soc. Rubber Ind, Jpn., Ed.) (1997) (in Japanese).

Urayama K, Kohjiya S, Yamamoto M, Ikeda Y, Kidera A: Formation Process of End-linked Networks by Gel Permeation Chromatography, *J. Chem. Soc., Faraday Trans.*, **93**, 3689-3693 (1997).

Kawamura T, Urayama K, Kohjiya S: Equilibrium Swelling and Elastic Modulus of End-linked Polydimethylsiloxane Networks in Theta Solvent, *J. Soc. Rheol., Jpn.*, **25**, 195-196 (1997).

Kohjiya S, Urayama K, Ikeda Y: Poly(Siloxane) Network of Ultra-high Elongation, *Kautsh. Gummi Kunst.*, **50**, 868-872 (1997).

Inoue T, Matsui H, Murakami S, Kohjiya S, Osaki K: Strain-induced Birefringence and Molecular Structure of Glassy Polymers, *Polymer*, **38**, 1215-1220 (1997).

Murakami S, Kawaguchi A: Structure Formation in the Drawing Process of Poly(ethylene-2,6-naphthalate), *Kobunshi Ronbunshu*, **54**, 183-198 (1997) (in Japanese).

Murakami S, Shimamura K, Kohjiya S: Deformation Behavior of Extruded Blown Film of High Density Polyethylene, *Nihon Reoroji Gakkaishi*, **25**, 193-194 (1997) (in Japanese).

Hirai A, Tsuji M and Horii F: Formation of Cellulose II crystal in bacterial cellulose, *Cell. Commun.*, **4**, 21-24 (1997) (in Japanese).

Hirai A, Tsuji M and Horii F: Culture conditions producing structure entities composed of Cellulose I and II in bacterial cellulose, *Cellulose*, **4**, 239-245 (1997).

Tsuji M, Fujita M and Kohjiya S: Correlation between the crystallite modulus along chain axis and the durability of crystallinity against electron irradiation for polymers, *Nihon Reoroji Gakkaishi*, **25**, 235-238 (1997) (in Japanese).

Tsuji M and Shimizu T: How fine details are identified by the latest nanoscopical techniques? –Ultrafine structures in synthetic fibers studied by electron microscopy and/or STM/AFM–, *SEN'I GAKKAISHI*, **53**, 137-141 (1997) (in Japanese).

Tsuji M and Vogl O: ICRIS '96: Controlled organization and molecular dynamics of polymers, Uji, Kyoto, Japan, *Polym. News*, **22**, 293-297 (1997).

Tsuji M and Tosaka M: Sample preparation and measuring methods • measured examples. in "*Kobunshi jikkengakukoza 6 Kobunshi no kozo (2) - Sanranjikken to Keitaikansatsu*" (Jpn. Soc. Polym. Sci. Ed.), Kyoritsu syuppan, Tokyo, 1997, 2-1, Densikenbikyo, 1.1 TEM, §1.1.2, 405-426 (in Japanese).

Tosaka M, Hamada N, Tsuji M, Kohjiya S, Ogawa T, Isoda S and Kobayashi T: Crystallization of Syndiotactic Polystyrene in β-form. 1. Positional Identification of Stacking Faults in the Solution Grown Single Crystals, *Macromolecules*, **30**, 4132-4136 (1997).

Fujita M, Hamada N, Tosaka M, Tsuji M and Kohjiya S: A TEM Study on Polyoxymethylene Rodlike Crystals Grown Epitaxially on NaCl, *J. Macromol. Sci., -Phys*, **B36**, 681-687 (1997).

Hamada N, Tosaka M, Tsuji M, Kohjiya S and Katayama K:

Crystallization of Syndiotactic Polystyrene in β-form. 2: Quantification of Stacking Faults in the Solution-Grown Single Crystals, *Macromolecules*, **30**, 6888-6892 (1997).

Tosaka M, Hamada N, Tsuji M and Kohjiya S: Crystallization of Syndiotactic Polystyrene in β-form. 3: Energetic Analysis of the Incorporation Mechanism of Stacking Faults into the Crystal, *Macromolecules*, **30**, 6592-6596 (1997)

Tsuji M, Tosaka M and Kohjiya S: Polymer crystals observed by high-resolution electron microscopy, *Ann. Rep. Res. Chem. Fibers, Jpn.*, **54**, 67-74 (1997) (in Japanese)

INERFACE SCIENCE

I. Solutions and Interfaces

Matubayasi N, Wakai C and Nakahara M: NMR Study of Water Structure in Super- and Subcritical Conditions, *Phys. Rev. Lett.*, **78**, 2573-2576, 4309 (1997).

Okamura E, Wakai C, Matubayasi N and Nakahara M: ^{14}N NMR Spectra Sensitively Reflect Surface Curvature and Segmental Motion of Hydrophilic Headgroups in Lipid Bilayers and Micelles, *Chem. Lett.*, 1061-1062 (1997).

Wakai C and Nakahara M: Attractive potential effect on the self-diffusion coefficients of a solitary water molecule in organic solvents, *J. Chem. Phys.*, **106**, 7512-7518 (1997).

Nakahara M, Yamaguchi T and Ohtaki H: The Structure of Water and Aqueous Electrolyte Solutions under Extreme Conditions, *Recent Res. Devel. in Physical Chem.*, **1**, 17-49 (1997).

Nakahara M, Tennoh T, Wakai C, Fujita E and Enomoto H: ^{13}C-NMR Evidence for Hydrogen Supply by Water for Polymer Cracking in Supercritical Water, *Chem. Lett.*, 163-164 (1997).

Matubayasi N and Nakahara M: Structure of Water at High Temperatures and Pressures, Koatsu-ryoku no Kagaku to Gijutsu (Rev. High Pressure Sci. Tech.), **6**, 16-23 (1997) (in Japanese).

Tatsumi K, Conard J, Nakahara M, Menu S, Lauginie P, Sawada Y and Ogumi Z: ^{7}Li NMR Studies on a Lithiated Non-graphitizable Carbon Fibre at Low Temperatures, *Chem. Commun.*, 687-688 (1997).

Nakahara M: Structure and Properties of Supercritical Water and Solutions, in "Handbook for Hydrothermal Sciences (Suinetsu-Kagaku)", *Gihoudou Shuppan*, 21-37 (1997) (in Japanese).

Sakai H and Umemura J : Effect of Infrared Radiation and Air Flow on Fourier Transform Infrared External Reflection Spectra of Langmuir Monolayers, *Langmuir*, **13**, 502-505 (1997).

Hasegawa T, Nishijo J, Kobayashi Y and Umemura J : Effect of Substrates on the Infrared External Reflection Spectra of Langmuir-Blodgett Films, *Bull. Chem. Soc. Jpn.*, **70**, 525-533 (1997).

Sakai H and Umemura J : Molecular Orientation Change in Langmuir Films of Stearic Acid and Cadmium Stearate on Surface Compression as studied by Infrared External Reflection Spectroscopy, *Bull. Chem. Soc. Jpn.*, **70**, 1027-1032 (1997).

Tano T and Umemura J : FT-IR Spectra and Molecular Orientation of Black Lipid Films in Air Interacting with Metal Ions, *Langmuir*, **13**, 5718-5725 (1997).

Tano T and Umemura J : Deviation from the Lambert Law in Ultrathin Films Such as Black Soap Films, *Appl. Spectrosc.*, **51**, 944-948 (1997).

Matubayasi N: Yuuden-ritsu (dielectric constant), *Kagaku (Chemistry)*, **52**, 42-43 (1997) (in Japanese).

Payne V A, Matubayasi N, and Murphy L R, and Levy R M: Monte Carlo Study of the Effect of Pressure on Hydrophobic Association, *J. Phys. Chem.*, **B101**, 2054-2060 (1997).

Matubayasi N: Mean-field theory of solutions: Chemical potential and solution structure in the superposition approximation, *bussei kenkyu*, **68**, 379-399 (1997) (in Japanese).

II. Molecular Aggregates

Izuoka A, Murase T, Tukada M, Ito Y, Sugawara T, Uchida A, Sato N and Inokuchi H: Crystal Structure and Solid State Reaction of Tetrabenzo[*de*,*hi*,*op*,*st*]pentacene Endoperoxide, *Tetrahedron Lett.*, **38**, 245-248 (1997).

Sato N: Molecular Electronic Relaxation in Organic Solids: *Electrical and Related Properties of Organic Solids*, Munn R W, Miniewicz A and Kuchta B (eds.), (Kluwer Academic Publishers, Dordrecht, 1997), pp. 157 - 166.

Inagaki Y , Shirotani I, Konno M, Sato N and Nishi H: Structure and Absorption Spectra of Thin Films of Triphenodithiazine, $C_{18}N_2S_2H_{10}$, *Mol. Cryst. Liq. Cryst.*, **296**, 397-407 (1997) .

Hasegawa M and Sato N: Correlation of Molecular Orientations at the Interface of Organic Double-Layered Thin Films, *Mol. Cryst. Liq. Cryst.*, **296**, 409-426 (1997).

Oda M and Sato N: A Theoretical Study on Solid-State Thermal Isomerization Reaction of Methyl 4-(Dimethylamino)-benzenesulfonate in the Energetic Aspect, *Chem. Phys. Lett.*, **275**, 40-45 (1997).

Wada S, Iida A, Asami K, Tachikawa E and Fujita T: Ion Channel Formation in Lipid Membranes and Catecholamine Secretion from Chromaffin Cells by Trichocellines A-II and B-II, 20 Residue Peptaiboles, *Biochim. Biophys. Acta*, **1325**, 209-214 (1997).

Koide N, Asami K and Fujita T: Ion-Channels of Hypelcins, Antibiotic Peptides, Formed in Planar Bilayer Lipid Membranes, *Biochim. Biophys. Acta*, **1326**, 47-53 (1997).

Iseda M, Nishio T, Han S Y, Yoshida H, Terasaki A and Kondow T: Electronic Structure of Vanadium Cluster Anions as Studied by Photoelectron Spectroscopy, *J. Chem. Phys.*, **106**, 2182-2186 (1997).

III. Separation Chemistry

Hasegawa H: Seasonal Changes in Methylarsenic Distribution in Tosa Bay and Uranouchi Inlet, *Applied Organometallic Chemistry*, **10**, 733-740 (1996).

Zhou D, Li Q, Huang C, Yao G, Umetani S, Matsui M, Ying L, Yu A, Zhao X: Room- Temperature Fluorescence, Phosphorescence and Crystal Structure of 4-Acyl Pyrazolone Lanthanides Complexes: $Ln(L)_3 \cdot H_2O$, *Polyhedron*, **16**, 1381-1389 (1997).

Sohrin Y, Tateishi T, Mito S, Matsui M, Maeda H, Hattori A, Kawashima M, Hasegawa H: Nutrients of Lake Biwa in the Unusually Cool and Hot Summers of 1993 and 1994, *Lakes & Reservoirs: Research and Management 1996*, **2**, 77-87 (1997).

Le Q.T.H, Umetani S, Suzuki M, Matsui M: a-Substituted b-Diketones: Effect of the a Substituent on the Complexation and Selectivity for Lanthanides, *J. Chem. Soc., Dalton Trans.*, 643-647 (1997).

Suzuki M, Umetani S, Matsui M, Kihara S: Oxidation of Ascorbate and Ascorbic Acid at the Aqueous/Organic Solution Interface, *J. Electroanal. Chem.*, **420**, 119-125 (1997).

Obata H, Karatani H, Matsui M, Nakayama E: Fundamental Studies for Chemical Speciation of Iron in Seawater with an Improved Analytical Method, *Marine Chemistry*, **56**, 97-106 (1997).

Tsurubou S, Umetani S, Matsui M: Solvent Extraction of Some Divalent Metal Ions with 4,4'-(1,3-Phenylenediacetoxy)bis(1-phenyl-3- methyl-5-pyrazolone), *Solvent Extr. Res. Dev., Jpn.*, **4**, 190-198 (1997).

Hasegawa H: The Behavior of Trivalent and Pentavalent Methylarsenicals in Lake Biwa, *Appl. Organometallic Chem.*, **11**, 305-311 (1997).

Umetani S, Kawase Y, Le Q T H, Matsui M: The Synergistic Extraction of Lanthanides with Trifluoroacetylcycloalkanones and Trioctylphosphine Oxide, *Chem. Lett.*, 771-772 (1997).

Sohrin Y, Matsui M, Kawashima M, Hojo M, Hasegawa H: Arsenic Biogeochemistry Affected by Eutrophication in Lake Biwa, Japan, *Environ. Sci. Technol.*, **31** (10), 2712-2720 (1997).

Le Q T H, Umetani S, Matsui M: Ion-size Recognition of Group 13 Metals (Al^{3+}, In^{3+}) with Modified β-Diketones, *J. Chem. Soc., Dalton Trans.*, 3835-3840 (1997).

Umetani S, Le Q T H, Matsui M: Molecular Design of Highly Selective Ligands for Group 13 Metals, *Anal. Sci.*, **13 Suppl**, 103-106 (1997).

Umetani S, Sasaki T, Matsui M, Tsurubou S, Kimura T, Yoshida Z: Complex Formation of Metal Ions with Sulfonated Crown Ethers in Water as Ion Size Selective Masking Reagents, *Anal. Sci.*, **13 Suppl**, 123-126 (1997).

Komatsu Y, Umatsni S: Triple-phase Separation of Alkaline Earth Metal Ions, *Anal. Sci.*, **13 Suppl**, 107-110 (1997).

Mukai H, Umetani S, Matsui M: The Synergic Extraction of Rare Earth Metals with Ortho-Substituted 1-Phenyl-3-methyl-4-aroyl- 5-pyrazolones and Trioctylphosphine Oxide, *Anal. Sci.*, **13 Suppl**, 145-148 (1997).

Tsurubou S, Sasaki T, Umetani S, Matsui M: Quantitative Separation of Alkaline Earths Using Diazapolyoxabicyclic Ligands as Ion-size Selective Masking Reagents, *Anal. Sci.*, **13 Suppl**, 127-130 (1997).

Li Q, Huang C, Yao G, Umatani S, Matsui M: Synthesis, Characterization and Luminescence of Tb^{3+} Mixed Ligand Complexes with 1-Phenyl-3-methyl-4-isobutyryl-5-pyrazolone and Neutral Ligands, *J. Chinese Rare Earth Soc.*, **15**, 295-299 (1997).

SOLID STATE CHEMISTRY

I. Artificial Lattice Alloys

Sugimoto T, Ueda K, Kanehisa N, Kai Y, Shiro M, Hosoito N, Takeda N and Ishikawa M: Weak-Ferromagnetism and Ferromagnetism in Tetrafluorotetracyanoquinodimethanide Salts, *ACS Symposium Series* 644, *Molecule-Based Magnetic Materials, Theory, Techniques, and Applications*, **Chap. 19**, 276-295 (1996).

Ueda K, Sugimoto T, Endo S, Toyota N, Kohama M, Yamamoto K, Suenaga Y, Morimoto H, Yamaguchi T, Munakata M, Hosoito N, Kanehisa N, Shibamoto Y and Kai Y: 1:2 TCNQ/$TCNQ^{\cdot}$ Mixed Salts Exhibiting Ferromagnetic Behavior at Room Temperature, *Chem. Phys. Lett.*, **261**, 295-300 (1996).

Passamani E C, Mibu K, Baggio-Saitovitch E and Shinjo T: ^{151}Eu Mössbauer Study of V/Eu, Cr/Eu, Fe/Eu, and Co/Eu Multilayers, *Conf. Proc.* **50** *"ICAME-95"*, I. Ortalli (Ed.), SIF, Bologna, 631-634 (1996).

Kobayashi Y, Sato H, Sugawara H, Aoki Y, Ono T, Shinjo T and Kamijo A: Transport Properties in Microstructured Multilayers, *Czechoslovak J. Phys.*, **46**, Suppl. S4, 2351-2352 (1996).

Mibu K, Nagahama T and Shinjo T: Reversible Magnetization Process and Magnetoresistance of Soft-Magnetic (NiFe)/ Hard-Magnetic (CoSm) Bilayers, *J. Magn. Magn. Mater*, **163**, 75-79 (1996).

Shinjo T, Ono T, Shigeto K and Sugita Y: Magnetism and Magnetoresistance of Multilayers Prepared on Microstructured Substrates, *Acta Physica Polonica A*, **91**, 27-36 (1997).

Emoto T, Hosoito N and Shinjo T: Magnetic Polarization of Conduction Electrons at Au Layers in Fe/Au Multilayers by ^{119}Sn Mössbauer Spectroscopy, *J. Phys. Soc. Jpn.*, **66**, 803-808 (1997).

Shigeto K, Ono T and Shinjo T: Magnetoresistance Study of Noncoupled-Type Multilayers Prepared on V-groove Substrates, *J. Phys. Soc. Jpn.*, **66**, 2425-2428 (1997).

Hamada S, Hosoito N and Shinjo T: Local Spin Polarization in Au Layers of Co/Au(111) Multilayers by ^{57}Fe Mössbauer Probes, *J. Phys. Soc. Jpn.*, **66**, 30-33 (1997).

Ishimatsu N, Venkataraman C T , Hashizume H, Hosoito N, Namikawa K and Iwazumi T: X-ray Reflectivity at the L Edges of Gd, *J. Synchrotron Rad.*, **4**, 175-179 (1997).

Ono T, Shigeto K, Shinjo T, Shintaku K and Moriya H: Giant Magnetoresistance of Multilayers Prepared on Replicas of V-Groove Substrates, *Jpn. J. Appl. Phys.*, **36**, L616-L618 (1997).

Hashizume H, Ishimatsu N, Sakata O, Hosoito N, Emoto T, Lee Ki-Bong, Lee Dong-Ryeol and Iwazumi T: X-Ray Circular Dichroic Bragg Reflections from a GdCo/Ag Multilayer, *Jpn. J. Appl. Phys.*, **36**, 4525-4530 (1997).

Ono T, Sugita Y, Shigeto K, Mibu K, Hosoito N and Shinjo T: Magnetoresistance Study of Co/Cu/NiFe/Co Multilayers Prepared on V-groove Substrates, *Phys. Rev. B*, **55**, 14457-14466 (1997).

Ono T, Shigeto K and Shinjo T: Magnetoresistance of Co/Cu(Ag)/NiFe/Cu(Ag) Multilayers Prepared on V-groove Substrates, *Physica B*, **237-238**, 267-268 (1997).

Ono T, Shigeto K and Shinjo T: GMR Properties of Co/Ag(Cu)/NiFe/Ag(Cu) Multilayers Prepared on V-groove Substrates, *Physica B*, **239**, 41-46 (1997).

Ono T and Shinjo T: GMR Properties of Multilayers Prepared on Microstructured Substrates, *Kotai Butsuri*, **32**, 212-220 (1997). (in Japanese)

Amaral L, Scorzelli R B, Paesano A, Brückman M E, Bustamante Dominguez A, Shinjo T, Ono T and Hosoito N: Mössbauer Study on Phase Separation in FeNi Multilayers under Ion Bombardment, *Surface Science*, **389**, 103-108 (1997).

Trhlík M, De Moor P, Mibu K, Severijns N, Shinjo T, Van Geert A and Vanneste L: Perpendicular Magnetic Anisotropy of Tb Magnetic Moments in Tb/Fe Multilayers, J. Magn. Magn. Mater., **165**, 408-410 (1997).

II. Artificial Lattice Compounds

Chong I, Terashima T, Bando Y, Takano M, Matsuda Y, Nagaoka T and Kumagai K: Growth of Heavily Pb-Substituted Bi-2201 Single Crystals by a Floating Zone Method, *Physica C*, **290**, 57-62 (1997).

Joko H, Fujiwara M, Nakanishi M, Fujii T, Takada J, Kusano Y, Takeda Y, Ikeda Y, Takano M and Bando Y: Li Doping into the Pb Substituted Bi-2212 Phase by Electrochemical Method, *Funtai oyobi Funmatsu Yakin*, **44**, 792-796 (1997) (in Japanese).

Takeuchi T, Ding H, Campuzano J C, Yokoya T, Takahashi T, Chong I, Terashima T and Takano M: ARPES Studies of Pb Substituted Bi2201 Compounds, *Physica C*, **282-287**, 999-1000 (1997).

Izumi M, Nakazawa K, Bando Y, Yoneda Y and Terauchi H: Magnetotransport of $SrRuO_3$ Thin Film on $SrTiO_3$ (001), *J. Phys. Soc. Jpn.*, **66**, 3893-3900 (1997).

Bando Y: Synthesis and Research of Materials, *Butsuri*, **52**, 170-174 (1997) (in Japanese).

Fujiwara M, Nakanishi M, Fujii T, Takada J, Kusano Y, Takeda Y, Ikeda Y, Takano M and Bando Y: Li Doping into the Bi-2212 Phase by Electrochemical Method, *Funtai oyobi Funmatsu Yakin*, **44**, 142-146 (1997) (in Japanese).

Chong I, Hiroi Z, Izumi M, Shimoyama J, Nakayama Y, Kishio K, Terashima T, Bando Y and Takano M: High Critical Current Density in the Heavily Pb-Doped $Bi_2Sr_2CaCu_2O_{8+\delta}$ Superconductor: Generation of Efficient Pinning Centers, *Science*, **276**, 770-773 (1997).

Kawahara T, Sugiuchi N, Komai E, Terashima T and Bando Y: Hole and Electron Doping in Ultrathin Films with the Infinite Layer Structure by Electric Field Effect, *Physica C*, **276**, 127-131 (1997).

Ikeda Y and Bando Y: Subsolidus Phase Relations in the BaO-TiO_2-Fe_2O_3 System, *J. Phys. IV France 7*, C1-343-344 (1997).

Fujiwara M, Nakanishi M, Kusano Y, Fujii T, Takada J, Takeda Y and Ikeda Y: Electrochemical Lithium Intercalation into the Bi-2212 Phase, *Physica C*, **279**, 219-224 (1997).

Chong I, Terashima T, Ikeda Y, Bando Y, Takano M, Matsuda Y, Nagaoka T and Kumagai K: Growth of Pb-Substituted Bi-2201 Single Crystal by Floating Zone Method, *Journal of the Korean Physical Society*, **31**, 40-42 (1997).

Terashima T and Bando Y: Growth Mechanism and Microstructure of Ultrathin $YBa_2Cu_3O_{7-\delta}$ Films, *Proceedings of The Fourth R.O.C. - Japan Joint Seminar on Crystallography, Nov. 11-12, 1996, Hsinchu, Taiwan, R.O.C., Taiwan, R.O.C.*, 259-266 (1997).

Chong I, Terashima T, Bando Y, Takano M, Matsuda Y, Nagaoka T and Kumagai K: Growth of Pb-Substituted Bi-2201 Single Crystal by Floating Zone Method, *Advances in Superconductivity IX: Proceedings of the 9th International Symposium on Superconductivity (ISS'96), Oct. 21-24, 1996, Sapporo, Japan (ed. Nakajima S and Murakami M), Springer-Verlag, Tokyo*, **1**, 449-452 (1997).

III. Multicomponent Materials

Kanno R, Shirane T, Kawamoto Y, Takeda Y, Takano M, Ohashi M and Yamaguchi Y: Synthesis, Structure, and Electrochemical Properties of a New Lithium Iron Oxide, $LiFeO_2$, with a Corrugated Layer Structure, *J. Electrochem. Soc.*, **143**, 2435-2442 (1996).

Hiroi Z, Amelinckx S, Tendeloo G V and Kobayashi N: Microscopic Origin of Dimerization in the CuO_2 Chains in $Sr_{14}Cu_{24}O_{41}$, *Phys. Rev. B*, **54**, 15849-15855 (1996).

Yamaura K, Takano M, Hirano A and Kanno R: Magnetic Properties of $Li_{1-x}Ni_{1+x}O_2$ ($0 \le x \le 0.08$), *J. Solid State Chem.*, **127**, 109-118 (1996).

Kobayashi N, Hiroi Z and Takano M: Compounds and Phase Relations in the SrO-CaO-CuO System under High Pressure, *J. Solid State Chem.*, **132**, 274-283 (1997).

Saitoh T, Sekiyama A, Kobayashi K, Mizokawa T, Fujimori A, Sarma D D, Takeda Y and Takano M: Temperature-Dependent Valence-Band Photoemission Spectra of $La_{1-x}Sr_xMnO_3$, *Phys. Rev. B*, **56**, 8836-8840 (1997).

Shimoyama J, Nakayama Y, Kitazawa K, Kishio K, Hiroi Z, Chong I and Takano M: Strong Flux Pinning up to Liquid Nitrogen Temperature Discovered in Heavily Pb-Doped and Oxygen Controlled Bi2212 Single Crystals, *Physica C*, **281**, 69-75 (1997).

Takeuchi T, Ding H, Campuzano J C, Yokoya T, Takahashi T, Chong I, Terashima T and Takano M: ARPES Studies of Pb Substituted Bi2201 Compounds, *Physica C*, **282-287**, 999-1000 (1997).

Joko H, Fujiwara M, Nakanishi M, Fujii T, Takada J, Kusano Y, Takeda Y, Ikeda Y, Takano M and Bando Y: Li Doping into the Pb Substituted Bi-2212 Phase by Electrochemical Method, *Funtai oyobi Funmatsu Yakin*, **44**, 792-796 (1997) (in Japanese).

Takano M, Azuma M, Fujishiro Y, Nohara M, Takagi H, Fujiwara M, Yasuoka H, Ohsugi S, Kitaoka Y and Eccleston R S: Impurity Effects on a 2-Leg Spin Ladder Compound $SrCu_2O_3$, *Physica C*, **282-287**, 149-152 (1997).

Hiroi Z: Beer and Electron Microscope - Record of Our Stay in Antwerp -, *Denshikenbikyo*, **32**, 176-178 (1997) (in Japanese).

Chong I, Hiroi Z, Izumi M, Shimoyama J, Nakayama Y, Kishio K, Terashima T, Bando Y and Takano M: High Critical Current Density in the Heavily Pb-Doped $Bi_2Sr_2CaCu_2O_{8+d}$ Superconductor: Generation of Efficient Pinning Centers, *Science*, **276**, 770-773 (1997).

Chong I, Terashima T, Bando Y, Takano M, Matsuda Y, Nagaoka T and Kumagai K: Growth of Heavily Pb-Substituted Bi-2201 Single Crystals by a Floating Zone Method, *Physica C*, **290**, 57-62 (1997).

Kaimori S, Kawsaki S, Azuma M and Takano M: High Pressure Synthesis of Ln_2CuSnO_6 (*Ln*=La, Pr, Nd, Sm), *Funtai oyobi Funmatsu Yakin*, **44**, 127-131 (1997) (in Japanese).

Azuma M, Fujishiro Y, Takano M, Nohara M and Takagi H: Switching of the Gapped Single Spin-Liquid State to an Antiferromagnetically Ordered State in $Sr(Cu_{1-x}Zn_x)_2O_3$, *Phys. Rev. B*, **55**, R8658-R8661 (1997).

Takano M: Superconductivity, *Kikan Kagaku Sosetsu*, **32**, 73-83 (1997) (in Japanese).

Mizokawa T, Ootomo K, Konishi T, Fujimori A, Hiroi Z, Kobayashi N and Takano M: Photoemission and X-Ray-Absorption Study of the Hole-Doped Ladder System $La_{1-x}Sr_xCuO_{2.5}$, *Phys. Rev. B*, **55**, R13373-R13376 (1997).

Nozawa K, Nohara M, Takagi H, Hiroi Z and Takano M: Transport Properties of a Quasi-One Dimensional Ladder Compound $La_{1-x}Sr_xCuO_{2.5}$, *Advances in Superconductivity IX: Proceedings of the 9th International Symposium on Superconductivity (ISS'96), Oct. 21-24, 1996, Sapporo, Japan (ed. Nakajima S and Murakami M), Springer-*

Verlag, Tokyo, **1**, 69-72 (1997).

Takano M and Onodera A: High Pressure Synthesis in Inorganic Systems, *Current Opinion in Solid State & Materials Science*, **2**, 166-173 (1997).

Fujiwara M, Nakanishi M, Fujii T, Takada J, Kusano Y, Takeda Y, Ikeda Y, Takano M and Bando Y: Li Doping into the Bi-2212 Phase by Electrochemical Method, *Funtai oyobi Funmatsu Yakin*, **44**, 142-146 (1997) (in Japanese).

Ohtani T, Honji S and Takano M: Phase Transitions in Quasi-One-Dimensional Selenide $BaNbSe_3$ and Superconductivity in $BaNb_2Se_5$, *J. Solid State Chem.*, **132**, 188-195 (1997).

Saitoh T, Mizokawa T, Fujimori A, Abbate M, Takeda Y and Takano M: Electronic Structure and Temperature-Induced Paramagnetism in $LaCoO_3$, *Phys. Rev. B*, **55**, 4257-4266 (1997).

Saitoh T, Mizokawa T, Fujimori A, Abbate M, Takeda Y and Takano M: Electronic Structure and Magnetic States in $La_{1-x}Sr_xCoO_3$ Studied by Photoemission and X-Ray-Absorption Spectroscopy, *Phys. Rev. B*, **56**, 1290-1295 (1997).

Chong I, Terashima T, Bando Y, Takano M, Matsuda Y, Nagaoka T and Kumagai K: Growth of Pb-Substituted Bi-2201 Single Crystal by Floating Zone Method, *Advances in Superconductivity IX: Proceedings of the 9th International Symposium on Superconductivity (ISS'96), Oct. 21-24, 1996, Sapporo, Japan (ed. Nakajima S and Murakami M), Springer-Verlag, Tokyo*, **1**, 449-452 (1997).

Chong I, Terashima T, Ikeda Y, Bando Y, Takano M, Matsuda Y, Nagaoka T and Kumagai K: Growth of Pb-Substituted Bi-2201 Single Crystal by Floating Zone Method, *Journal of the Korean Physical Society*, **31**, 40-42 (1997).

Kageyama H, Yoshimura K, Kosuge K, Azuma M, Takano M, Mitamura H and Goto T: Magnetic Anistoropy of $Ca_3Co_2O_6$ with Ferromagnetic Ising Chains, *Journal of the Physical Society of Japan*, **66**, 3996-4000 (1997).

IV. Amorphous Materials

Kim S-H and Yoko T: Nonlinear Optical Properties of TeO_2-Based glasses: PbX_2 (X=F, Cl and Br)-TeO_2 Binary Glasses, *Metals. Materials and processes*, **8**, 291-300 (1996).

Uchino T, Kim S-H, Yoko T and Fukunaga T, Strucutre of TeO_2 Glass from Neutron Radial Distribution Functions, Raman Spectra and Ab Initio Molecular Orbital Calculations, *J. Ceram. Soc. Jpn.*, **105**, 201-5 (1997).

Terashima K, Uchino T, Hashimoto T and Yoko T: Structure and Nonlinear Optical Properties of BaO-TiO_2-B_2O_3 Glasses, *J. Ceram. Soc. Jpn.*, **105**, 288-293 (1997).

Monde T, Nakayama N, Tachiiri N, Hukube H, Nemoto F, Yoko T and Konakahara T: Adsorption Characteristics of the Silica-Gels Treated with Fluorinated Silylation Agents, *J. Colloid and Interface Science*, **185**, 111-18 (1997).

Hashimoto T, Ishibashi K and Yoko T: Third-Order Nonlinear Optical Susceptibility of Pb-Complex Perovskite Thin Films Prepared by the Sol-Gel Method, *J. Sol-Gel Science and Technology*, **9**, 211-218 (1997).

Terashima K, Hashimoto T and Yoko T: Nonlinear Optical Properties of B_2O_3-Based Glasses: PbO-Bi_2O_3-B_2O_3 Heavy Metal Oxide Glasses, *Phys. Chem. Glasses*, **38**, 211-217 (1997).

Innocenzi P, Kozuka H and Yoko T: Fluorescence Properties of $Ru(bpy)_3^{2+}$ Complexes Incorporated in Sol-Gel-Derived Silica Coating Films, *J. Phys. Chem.*, B, **101**, 2285-91 (1997).

Kitaoka K, Kozuka H, Hashimoto T, and Yoko T: Preparation of $La_{0.5}Li_{0.5}TiO_3$ Perovskite Thin Films by Sol-Gel Method, *J. Mater. Sci.*, **32**, 2063-70 (1997).

Zhao G-L, Kozuka H and Yoko T: Effects of the Incorporation of Silver and Gold Nanoparticles on the Photoanodic Properties of Rose Bengal Sensitized TiO_2 Films Electrodes Prepared by Sol-Gel Method, *Solar Energy Mater. Solar Cells*, **46**, 219-231 (1997).

Uchino T and Yoko T: Ab Initio Molecular Orbital Calculations on the Boson Peal Frequencies of Molecular Glasses, *Progress of Theoretical Physics Supplement*, **126**, 147-150 (1997).

Ohyama M, Kozuka H and Yoko T: Sol-Gel Preparation of ZnO Films with Extremely Preferred Orientation along the (002) Plane from Zinc Acetate Solution, *Thin Solid Films*, **306**, 78-85 (1997).

Terashima K, Tamura S, Kim S-H and Yoko T: Structure and Nonlinear Optical Properties of Lanthanide Borate Glasses, *J. Am. Ceram. Soc.*, **80**, 2903-09 (1997).

Uchino T and Yoko T: Ab Initio Molecular Orbital Calculations on the Structure and the Low-Frequency Vibrational Modes in B_2O_3 and Alkali Borate Glasses, in Borate Glasses, Crystals & Melts, eds by AC Wright, SA Feller and AC Hannon, *The Society of Glass Technology*, Scheffield (1997) pp 417-424

Kozuka H: Metal Nanoparticles in Gel-Derived Oxide Coating Films: Control and Application of Surface Plasma Resonance, *SPIE*, **3136**, 304-314 (1997).

Lin H, Yanagi T, Seo W-S, Kuwabara K and Koumoto K: Crystal Growth of Hydroxyapatite under Langmuir Monolayers, *Phosphorus Research Bulletin*, **6**, 39-42 (1996).

Lin H, Kuroiwa N, Seo W-S, Kuwabara K and Koumoto K: Preparation of Metallic Crystals by Langmuir-Blodgett Technique, *Molecular Crystals and Liquid Crystals*, **295**, 129-132 (1997).

Lin H and Koumoto K: Crystallization Control Based on Molecular Recognition phenomena at Inorganic-Organic Interfaces, *Catalysts and Catalysis*, **39(7)**, 572-579 (1997). (in Japanese)

FUNDAMENTAL MATERIAL PROPERTIES

I. Molecular Rheology

Osaki K, Watanabe H, Inoue T: Creep Behavior of the Factorable BKZ Constitutive Model *Nihon Reoroji Gakkaishi*, **25**, 173–174(1997)

Urakawa O, Watanabe H: Dielectric Relaxation of Dipole-Inverted cis-Polyisoprene in Solutions: Concentration Dependence of the Second Mode Relaxation Time *Macromolecules*, **30**, 652–654 (1997).

Watanabe H: Linear Viscoelasticity of Polymer Melts and

Solutions", in Osaki K Ed., "Experimental Methods for Polymers (Kobunshi Jikken-Gaku)", Kyoritsu (Tokyo), Vol.8, Chapter 4, pp. 165–213, 1997.(in Japanese)

Watanabe H: Rheology of Diblock Copolymer Micellar Systems *Acta Polymerica*, **48**, 215–233 (1997).

Watanabe H, Sato T, Osaki K, Yao ML,Yamagishi A: Rheological and Dielectric Behavior of a Styrene-Isoprene-Styrene Triblock Copolymer in Selective Solvents: 2.Contribution of Loop-type Middle Blocks to Elasticity and Plasticity *Macromolecules*, **30**, 5877–5892(1997).

Watanabe H, Yao ML, Sato T, Osaki K: Non-Newtonian Flow Behavior of Diblock Copolymer Micelles: Shear-Thinning in a Nonentangling Matrix *Macromolecules*, **30**, 5905–5912 (1997).

Watanabe H: Rheology of Suspensions *J. Jap. Soc. Col. Mat.*, **70**, 468–475 (1997).

Watanabe H, Yao ML,Osaki K, Shikata T, Niwa H, Morishima Y: Nonlinear Rheology of A Concentrated Spherical Silica Suspension: 2. Role of Strain in Shear-Thickening *Rheol. Acta*, **36**(5), 524–533 (1997).

Inoue T, Osaki K: Rheo-optics in Osaki K Ed., "Experimental Methods for Polymers (Kobunshi Jikken-Gaku)", Kyoritsu (Tokyo), Vol.8, Chapter 4, pp. 301–324, 1997.(in Japanese)

Inoue T, Hwang EJ, Osaki K: Birefringence of amorphous polyarylates: 2. Dynamic Measurement on a Polyarylate with Low Optical Anisotropy *Polymer*, **5**, 1029–1034(1997).

Inoue T, Matsui H, Murakami S, Kojiya S, Osaki K: Strain - Induced Birefringence and Molecular Structure of Glassy Polymers *Polymer*, **5**, 1215–1220(1997).

Inoue T, Matsui H,Osaki K: Molecular Origin of Viscoelasticity and Chain Orientation of Glassy Polymers, *Rheol. Acta*, **36**, 239–244 (1997).

II. Polymer Materials Science

Imai M and Kaji K: Ordering Process in the Induction Period of Polymer Crystallization, *Kotaibutsuri*, **32**, 449-458 (1997). (in Japanese)

Kaji K and Imai M: Dynamics in the Induction Period of Polymer Crystallization, *Kobunshi*, **46**, 765-771 (1997). (in Japanese)

Nomura S and Kaji K: From the Micell Model to the Fringed-Micell Model, *Sen'i gakkaishi*, **53**, 129-131 (1997). (in Japanese)

Kaji K: From the Fringed-Micell Microfibril Model to the Shish-Kebab Model, *Sen'i gakkaishi*, **53**, 132-136 (1997). (in Japanese)

Yamamuro O, Tsukushi I, Matsuo T, Takeda K, Kanaya T and Kaji K: Inelastic neutron scattering study of low-energy excitations in vapor-deposited glassy propylene, *J. Chem. Phys.*, **105**, 2997-3002 (1997).

Kanaya T, Kaji K, Bartos J and Klimova M: Onset of the Fast Process in Amorphous Polypropylene as Detected by Quasielastic Neutron Scattering and Electron Spin Resonance Techniques, *Macromolecules*, **30**, 1101-1104 (1997).

Kanaya T, Tsukushi I and Kaji K: Non-Gaussian Parameter and Heterogeneity of Amorphous Polymers, *Prog. Theor. Phys. Suppl.*, **126**, 133-140 (1997).

Yamamuro O, Tsukushi I, Matsuo T, Takeda K, Kanaya T and Kaji K: Low Energy Excitations in Simple Molecular Glasses, *Prog. Theor. Phys. Suppl.*, **126**, 93-96 (1997).

Baros J, Kristiak J and Kanaya T: Free volume and microscopic dynamics in amorphous polymers, *Physica*, **B 234/236**, 435-436 (1997).

Bartos J, Bandzuch P, Sausa O, Kristiakova K, Kristiak J, Kanaya T and Jenninger: Free Volume Microstructure and Its Relation to the Chain Dynamics in cis-1,4-Polybitadiene As Seen by Positron Annihilation Lifetime Spectroscopy, *Macromolecules*, **30**, 6906-6912 (1997).

Kanaya T: Dynamics of Glassy Polymers and Glass Transition, *Molecular Electronics and Bioelectronics*, **8**, 2-16 (1997).(in Japanese)

Kanaya T: Slow Motion of Macromolecules, *RADIOISOTOPES*, **46**, 317-321 (1997).(in Japanese)

Kanaya T, Shibata K and Ikeda S: High Energy-resolution Spectrometer LAM-80ET, *Neutron News*, **8**, 34-37 (1997).

Kanaya T and Izumi Y: New Experimental Polymer Science 6, chap. 3, sec. 3 and 4, ed. The Society of Polymer Science, Japan, Kyoritsu Press, Tokyo, 333-351, 351-357 (1997). (in Japanese)

Kanaya T: Anomalous Heat Capcity at low Temperatures and Low Energy Excitations in Glassy Polymers - Inelastic Neutrons Scattering in Polymer Research, *Kobunshi Kako*, **46**, 40-43 (1997). (in Japanese)

Nishida K, Urakawa H, Kaji K, Gabrys B and Higgins J S: Electrostatic Persistence Length of NaPSS Polyelectrolytes Determined by a Zero Average Contrast SANS Technique, *POLYMER*, **38**, 6083-6085 (1997).

III. Molecular Motion Analysis

Horii F, Masuda K and Kaji H: CP/MAS ^{13}C NMR Spectra of Frozen Solutions of Poly(vinyl alchol) with Different Tacticities, *Macromolecules*, **30**, 2519-2520 (1997).

Ishida H, Kaji H and Horii F: Solid-State NMR Analyses of the Structure and Chain Conformation of Thermotropic Liquid Crystalline Polyurethane Crystallized from the Melt through the Liquid Crystalline State, *Macromolecules*, **30**, 5799-5803 (1997).

Kaji H and Horii F: One- and Two-Dimensional Solid-State ^{13}C NMR Analyses of the Solid Structure and Molecular Motion of Poly(ε-caprolactone) Isothermally Crystallized from the Melt, *Macromolecules*, **30**, 5791-5798 (1997).

Kuwabara K, Kaji H and Horii F: Solid-State NMR Analyses of the Crystalline-Noncrystalline Structure for Metallocene-Catalyzed Linear Low-Density Polyethylene, *Macromolecules*, **30**, 7516-7521 (1997).

Horii F, Yamamoto H and Hirai A: Microstructural Analysis of Microfibrils of Bacterial Cellulose, *Macromol. Symp.*, **120**, 197-205 (1997).

Hirai A, Tsuji M and Horii F: Culture Conditions Producing Structure Entities Composed of Cellulose I and II in Bacterial Cellulose, *Cellulose*, **4**, 239-245 (1997).

Horii F: Bacterial Cellulose—Structural Formation in the Biogenesis, *Kagaku*, **52**, 70-71 (1997) (in Japanese).

Hirai A, Tsuji M and Horii F: Formation of Cellulose II Crystal in Bacterial Cellulose, *Cellulose Commum.*, **4**, 21-24 (1997) (in Japanese).

Nonaka T and Horii F: New Polymeric Materials as Speaker Cones, *Koubunshi Kakou*, **46**, 368-373 (1997) (in Japanese).

Kaji H, Tai T and Horii F: Two-Dimensional Solid-State NMR Analyses of Medium-Range Molecular Motion of Polymers, *Proc. Soc. Solid-State NMR Mater.*, **No. 21** , 35-39 (1997) (in Japanese).

Kaji H: Analyses of Conformation and Local Structure of Polymers by Two-Dimensional Solid-State NMR Method, *Kaigai Koubunshi Kenkyu*, **43**, 107-108 (1997) (in Japanase).

ORGANIC MATERIALS CHEMISTRY

I. Polymeric Materials

Fukuda T, Ide N and Ma Y-D: Propagation and Termination Processes in Free Radical Copolymerization, *Macromol. Symp*., **111**, 305-315 (1996).

Takaragi A, Sugiura M, Minoda M, Miyamoto T and Watanabe J: Oligosaccharide-based Thermotropic Liquid Crystals 4; Synthesis of Cellobiose-based Twin and Triplet Derivatives and Their Mesophase Properties, *Macromol. Chem. Phys.*, **198**, 2583-2598 (1997).

Nishimura H, Donkai N and MiyamotoT: Temperature-Responsive Hydrogels from Cellulose, *Macromol. Symp.*, **120**, 303-313 (1997).

Nishimura H, Donkai N and Miyamoto T: Preparation and Properties of a New Type of Comb-shaped, Amphiphilic Cellulose Derivative, *Cellulose*, **4**, 89-98 (1997).

Liu H-Q, Zhang L-N, Takaragi A and Miyamoto T: Effect of Substituent Distribution on Water Solubility of *O*-Methylcellulose, *Cellulose*, **4**, 321-327 (1997).

Liu H-Q, Zhang L-N, Takaragi A and Miyamoto T: Water Solubility of Regioselectively 2,3-*O*-Sbstituted Carboxymethylcellulose, *Macromol. Rapid Commun.*,**18**, 921-925 (1997).

Goto A, Terauchi T, Fukuda T and Miyamoto T: Gel Permeation Chromatographic Determination of Activation Rate Constants in Nitroxide-Controlled Free Radical Polymerization, 1 Direct Analysis by Peak Resolution, *Macromol. Rapid Commun.*, **18**, 673-682 (1997).

Fukuda T and Goto A: Gel Permeation Chromatographic Determination of Activation Rate Constants in Nitroxide-Controlled Free Radical Polymerization, 2 Analysis of Evolution of Polydispersities, *Macromol. Rapid Commun.*, **18**, 683-688 (1997).

Ohno K, Tsujii Y and Fukuda T: Mechanism and Kinetics of Nitroxide-Controlled Free Radical Polymerization. Thermal Decomposition of 2,2,6,6-Tetramethyl-1-polystyroxypiperidines, *Macromolecules*, **30**, 2503-2506 (1997).

Ide N and Fukuda T: Nitroxide-Controlled Free Radical Copolymerization of Vinyl and Divinyl Monomers. Evaluation of Pendant-Vinyl Reactivity, *Macromolecules*, **30**, 4268-4271 (1997).

Goto A and Fukuda T: Effects of Radical Initiator on Polymerization Rate and Polydispersity in Nitroxide-Controlled Free Radical Polymerization, *Macromolecules*, **30**, 4272-4277 (1997).

Goto A and Fukuda T: Mechanism and Kinetics of Activation Processes in A Nitroxide-Mediated Polymerization of Styrene, *Macromolecules*, **30**, 5183-5186 (1997).

Okamura H, Terauchi T, Minoda M, Fukuda T and Komatsu K: Synthesis of 1,4-Dipolystyryldihydro[60]fullerenes by Using 2,2,6,6-Tetramethyl-1-polystyroxypiperidine as a Radical Source, *Macromolecules*, **30**, 5279-5284 (1997).

Gawronski M, Donkai N, Fukuda T and Miyamoto T: Triple Helix of the Polysaccharide Cinerean in Aqueous Solution, *Macromolecules*, **30**, 6994-6996 (1997).

Ide N, Oguchi A, Tsujii Y, Fukuda T, Miyamoto T, Higashida N and Chujo Y: Gelation of Styrene-Acrylonitrile Copolymer via Cyclodiborazane Formation, *Nihon Reoroji Gakkaishi*, **25,** 197-198 (1997). (in Japanese)

Fukuda T, Ohno K, Goto A, Tsujii Y and Miyamoto T: Synthesis of New Polymer Materials by "Living" Radical Polymerization, *Kasen-Kouenshu*, **54**, 1-10 (1997). (in Japanese)

II. High-Pressure Organic Chemistry

Nishinaga T, Kawamura T, Komatsu K: Synthesis, Structure, and Redox Behavior of the Dehydroannulenes Fused with Bicyclo[2.2.2]octene Frameworks, *J. Org. Chem.*, **62**, 5354-5362 (1997).

Matsuura A, Nishinaga T, Komatsu K: Synthesis and Electronic Properties of Anthracene Fully Annelated with Bicyclo[2.2.2]octene Frameworks,
Tetrahedron Lett., **38**, 3427-3430 (1997).

Matsuura A, Nishinaga T, Komatsu K: Reactions of a Novel Benzyne Annelated with Two Bicyclo[2.2.2]octene Units, *Tetrahedron Lett.*, **38**, 4125-4128 (1997).

Wang G-W, Komatsu K, Murata Y, Shiro M: Synthesis and X-Ray Structure of Dumb-bell-shaped C_{120}, *Nature*, **387**, 583-586 (1997).

Murata Y, Shiro M, Komatsu K: Synthesis, X-Ray Structure, and Properties of the First Tetrakisadduct of Fullerene C_{60} Having a Fulvene-Type π-System on the Spherical Surface, *J. Am. Chem. Soc.*, **119**, 8117-8118 (1997).

Tanaka T, Kitagawa T, Komatsu K, Takeuchi K: Synthesis of a Hydrocarbon Salt Having a Fullerene Framework: *J. Am. Chem. Soc.*, **119**, 9313-9314 (1997).

Kitagawa T, Tanaka T, Takata Y, Takeuchi K, Komatsu K: Ionically Dissociative Hydrocarbons Containing the C_{60} Skeleton: *Tetrahedron*, **53**, 9965-9976 (1997).

Mori S, Karita T, Komatsu K, Sugita N, Wan TSM: High-Pressure Synthesis of Cycloadduct of Fullerene C_{60} with 2H-Pyran-2-one: *Synth. Commun.*, **27**, 1475-1482 (1997).

Kudo K, Ikoma F, Mori S, Komatsu K, Sugita N: Synthesis of Oxalate from Carbon Monoxide and Carbon Dioxide in the Presence of Caesium Carbonate, *J. Chem. Soc.*, Perkin Trans.2, 679-682 (1997).

Kudo K, Oida Y, Mori S, Komatsu K, Sugita N: Palladium(II)-Catalyzed Hydroesterification of Enol Esters: Remarkable a-Substituent Effect upon Regioselectivity, *React. Kinet. Catal. Lett.*, **59**, 29-33 (1996).

Okamura H, Terauchi T, Minoda M, Fukuda T, Komatsu K: Synthesis of 1,4-dipolystyryldihydro[60]fullerenes by Using 2,2,6,6-Tetramethyl-1-polystyroxypiperidine as a Radical Source, *Macromolecules*, **30**, 5279-5284 (1997).

Okamura H, Minoda M, Komatsu K, Miyamoto T: Synthesis of C60-Capped Vinyl Ether Oligomers by Living Cationic Polymerization Technique, *Macromolecular Chem. Phys.*, **198**, 777-786 (1997).

Komatsu K, Wang G-W, Murata Y, Shiro M: Synthesis of the Fullerene Dimer C_{120} by a Solid State Reaction, *Fullerens:*

Recent Advances in the Chemistry and Physics of Fullerenes and Related Materials, R. S. Ruoff and K. M. Kadish Eds; Electrochemical Society, Pennington, N.J., **4**, 290-297 (1997).

Komatsu K, Murata Y: Synthesis and Electrochemical Behavior of a Fullerenyl Anion Having Five Organic Addends Around the cyclopentadienide Ring on the C_{60} Surface, *Fullerens: Recent Advances in the Chemistry and Physics of Fullerenes and Related Materials*, R. S. Ruoff and K. M. Kadish Eds; Electrochemical Society, Pennington, N.J., **4**, 199-208 (1997).

Komatsu K: The Organic Chemistry of Fullerene, *SUT Bulletin*, **14** (12), 29-33 (1997) (in Japanese).

SYNTHETIC ORGANIC CHEMISTRY

I. Synthrtic Design

Yamaguchi S, Ohno S, and Tamao K: Pd(II)-Catalyzed Oxidative Homo-Coupling of Aryl-Metal Compounds Using Acrylate Dibromide Derivatives as Effective Oxidants, *Synlett*, 199-1201 (1997).

Kawachi A, Tanaka Y, and Tamao K: Synthesis and Structures of Tris[2-(dimethylamino)phenyl]silane and -germane Compounds, *Organometallics*, **16**, 5102-5107 (1997).

Toshimitsu A, Hirosawa C, Nakano K, Mukai T, and Tamao K: Stereospecific Transformations of Chiral Compounds Using Anchimeric Assistance of Arylthio and Arylseleno Group, *Phosphorus, Sulfur, and Silicon*, **120 &121**, 355-356 (1997).

Toshimitsu A, Terada M, and Tamao K: Intramolecular Cyclization Reaction via a Sterically Protected Episelenonium Ion Intermediate, *Chem. Lett.*, 733-734 (1997).

Yamaguchi S, Jin R.-Z, Tamao K, and Shiro M: Silicon-Catenated Silole Oligomers: Oligo(1,1-silole)s, *Organometallics*, **16**, 2486-2488 (1997).

Yamaguchi S, Jin R.-Z, Tamao K, and Shiro M: Synthesis of a Series of 1,1-Difunctionalized Siloles, *Organometallics*, **16**, 2230-2232 (1997).

Kawachi A and Tamao K: Preparations and Reactions of the Functionalized Silyllithiums (Accounts), *Bull. Chem. Soc. Jpn.*, **70**, 945-955 (1997).

Yamaguchi S, Jin R.-Z, Shiro M, and Tamao K: A New Example of the Linear Disiloxanes: Synthesis and X-ray Crystal Structure of Bis(2-silolyl)tetramethyldisiloxane, *Chem. Heterocyclic Comp.*, **356**, 180 - 185 (1997).

Tamao K, Sun G.-R, Kawachi A, and Yamaguchi S: Regioselective Synthesis of Polyfunctionalized Alkyl-Trisilanes and Tetrasilanes via Reductive Cross-Coupling Reaction of (Amino)alkylsilyl Chlorides with Lithium, *Organometallics*, **16**, 780-788 (1997).

Kawachi A, Doi N, and Tamao K: The Sila-Wittig Rearrangement, *J. Am. Chem. Soc.*, **119**, 233-234 (1997).

II. Fine Organic Synthesis

Nishide K, Nakamura D, Yokota K, Sumiya T, Node M, Ueda M and Fuji K: A Silver Salt-Iodine Reagent System for the Deprotection of Monothioacetals and Dithioacetals, *Hetrocycles*, **44**, 393-404 (1997).

Aoki H, Fuji K and Miyajima K: Effects of blood on the uptake of charged liposomes by perfused rat liver: cationic glucosamine-modified liposames interct with erthrocyte and escape phagocytosis by macrophages, *Internat. J. Pharmaceutics*, **149**, 15-23 (1997).

Aoki H, Tottori T, Sakurai F, Fuji K and Miyajima K: Effects of positive charge density on the liposomal surface on disposition kinetics of liposomes in rats, *Internat. J. Pharmaceutics*, **156**, 163-174 (1997).

Kawabata T, Nagato M, Takasu K and Fuji K: Nonenzymatic Kinetic Resolution of Racemic Alcohols through an "Induced Fit" Process, *J. Am. Chem. Soc.*, **119**, 3169-3170 (1997).

Aoki H, Fujita M, Sun C, Fuji K and Miyajima K: High-Efficiency Entrapment of Superoxide Dismutase into Cationic Liposomes Containing Synthetic Aminoglycolipid, *Chem. Pharm. Bull.*, **45**, 1327-1331 (1997).

Fuji K, Sakurai M, Kinoshita T, Tada T, Kuroda A and Kawabata T: Assessment of the Activity of 8-Diphenylphosphino-8'-methoxy-1,1'-binaphthyl as a Ligand for Palladium-Catalyzed Reactions, *Chem. Pharm. Bull.*, **45**, 1524-1526 (1997).

Tanaka K, Asakawa N, Nurruzzaman M and Fuji K: Use of 8,8'-dihydroxy-1,1'-binaphthalene as a chiral anxiliary for asymmetric Diels-Alder cycloadditions, *Tetrahedron: Asymmetry*, **8**, 3637-3645 (1997).

Tanaka K, Watanabe T, Ohta Y and Fuji K: Formation of non-racemic *E* -and *Z* -olefins based on discrimination of enantiotopic carbonyl groups in a-diketones by a chiral phosphonate reagent, *Tetrahedron Lett.*, **38**, 8943-8946 (1997).

BIOORGANIC CHEMISTRY

I. Bioorganic Reaction Theory

Ishihara K, Nishitani M, Yamaguchi H, Nakajima N, Ohshima T, Nakamura K: Preparation of Optically Active α-Hydroxy Esters: Stereoselective Reduction of α-Keto Esters Using Thermophilic Actinomycetes. *J. Ferment. Bioeng.*, **84**, 268-270 (1997).

Horiuchi A, Ikeda A, Kanamori M, Hosokawa H, Sugiyama T, Takahashi T: A New Synthesis of *trans*-Iodohydrins Using Iodine-cerium(IV) Salts. *J. Chem. Res., Synop.*, 60-61 (1997).

Kano K, Negi S, Kawashima A, Nakamura K: Optical Resolution of 1-Arylethanols Using Transesterification Catalyzed by Lipases. *Enantiomer*, **2**, 261-266 (1997).

Kawai Y, Takanobe K, Ohno A: Stereochemical Control in Microbial Reduction. XXIX. Mechanism of Stereochemical Control with an Additive in the Diastereoselective Reduction by *Geotrichum candidum*. *Bull. Chem. Soc. Jpn.*, **70**, 1683-1686 (1997).

Kawai Y, Kunitomo J, Ohno A: A Novel Function of an Atropisomeric Flavin Model as a Host Compound. *Acta Crystallogr.*, **C53**, 513-515 (1997).

Kawai Y, Ohno A: Fundamentals of Biofine Chemicals. Enzymes in Organic Synthesis. *Kikan Kagaku Sosetsu*, **33**, 7-19 (1997) (in Japanese).

Kimura T, Hanzawa M, Horn E, Kawai Y, Ogawa S, Sato R: Preparation and Conformational Analysis of 6,10-Disubstituted[1,2,3]trithiolo[h]benzopentathiepin Monooxides. *Tetrahedron Lett.*, **38**, 1607-1610 (1997).

Nakajima N, Ishihara K, Matsumura S, Hamada H, Nakamura K, Furuya T: Lipase-catalysed Synthesis of Arbutin Cinnamate in an Organic Solvent and Application of Transesterification to Stabilize Plant Pigments. *Biosci. Biotech. Biochem.*, **61**, 1926-1928 (1997).

Nakamura K, Kondo S, Kawai Y, Nakajima N, Ohno A: Amino Acid Sequence and Characterization of Aldo-keto Reductase

from Bakers' Yeast. *Biosci. Biotechnol. Biochem.*, **61**, 375-377 (1997).

Nakamura K: Artificial Regulation of Biocatalytic Reaction. *Kagaku to Seibutsu*, **35**, 590-598 (1997) (in Japanese).

Ogawa S, Kikuchi M, Kawai Y, Sato R: Synthesis, Structure, and One-electron Redox Reactions of Novel Benzodithiolium Salts. *Phosphorus, Sulfur and Silicon*, **120-121**, 433-434 (1997).

Ohno A: The Simplest Reaction in Organic Chemistry - Transition State of Proton - Transfer Reaction. Maruzen, Tokyo (1997) (in Japanese).

Ohno A: Organic Chemistry of Enzyme Catalysis. Maruzen, Tokyo (1997) (in Japanese).

Ohno A, Kunitomo J, Kawai Y: Physical Properties of Atropisomeric 5-Deazaflavin Derivatives. *Tetrahedron*, **53**, 4601-4610 (1997).

Okamura M, Hazama K, Ohta M, Kato K, Horaguchi T, Ohno A: Exalted Resonance Effect in the Aryl-assisted Solvolyzes of 2-Aryl-2-(trifluoromethyl)ethyl m-Nitrobenzenesulfonates. *Chem. Lett.*, 973-974 (1997).

Tanaka K, Kume T, Takimoto T, Kitahara Y, Suzuki H, Osuga H, Kawai Y: Synthesis, Structure and Properties of [7]Heterohelicenes Possessing Phenolic Hydroxy Functions. *Chem. Lett.*, 501-502 (1997).

Yamazaki N, Okamura M, Kawai Y, Mikata Y, Ohno A: Stereospecific Redox Reaction Directed by a Sulfinyl Group. *Phosphorus, Sulfur and Silicon*, **120-121**, 445-446 (1997).

Yasui S, Tsujimoto M, Shioji K, Ohno A: Dichotomy in the Reactivity of Trivalent Phosphorus Compounds Z_3P (Z=Ph, nBu, OR) Observed in the Photoreaction with a Ruthenium Complex. *Chem. Ber.*, **130**, 1699-1707 (1997).

II. Bioactive Chemistry

Ishiguro T, Saito J, Yawata H, Otsuka M, Inoue T, Sugiura Y: Fluorescence Detection of Specific Sequence Nucleic Acids by Oxazole Yellow-Linked Oligonucleotides. Homogeneous Quantitative Monitoring of in vitro Transcription. *Nucleic Acids Res.*, **24**, 4992-4997 (1996).

Sugiura Y, Nagaoka M: Reccognition of DNA Sequence and DNA Bending. Molecular Design for Artificial Repressors. *J.Syn.Org.Chem.Jpn.*, **55**, 384-392 (1997) (in Japanese).

Otsuka M, Fujita M, Sugiura Y, Yamamoto T, Inoue J, Maekawa T, Ishii S: Synthetic Inhibitors of Regulatory Proteins Involved in the Signaling Pathway of the Replication of Human Immunodeficiency Virus I. *Bioorg. Med.Chem.*, **5**, 205-215 (1997).

Sugiura Y, Totsuka R, Araki M, Okuno Y: Selective Cleavage of $tRNA^{Phe}$ with Secondary and Tertiary Structures by Enediyne Antitumor Antibiotics. *Bioorg. Med. Chem.*, **5**, 1229-1234 (1997).

Kigoshi H, Kitamura Y, Fujita T, Ohashi E, Atsumi T, Mutou T,Yamada K, Kusakabe T, Sasaki D, Sugiura Y: New Synthetic Analogues of the Bracken Ultimate Carcinogen. Elevation of Stability and Alteration of DNA Alkylation Site Selectivity. *Tetrahedron Lett.*, **38**, 3235-3238 (1997).

Morii T, Saimei Y, Okagami M, Makino K, Sugiura Y: Factors Governing the Sequence-Selective DNA Binding of Geometrically Constrained Peptide Dimers. *J. Am. Chem. Soc.*, **119**, 3649-3655 (1997).

Takahashi T, Yamada T, Matsumoto T, Sugiura Y: Synthesis of Nine-Membered, Masked Enediyne Analogues with DNA Intercalators and Its DNA Cleaving Activities. *Angew. Chem. Int. Ed. Engl.*, **36**, 1524-1526 (1997).

Saegusa N, Yokono M, Matsushita K, Sugiura Y: Different Contributions of Three Zinc Fingers of Transcription Factor Sp1 to DNA Recognition: Novel Binding Mode of N-Terminal Finger1. *Nucleic Acids Res. (Sym.Ser.)*, **37**, 151-152 (1997).

Kamiuchi T, Imanishi M, Abe E, Sugiura Y: New Multi Zinc Finger Protein. Biosynthetic Design and Characteristics of DNA Recognition. *Nucleic Acids Res. (Sym.Ser.)*, **37**, 153-154 (1997).

Aizawa Y, Morii T, Sugiura Y: Selective Recognition of Tandemly Repeated DNA Sequences by Homo- and Hetero-Dimers of Short Peptides. *Nucleic Acids Res. (Sym.Ser.)*, **37**, 311-312 (1997).

III.Molecular CLinical Chemistry

Ueda K: Possible role of poly(ADP-ribose) synthetase in neuronal degeneration., *Acta Neurobiologiae Experimentalis*, **57**, S47 (1997).

Li S, Mallory M, Alford M, Tanaka S, Masliah E: Glutamate transporter alterations in Alzheimer's disease are possibly associated with abnormal APP expression., *J. Neuropathol. Exp. Neurol.*, **56**, 901-911 (1997).

Ueda, K: Poly(ADP-ribose) synthetase : A multifunctional guardian of genomic DNA., *Proc. of 16th Annual Convention of Indian Association for Cancer Research and National Symposium on New Insights into the Molecular Mechanism of Oncogenesis*, 2-3 (1997).

Adachi, Y, Nishikimi, A, Teraoka, H, Ueda, K: Apoptotic degradation and subcellular localization of PARP regulated by phoshorylation., *Proc. of 12th International Symposium on ADP-ribosylation Reactions : From Bacterial Pathogenesis to Cancer*, 56 (1997).

Ariumi Y, Masutani M, Copeland TD, Mimori T, Sugimura T, Ueda K, Hatanaka M: Interaction of DNA-dependent protein kinase with poly(ADP-ribose) polymerase (PARP)., *Proc. of 12th International Symposium on ADP-ribosylation Reactions : From Bacterial Pathogenesis to Cancer*, 106 (1997).

Ueda K, Nishikimi A, Ariumi Y, Tokime T, Teraoka H, Strosznajder J, Tanaka S, Adachi Y: Poly(ADP-ribose) synthetase as a genome guardian., *Proc. of 1st Japan-Italy Bilateral Seminar on ADP-ribose and Nitric Oxide: Role in Cell Differentiation, Growth and Death*, 9-11 (1997).

Ueda K: Present status and future of gene diagnosis., in *Gene Diagnosis and Therapy 97"* (M. Muramatsu, ed), Igaku-shoin, 7-10 (1997). (in Japanese)

Ueda K: Gene and diseases; introduction., in *Progress of Molecular Biology (vol. 4), Medical Molecular Biology*, Asakura-shoten, 132-135 (1997). (in Japanese)

Ueda K: Gene and diseases; gene diagnosis., in *Progress of Molecular Biology (vol. 4), Medical Molecular Biology*, Asakura-shoten, 142-146 (1997). (in Japanese)

Tanaka S, Ueda K: Molecular genetics of Alzheimer's disease., *Gene & Medicine*, **1**, 62-71 (1997). (in Japanese)

Tanaka S: Gene diagnosis of Alzheimer's disease., *Saishin-Igaku*, **52**, 2160-2169 (1997). (in Japanese)

MOLECULAR BIOFUNCTION

I. Functional Molecular Conversion

Hiratake J and Oda J: Aminophosphonic and Aminoboronic Acids As a Key Element of Transition-State Analogue Inhibitor of Enzymes, *Biosci. Biotech. Biochem*, **61**, 211-218 (1997).

Hiratake J and Oda J: Organic Synthesis and Catalytic Antibodies, *J. Synthetic Org. Chem*., Japan, **55**, 452-459 (1997). (in Japanese)

Hiratake J: Transition-state Analogues: the Point of Contact between Enzyme Catalysis and Organic Chemistry, *Enzyme Engineering News* **38**, 21-25 (1997). (in Japanese)

Kato H and Oda J: Four-dimensional Structure of Enzyme: Watching enzyme at work by Time-Resolved X-Ray Crystallography, *Bioscience and Industry*, **55** (7), 32-34 (1997). (in Japanese)

Kato H: Supporting strategies of Protein Crystallization by Dynamic Light Scattering, *Nippon Kessyou Gakkaishi*, **39**, 315-319 (1997). (in Japanese)

Koiwa H, Kato H, Nakatsu T, Oda J, Yamada Y and Sato F: Purification and Characterization of Tobacco Pathogenesis-Related Protein PR-5d, an Antifungal Thaumatin-like Protein, *Plant Cell Physiol.*, **38**, 783-791 (1997).

Oda J: Reaction Mechanism of Glutathione Synthetase, *Kagaku*, 52(9), **23** (1997). (in Japanese)

II. Molecular Microbial Science

Liu J.-Q., Kurihara T, Miyagi M, Tsunasawa S, Nishihara M, Esaki N, Soda K: Paracatalytic Inactivation of L-2-Haloacid Dehalogenase from *Pseudomonas* sp. YL by Hydroxylamine, *J. Biol. Chem.*, **272**, 3363-3368 (1997)

Mihara H, Kurihara T, Yoshimura T, Soda K, Esaki N: Cysteine Sulfinate Desulfinase, a NIFS-like Protein of *Escherichia coli* with Selenocysteine Lyase and Cysteine Desulfurase Activities, *J. Biol. Chem.*, **272**, 22417-22424 (1997)

Galkin A, Kulakova L, Ohshima T, Esaki N, Soda K: Construction of a New Leucine Dehydrogenase with Preferred Specificity for $NADP^+$ by Site-directed Mutagenesis of the Strictly NAD^+-specific Enzyme. *Protein Engineering*, **10**, 687-690 (1997)

Inoue H, Inagaki K, Eriguchi S, Tamura T, Esaki N, Soda K, Tanaka H: Molecular Characterization of the *mde* Operon Involved in L-Methionine Catabolism of *Pseudomonas putida*, *J. Bacteriol.*, **179**, 3956-3962 (1997)

Nardi-dei V, Kurihara T, Park C, Esaki N, Soda K: Bacterial DL-2-Haloacid Dehalogenase from *Pseudomonas* sp. Strain 113: Gene Coning and Structural Comparison with D- and L-2-Haloacid Dehalogenases, *J. Bacteriol.*, **179**, 4232-4238 (1997)

Galkin A, Kulakova L, Yoshimura T, Soda K, Esaki N: Synthesis of Optically Active Amino Acids from a-Keto Acids with *Escherichia coli* Cells Expressing Heterologous Genes, *Appl. Environ. Microbiol.*, **63**, 4651-4656 (1997)

Galkin A, Kulakova L, Yamamoto H, Tanizawa K, Tanaka H, Esaki N, Soda K: Conversion of a-Keto Acids to D-Amino Acids by Coupling of Four Enzyme Reactions, *J. Ferment. Bioeng.*, **83**, 299-300 (1997)

Liu L, Yoshimura T, Endo K, Esaki N, Soda K: Cloning and Expression of the Glutamate Racemase Gene of *Bacillus pumilus*, *J. Biochem.*, **121**, 1155-1161 (1997)

Kishimoto K, Yoshimura T, Soda K, Esaki N: Mutation of Arginine 98, Which Serves as a Substrate-Recognition Site of D-Amino Acid Aminotransferase, Can Be Compensated for by Mutation of Tyrosine 88 to an Arginyl Residue, *J. Biochem.*, **122**, 1182-1189 (1997)

Soda K, Esaki N, Kurihara T, Liu J.-Q, Nardi-Dei V, Nishihara M, Hata Y, Fujii T, Hisano T, Tsunaswa S. Miyagi M: 2-haloacid Dehalogenase: Structure and Catalytic Mechanism, *Mechanisms of Biohalogenation and Dehalogenation* (D. B. Janssen, K. Soda and R. Wever eds.),157-166 (1997)

Kurihara T, Nardi-Dei V, Park C, Esaki N, Soda K, Tsunaswa S. Miyagi M: Characteristics of DL-2-haloacid Dehalogenase, *Mechanisms of Biohalogenation and Dehalogenation* (D. B. Janssen, K. Soda and R. Wever eds.),167-174 (1997)

Esaki N, Yoshimura T: Classification of Pyridoxal Enzymes Based on Stereospecificity of Hydrogen Transfer, *RADIOISOTOPES*, **46**, 327-329 (1997) (in Japanese)

MOLECULAR BIOLOGY AND INFORMATION

I. Biopolymer Structure

Fujii T, Hata Y, Oozeki M, Moriyama H, Wakagi T, Tanaka N and Oshima T: The Crystal Structure of Zinc-Containing Ferredoxin from the Thermoacidophilic Archaeon *Sulfolobus* sp. Strain 7, *Biochemistry*, **36**, 1505-1513 (1997).

Fujii T, Wakagi T and Hata Y: The Structure of a Thermoacidophilic Archaeal Ferredoxin with a Novel Zinc Binding Center Crucial for Thermostabilization, *J. Inorg. Biochem.* **67**, 264 (1997).

Hata Y and Fujii T: Crystallograhic Analysis of the Tertiary Structure and Reaction Mechanism of L-2-Haloacid dehalogenase, *Nippon Kesshougaku Kaishi*, **39**, 358-365 (1997) (in Japanese).

Ishiguro R and Takahashi S: ATR-IR spectroscopy and studies of lipid-peptide interaction, *Jasco Report*, **39**, 12-19 (1997) (in Japanese).

Kojoh K, Fujii T, Matsuzawa H and Wakagi T: A Dicluster Ferredoxin from the Thermoacidophilic Archaeon *Sulfolobus* sp. strain 7 is Highly Stabilized by its Inherent Zinc and N-Terminal Extra Stretch, *J. Inrog. Biochem.*, **67**, 265 (1997).

Kumar A, Reddy V S, Yushibov V, Chipman P R, Hata Y, Fita I, Fukuyama K, Rossmann M G, Loesch-Fries L S, Baker T and Johnson J E: The Structure of Alfalfa Mosaic Virus Capsid Protein Assembled as a T=1 Icosahedral Particle at 4.0-Å Resolution, *J. Virology*, **71**, 7911-7916 (1997).

Ozawa S, Hayashi R, Mazuda A, Ito T. and Takahashi S: Reconstitution of bacteriorhodopsin from a mixture of a proteinase V8 fragment and two synthetic peptides, *Biochem. Biophys. Acta*, **1323**, 145-153 (1997).

Sano Y, Inoue H, Kajiwara K, Hiragi Y and Isoda S: Structural Analysis of A-Protein of Cucumber Green Mottle Mosic Virus and Tobacco Mosic Virus by Synchrotron Small-Angle Scattering, *J. Protein Chem.*, **16**, 151-159 (1997).

Tokioka K, Masuda S, Fujii T Hata Y and Yamamoto Y: Asymmeric Cycloaddition of Anthrone with *N*-Substituted Maleimides with C_2-Chiral Pyrrolidines, *Tetrahedron*, **8**, 101-107 (1997).

Watanabe K, Hata Y, Kizaki H, Katsube Y and Suzuki Y: The Refined Crystal Structure of *Bacillus cereus* Oligo-1,6-glucosidase at 2.0 Å Resolution: Structural Characterization of Proline-substitution Site for Protein Thermostabilization, *J. Mol. Biol.*, **269**, 142-153 (1997).

Yamamoto A, Hata T, Tomoo K, Ishida T, Fujii T, Hata Y, Murata M and Kitamura K: Binding Mode of CA074, a Specific Irreversible Inhibitor, to Bovine Carthepsin B as Determined by X-Ray Crystal Analysis of the Complex, *J. Biochem.*, **121**, 974-977 (1997).

II. Molecular Biology

Goto K: Molecular Mechanisms of Petal and Stamen Development in *Arabidopsis*. *J Reprod Develop*, **43**, 19-20 (1997).

Kudo M and Goto K: Mechanism in Arrangements of Flower Organs. *Iden*, **51**, 27-33 (1997) (in Japanese).

Nevalainen L T, Aoyama T, Ikura M, Crivici A, Yan H, Chua N-H and Nairn A C: Characterization of Novel Calmodulin-binding Peptides with Distinct Inhibitory Effects on Calmodulin-dependent Enzymes. *Biochem J*, **321**, 107-115 (1997).

Aoyama T and Chua N-H: A Glucocorticoid-mediated Transcriptional Induction System in Transgenic Plants. *Plant J*, **11**, 605-612 (1997).

Oka A, Aoki M and Aoyama T: Phosphoprotein Phosphatases and Signal Transduction in Plant Cells. *Tanpakushitsu-Kakusan-Kouso*, **42**, 736-743 (1997) (in Japanese).

III. Biological Information Science

Bono H, Goto S, Ogata H, Kanehisa M: Genome Scale Prediction of Two-component Signal Transducers from the Knowledge of Regulatory Interactions, *8th Workshop on Genome Informatics*, 260-261 (1997).

Hattori M, Kanehisa M: The Construction of the Knowledge Base on Apoptotic Molecular Interactions, *8th Workshop on Genome Informatics*, 276-277 (1997).

Kanehisa M: Linking databases and organisms - GenomeNet resources in Japan. *Trends Biochem. Sci.*, **22**, 442-444 (1997).

Kanehisa M: A database for post-genome analysis. *Trends Genet.*, **13**, 375-376 (1997).

Kanehisa M: Network based analysis of genetic information, In "*Introduction to Genetic Engineering*" (T. Yamamoto, ed.), Yodosha, (1997) (in Japanese).

Kanehisa M: *"Human Genome Project", Series Biophysics* **Vol. 11**, Kyoritsu Shuppan, (1997) (in Japanese).

Kawashima S, Katayama T, Kanehisa M: Construction of Molecular Interaction Database and Searching for similar Pathways, *8th Workshop on Genome Informatics*, 298-299 (1997).

Kihara D, Kanehisa M, Takagi T: Internet Resources for Genome Research. *Protein, Nucleic Acid and Enzyme*, **42(suppl.)**, 3090-3099 (1997) (in Japanese).

Kihara D, Kanehisa M: Detection of Membrane Proteins in the Whole Genome sequences, *8th Workshop on Genome Informatics*, 300-301 (1997).

Nishioka K, Goto S, Kanehisa M: Present Status of LIGAND Chemical Database for Enzyme Reactions, *8th Workshop on Genome Informatics*, 316-317 (1997).

Sato K, Katsurada T, Kimura Y, Kanehisa M: Integrated GENES database in KEGG. *8th Workshop on Genome Informatics*, 334-335 (1997).

Suzuki K, Kanehisa M: Database and prediction of sequence motifs on protein molecular interactions. *8th Workshop on Genome Informatics*, 344-345 (1997).

Takazawa F, Kanehisa M, Mitaku S: Analysis of amphiphilic periodicity of alpha-helices: detection of edges of helices and functional residues in proteins. *8th Workshop on genome Informatics*, 348-349 (1997).

Tomii K and Kanehisa M: Current Status of Pathway Analysis, *Protein, Nucleic Acid and Enzyme*, **42(suppl.)**, 3026-3032 (1997) (in Japanese).

NUCLEAR SCIENCE RESEARCH FACILITY

I. Particle and Photon Beams

II. Beams and Fundamental Reaction

Fujieda M, Ezura E, Mori Y, Nakayama H, Ohmori C, Saito K, Sawada S, Takagi A, Tanabe Y, Toda M, Uesugi T, Yamamoto M and Yoshii M: A Broad Band RF Cavity for JHF Synchrotrons, *Proc. of the 11th Symposium on Accelerator Science and Technology, Harima Science Garden City, Hyogo, Japan*, 209-211 (1997).

Morita A, Inoue M, Noda A, Iwashita Y, Shirai T, Urakabe E, Hiramoto K and Noda K: Octupole Magnet for Expansion of Irradiation Area, *Proc. of the 11th Symposium on Accelerator Science and Technology, Harima Science Garden City, Hyogo, Japan*, 399-401 (1997).

Noda A, Fujita Y, Hiramoto K, Hirota J, Iwashita Y, Nishi M, Noda K, Shirai T, Tadokoro M, Torikoshi M, Urakabe E, Yamada S, and Inoue M: Development of Proton Synchrotron Dedicated for Cancer Therapy at Kyoto University, Proc. of the 6th China-Japan Joint Symposium on Accelerators for Nuclear Science and Their Applications, Chengdu, China, 308-311 (1996) .

Noda A, Fujita H, Inoue M, Iwashita Y, Shirai T, Sugimura T, Tonguu H and Mashiko K: Stretcher Mode of the Electron Storage Ring, KSR, Beam Science and Technology, **2**, 36-38 (1997).

Noda A, Dewa H, Fujita H, Ikegami M, Inoue M, Iwashita Y, Kakigi S, Kando M, Mashiko K, Okamoto H, Shirai T, Sugimura T and Tonguu H: Electron Storage and Stretcher Ring, KSR, *Proc. of the 5th European Particle Accelerator Conference, Sitges(Barcelona), Spain*, 451-453 (1996).

Saito K, Hirota J, Katane M, Tadokoro M, Iwashita Y, Noda A, and Inoue M: An Untuned RF Cavity using Multifeed Coupling, *Nucl. Instrum. & Meth.* **A401**, 133-143 (1997).

Noda A, Inoue M, Iwashita Y, Tonguu H, Fujita H, Shirai T and Sugimura T: Stretcher Mode of KSR, *Proc. of the 11th Symposium on Accelerator Science and Technology, Harima Science Garden City, Hyogo, Japan*, 59-61 (1997).

Noda A, Iwashita Y, Inoue M, Morita A, Shirai T, Nishi M, Hiramoto K, Hirota J, Tadokoro M and Umezawa M: Development of Compact Proton Synchrotron with Combined Function Dedicated for Cancer Therapy, *Proc. of the 11th Symposium on Accelerator Science and Technology, Harima Science Garden City, Hyogo, Japan*, 314-316 (1997).

Umezawa M, Hiramoto K, Nishi M, Tadokoro M, Hirota J, Iwashita Y and Noda A: A New Dipole Bending Magnet with Improved Magnetic Field Distribution, *Proc. of the 11th Symposium on Accelerator Science and Technology, Harima Science Garden City, Hyogo, Japan*, 380-382 (1997).

Hiramoto K and Noda A: Tune Change due to Ripple of Magnetic Field in a Synchrotron of Combined Function Lattice, *Proc. of the 11th Symposium on Accelerator Science and Technology, Harima Science Garden City, Hyogo, Japan*, 496-498 (1997).

Shirai T, Bisoffi G and Andrev V: Design of the Superconducting RFQ1 Cavity for the PIAVE Linac, *L.N.L.-I.N.F.N Report* **124/97** (1997).

Sugimura T, Shirai T, Iwashita Y, Tonguu H, Noda A, Fujita H and Inoue M: The Emittance Measurement of 100 MeV Electron Linac at ICR, *Beam Science and Technology*, **2**, 30-33 (1997).

Ao H and Iwashita Y: Study of the Coaxial Bridge Coupler for the DAW, *Beam Science and Technology*, **2**, 11-12 (1997).

Ikegami M and Okamoto H: Can Beam Haro be Scraped ?, *Beam Science and Technology*, **2**, 20-22 (1997).

Hayakawa Y, Seto M, Maeda Y, Shirai T and Noda A: Observation of Parametric X-Ray radiation from 80 MeV Electron Beams, *Beam Science and Technology*, **2**, 8-10 (1997).

Urakabe E, Inoue M, Iwashita Y, Kanazawa M, Shirai T, Tadokoro M, Nishi M, Noda A, Torikoshi M, Noda K and Fujita Y: Parallel Plate Ionization Chamber for Studying the Time Structure of Slow Extracted Beam, *Beam Science and Technology*, **2**, 23-29 (1997).

Urakabe E, Inoue M, Iwashita Y, Kanazawa M, Shirai T, Sugimura T, Tadokoro M, Nishi M, Noda A, Torikoshi M, Noda K and Fujita Y: Parallel Plate Ionization Chamber for the Medical-use Heavy-ion Beams, *Proc. of the 11th Symposium on Accelerator Science and Technology, Harima Science Garden City, Hyogo, Japan*, 308-310 (1997).

Kihara T, Okamoto H and Iwashita Y: A Possible 3D Laser Cooling Scheme in a Storage Ring, *Proc. of the 11th Symposium on Accelerator Science and Technology, Harima Science Garden City, Hyogo, Japan*, 481-483 (1997).

Tonguu H, Fujita H, Inoue M, Iwashita Y, Noda A, Shirai T and Sugimura T: Status of Pulse Stretcher,KSR, *Proc. of the 22nd Linear Accelerator Meeting in Japan, Sendai, Japan*, 296-298 (1997).

Kapin V: A New Analysis of 4-rod RFQ Linac with Intrinsic Field Distortions, *Jpn J. Appl. Phys.*, **Vol. 36**(1997), Pt 1, No.4A, pp.2415-2427.

Inoue M, Ao H, Dewa H, Fujisawa H, Ikegami M, Iwashita Y, Kakigi S, Kando, M, Kapin V, Kihara T, Noda A, Okamoto H, Shirai T, Sugimura T and Tonguu H: Linacs and Beam Physics at ICR Kyoto University, *Proc. of the 6th China-Japan Joint Symposium on Accelerators for Nuclear Science and their Applications, Chengdu*,74-77 (1997).

Inoue M, Noda A, Iwashita Y, Okamoto H and Shirai T: Pulsed Neutron source based on Accelerator-subcritical-assembly, *Proceedings of the 7th International Symposium on Advanced Nuclear Enrgy Research Recent Progress in Accelerator Beam Application, Takasaki, Japan*, 462-465 (1997).

Kawase Y, Inoue M and future plan working group: Nutron Factory Project at KURRI, *Proc. of the 11th Symposium on Accelerator Science and Technology, Harima Science Garden City, Hyogo, Japan*, 133-135 (1997).

Okamoto H, Ikegami M: Simulation study of halo formation in breathing round beams, *Physical Review* **E55**, 4694-4705 (1997).

Ikegami M, Okamoto H: Halo Formation from Mismatched Axisymmetric Beams in a Periodic Focusing Channel, *Jpn. J. Appl. Phys.*, **Vol. 36**, 7028-7034 (1997).

Kando M, Nakajima K, Arinaga M, Kawakubo T, Nakanishi H,Ogata A, Kozawa T, Ueda T and Uesaka M: Interaction of Terawatt Laser with Plasma, *J. of Nuclear Materials*, **248**, 405-407 (1997).

Kando M, Ahn H, Kotaki H, Tani K, Watanabe T, Ueda T, Uesaka M, Kishimoto Y, Nakajima K, Arinaga M, Nakanishi H and Ogata A: Formation of Self-Channeling and Electron Jet in an Underdense Plasma Excited by Ultrashort High Intensity Laser Pulses: *7th Workshop on Advanced Accelerator Concepts, AIP Conference Proceedings* **398**, 390-399 (1997).

Kando M, Kotaki H, Dewa H, Ahn H, Sakai F, Kondoh S, Ueda T, Watanabe T, Uesaka M, Nakanishi H, Nakajima K and Ogata A: Laser Wakefield Acceleration Experiments, *Proc. of the 11th Symposium on Accelerator Science and Technology, Harima Science Garden City, Hyogo, Japan*, 513-515 (1997).

Kando M, Ahn H, Dewa H, Kotaki H, Nakanishi H, Ogata A, Ueda T, Uesaka M, Watanabe T, and Nakajima K: Laser Wakefield Electron Acceleration over 100 MeV Driven by a Femtosecond Terawatt Laser Pulse, *JAERI-memo* 09-143 (1997).

Kakigi S and Shirai T: Shielding for the 100 MeV Electron Linac at ICR, *Beam Science and Technology*, **2**, 1-7 (1997).

Okihana A, Ushiro K, Yoshimura T, Kakigi S and Sekioka T: Quasifree Processes in the $_{6}$Li Breakup Reaction by Alpha Particles, *Nucl. Phys.*, **A614**, 71-85 (1997).

Iwashita Y: Phase Stability improvement of ICR Proton Linac, *Beam Science and Technology*, **2**, 13-14 (1997).

Iwashita Y: Alignment Error of Q-Magnet in KSR, *Beam Science and Technology*, **2**, 34-35 (1997).

Saito K, Hirota J, Noda F, Iwashita Y, Noda A and Inoue M: An Untuned RF Cavity Loaded with Fe-based Nanocrystalline FINEMET Cores, *Beam Science and Technology*, **2**, 15-19 (1997).

Iwashita Y: PISCES II: 2.5D RF Cavity Code, *Proc. Computational Accelerator Physics, Williamsburg, Virginia, AIP conference Proceedings* **391**, 119-124 (1996).

Iwashita Y: Ferro-magnetic material Loaded Untuned RF Cavity for Synchrotron, *JJAP* **36**, L727-L728, Part 2, No.6A (1997).

Iwashita Y: Accuracy of Eigenvalue with Hybrid Elements on Axisymmetric Domains, *Proc. of the 11th Conference on the Computation of Electromagnetic Fields, Rio de Janeiro, Brazil*, 165-166 (1997).

Yamamoto K, Matsuki S, and Ogawa I: Quantum calculation of axion-photon-Rydberg atom interactions in resonant cavities, *Proc. International Symposium on Dark Matter in the Universe and its Direct Detection, Tokyo*, 129 - 134 (1997).

Ogawa I, Kishimoto Y, Tada M, Matsuki S, Yamamoto K, Masaike A, Watanabe S, and Matsuzawa M: Search for dark matter axions with Rydberg atoms in resonant cavities, *Proc. International Symposium on Dark Matter in the Universe and its Direct Detection, Tokyo*, 175 - 180 (1997)

RESEARCH FACILITY OF NUCLEIC ACIDS

Fujibuchi W, Goto S, Migimatsu H, Uchiyama I, Ogiwara A, Akiyama Y and Kanehisa M: DBGET/LinkDB: an Integrated Database Retrieval System. *Proc. Pacific Symposium on Biocomputing '98*, 683-694 (1997).

Fujibuchi W and Kanehisa M: KEGG: Kyoto Encyclopedia of Genes And Genomes, *Genes and Medicine*, **1**, 119-124 (1997) (in Japanese).

Fujibuchi W and Kanehisa M: Prediction of gene expression specificity by promoter sequence patterns. *DNA Res.*, **4**, 81-90 (1997).

SEMINARS

Professor Odile Eisenstein
Universite de Montpellier 2, France
“Structures of Transition Metal Unsaturated Complexes: A High Sensitivity to the Nature of the Ligands”
Tuesday 7 January 1997

Professor Jack R. Norton
Colorado State University, USA
“A General Mechanism for the Formation and Fragmentation of Metallacyclobutanes. Effect of Metals on Cycloaddition Rules.”
Saturday 11 January 1997

Dr.Dieter Neher
Max-Planck-Institut fuer Polymerforschung, Germany
“Polymer Light Emitting Diodes: Tuning of Color and Efficiency”
Thursday 16 January 1997

Professor Richard G. Jones
University of Kent, Canterbury, UK
“Recent Advances in Understanding The Synthesis of Polysilanes by The Wurtz Reductive-Coupling Reaction.”
Monday 20 January 1997

Professor Ryu Sato
Department of Applied Chemistry and Molecular Science, Faculty of Engineering, Iwate University, Japan
“Chemistry of Polycarcogenoheterocycles”
Wednesday 22 January 1997

Professor Junji Inanaga
Institute for Fundamental Research of Organic Chemistry, Kyushu University, Japan
“Organic Synthesis Using Rare Earth Metal. Resent Development”
Thursday 23 January 1997

Professor Hideo Kitamura
High Energy Accelerator Research Organization/ Japan Synchrotron Radiation Research Institute
“Photon Beam Line Strategy of SPring-8”
Tuesday 28 January 1997

Dr.Silvia Mittler-Neher
Max-Planck-Institut fuer Polymerforschung, Mainz, Germany
“Integrated optics for communication, microscopy and sensing”
Wednesday 5 February 1997

Dr. Anthony J Ryan
Materials Science Centre, UMIST, Manchester, UK
"Semi-Crystalline Block Copolymers"
Wednesday 5 February 1997

Professor Andrews D. Hamilton
Department of Chemistry, University of Pittsburgh, USA
"New Approachs to Artificial Receptor Design"
Tuesday 18 February 1997

Dr. Motoharu Mizumoto
Japan Atomic Energy Research Institute
“High Current Accelerator for the Neutron Science”
Tuesday 20 February 1997

Dr.Michael Klaus Engel
Kawamura Institute of Chemical Research, Japan
“New Porphyrazine and Phthalocyanine Single crystals”
Monday 24 February 1997

Dr. Sanjay Rastogi
Centre of Polymer and Composites, Techische Universiteit Eindhoven, Eindhoven, Netherlands,
"Chain Mobility in Crystalline Polymers - a novel rout for welding and processing"
Wednesday 5 March 1997

Dr. Giovanni Bisoffi
Italian National Institute for Nuclear Physics, Legnaro, Italy
“LNL Linac and New Injector Project”
Wednesday 5 March 1997

Dr. Luigi Tecchio
Italian National Institute for Nuclear Physics, Legnaro, Italy
“The Crystal Storage Ring Project”
Wednesday 5 March 1997

Dr. Andrew M. Sessler
Lawrence Berkeley National Laboratory, USA
“Beam Dynamics of Muon Colliders”
Thursday 6 March 1997

Dr. Manfred Grieser
Max-Planck-Institut, Heidelberg, Germany
“Activities at the Heavy Ion Storage Ring at MPI Heidelberg”
Friday 7 March 1997

Professor Hisanori Suzuki
Institute of Biochemistry, Faculty of Medicine, University of Verona, Verona, Italy
"Regulation on the Expression of Nitric Oxide Synthases"
Tuesday 11 March 1997

Professor Masaru Matsuoka
Kyoto Women’s University, Department of Materials Science
“Molecular Interaction and Self-organization”
Thursday 13 March 1997

Dr. Annette Thierry
Institut Charles Sadron, France
“Epitaxial Orientation of Polymer Thin Films with Special Properties: The case of Polydiacetylenes”
Monday 24 March 1997

Professor Xiujian Zhao
Wuhan University of Technology, China
"Formation and Structures for Chalcohalide Glasses"
Wednesday 26 March 1997

Dr. Alper Garren
Lawrence Berkeley National Laboratory, USA
“Useful Lattice Structures”
Wednesday 26 March 1997

Professor Kenneth R. Poeppelmeier
Department of Chemistry, Northwestern University,

Evanceton USA
“Understanding the Synthesis of Layered Cuprates”
Thursday 3 April 1997

Professor Kenneth R. Poeppelmeier
Department of Chemistry, Northwestern University, Evanveton USA
“Optimal Stability in Multiphase Oxidation Catalysts and Some Remarkable Solid State Chemistry in the Mg-V-Mo-O system”
Thursday 10 April 1997

Professor P. Braunstein
University of Louis Pasteur, France
“Bimetallic Reactivity”
Saturday 26 April 1997

Dr. Masatomo Yonezawa
Chief Engineer
Research and Development Group, NEC Corporation
“Li Seondary Battery : Current State in the Fundamental Research and the Applications”
Monday 12 May 1997

Professor Krzysztof Matyjaszewski
Carnegie Mellon University, Pittsburgh, USA
Atom-Transfer Radical Polymerization: Novel Route to Narrow-Polydispersity Polymers of Various Architectures, Shapes, Compositions, and Functionalities
Thursday 15 May 1997

Dr.Ralph Nelson
DuPont
“Informal Talk about the Particle Technology Group at DuPont”
Friday 6 June 1997

Professor Hiromi Kitano
Toyama University, Toyama, Japan
Dynamics at the Interface between Polymer and Water
Monday 9 June 1997

Dr. Johan Heuts
University of New South Wales, Sydney, Australia
The Use of Controlled Radical Polymerization Techniques for the Study of Fundamental Copolymerization Kinetics
Friday 24 June 1997

Dr. Michael K. Georges
The Xerox Research Center of Canada, Mississauga, Canada
The Synthesis of Poly(alkyl acrylate)s by the Stable Free Radical Polymerization Process
Friday 24 June 1997

Dr. George A. Kraus
Department of Chemistry, Iowa State University, U.S.A.
“New Synthetic Approaches to Kainic Acid Derivatives”
Thursday 26 June 1997

Professor Robert West
Department of Chemistry, University of Wisconsin, Madison, USA
"Recent Advance in the Chemistry of Novel Aromatics Containing Si and Ge"
Saturday 28 June 1997

Professor Duy H. Hua
Department of Chemistry, Kansas State University, U.S.A.
“Sulfinyl Ketimines and Sulfinimines in the Asymmetric Syntheses of Alkaloids and Amino Acids”
Friday 18 July 1997

Professor Klaus Hafner
Institut für Organische Chemie, Technische Hochschule Darmstadt, Darmstadt, Germany
"Syntheses and Dynamic Properties of Chiral Heptalenes"
Monday 4 August 1997

Professor Dafu Cui
Institute of Electronics, Chinese Academy of Science, China
"Research of Chemical Sensor in the State Key Laboratory of Transducer Technology"
Wednesday 20 August 1997

Professor Norbert Karl
Universität Stuttgart, Germany
“Vapor-Deposited Organic Thin Films For Molecular Electronics”
Monday 1 September 1997

Dr. Ching-i Huang
Department of Chemistry, University of Minnesota, Minneapolis, USA
"The Effects of Neutral and Selective Solvents on Ordered Block Copolymer Solutions"
Wednesday 3 September 1997

Professor Dr. Ulrich Buchenau
Institut für Festkörperforschung, Forschungzentrum Jülich, Germany,
"Relaxation in Polymer Glasses"
Tuesday 9 September 1997

Professor Dr. Helumuth Hoffmann
Department of Inorganic Chemistry, Technical University of Vienna, Austria
“Infrared Reflection Spectroscopy of Organic Monolayer Films”
Wednesday 10 September 1997

Professor Aiqiao Mi
Union Laboratory of Asymmetric Synthesis, Chengdu Institute of Organic Chemistry, China
“Design and Synthesis of Chiral Ligands and Asymmetric Catalytic Reactions”
Wednesday 17 September 1997

Professor Shigeru Torii
Faculty of Technology, Okayama University, Japan
“Recent Develepment of Asymmetric Induction by Means of Electrolysis”
Friday 17 September 1997

Professor Gaorong Han
Institute of Inorganic Materials, Department of Materials, Zhejiang University, China
"Amorphous Silicon and Its Application in a Liquid Crystal Light Valve Device"
Friday 19 September 1997

Professor Ho Chee Cheong
Universiti Malaya, Malaysia
“Recent Advances in Characterization of Natural Latex Film Surface”

Saturday 20 September 1997

Professor Michael Ilavsky
Charles University, Czech
“Structure, Formation and Physical Properties of Model End-linked Networks”
Monday 22 September 1997

Professor J. C. Grenier
Bordeau Univewrsity, France
“New Chimie-Douce (Soft Chemistry) Processes in Solid State Chemistry”
Monday 22 September 1997

Professor Giorgio Morelli
Istituto Nazionale della Nutrizione, Rome, Italy
“Homeodomain-Leucine Zipper Proteins of the HD-ZIP III and IV Families in the Control of Plant Growth”
Monday 29 September 1997

Professor Ida Ruberti
Centro di studio per gli Acidi Nucleici, CNR, Rome, Italy
“Homeodomain-Leucine Zipper Proteins of the HD-ZIP I and II Families in the Control of Plant Growth”
Monday 29 September 1997

Professor Reinhart Keese
Universitat Bern, Switzerland
“Transition Metal Induced Syntheses of Fenestranes”
Wednesday 1 October 1997

Dr. Patrick Bruno
Institut d'…lectronique Fondamentale, UniversitÈ Paris-Sud, France
“Interlayer Exchange Coupling”
Thursday 9 October 1997

Professor Richard Neidlein
Department of Pharmaceutical Chemistry, University of Heidelberg, Heidelberg, Germany
"Metallacycles and Heterocycles: New Synthetic Results"
Monday 13 October 1997

Professor Norimasa Okui
Faculty of Engineering, Tokyo Institute of Technology, Tokyo, Japan,
"Crystallization of Polymers"
Friday 17 October 1997

Professor Peter M. Levy
Department of Physics, New York University, USA
“Fundamental Limit to Small Scale Magnetoresistive Memory and Sensors”
Tuesday 21 October 1997

Professor Dr. Oliver Lindqvist
Department of Environmental Chemistry, Gothenburg University and Chalmers University of Technology, Sweden
“Environmental Aspects on Energy Conversion”
Wednesday 22 October 1997

Professor Guo-Qiang Lin
Shanghai Institute of Organic Chemistry, China
“Chiral Synthesis of Polyhydroxy Aza-rings, Amines and the Restricted Biaryl Compounds”
Thursday 23 October 1997

Dr. Christopher J. G. Plummer
Lausanne Federal Institute of Technology, Switzerland
“TEM and HREM Investigations of Morphology and Deformation in Semicrystalline Polymers”
Friday 24 October 1997

Professor Tien-Yau Luh
National Taiwan Unversity
“Synthetic Applications of the Dithioacetal Functionality”
Tuesday 28 October 1997

Professor Ken Feldmann
Department of Plant Science, Arizona University, Tucson, Arizona, USA
“Brassinosteroids and Dwarf in *Arabidopsis thaliana*”
Wednesday 29 October 1997

Professor T. Don Tilley
University of California, Berkeley, USA
“Transition Metal Coupling Routes to New Polymers and Macrocycles”
Saturday 1 November 1997

Professor Brian Halton
School of Chemical & Physical Sciences, Victoria University of Wellington, Wellington, New Zealand
"Strained Molecules and Novel Ring-Systems: Discoveries with Cycloproparenes"
Tuesday 4 November 1997

Professor Pierre Deslongchamps
Department of Chemistry, University of Sherbrooke, Canada
“Transannular Diels-Alder Reaction and the Synthesis of Diterpenes and Steroids”
Tuesday 4 November 1997

Professor David M. Hodgson
University of Oxford, UK
“Carbenes, Carbenoids and Enantioselective Desymmetrisation”
Wednesday 5 November 1997

Dr. Kazuhisa Nakajima
High Energy Accelerator Research Organization
“Laser Acceleration and Topics of Related Physics”
Tuesday 5 November 1997

Professor Stephen L. Buchwald
Department of Chemistry, Massachusetts Institute of Technology, U.S.A.
“Metal-Catalyzed Carbon-Heteroatom Bond Formation in Organic Synthesis”
Friday 7 November 1997

Professor Amos B. Smith, III
Department of Chemistry, University of Pennsylvania, U.S.A.
“The Spongistatin Antitumor Agents: Architecturally Complex Synthetic Targets”
Saturday 8 November 1997

Dr. Mathias Floersheimer
Department of Physics, University Muenster, Germany
”Second Harmonic Imaging of Surface Order and Symmetry”
Thursday 13 November 1997

Professor Jozef Drabowicz
Polish Academy of Sciences in Lodz, Poland
“Studies on Sulfur Compounds: Synthetic and Stereochemical Aspects”
Thursday 13 November 1997

Professor Edmunds Lukevics
Latvian Institute of Organic Synthesis, Latvia
“Synthesis, Structure and Biological Properties of Germatranes”
Friday 14 November 1997

Dr. Alexey V. Latyshev
Institute of Semiconductor Physics, Academy of Science, Novosibirsk, Russia
“Electromigration on Si Surfaces”
Tuesday 18 November 1997

Professor Thomas S. Livinghouse
Montana State University, USA
“Enantio- and Diastereo- Controlled Chemical Synthesis via Transition Metal Complexes”
Wednesday 19 November 1997

Dr. Yamanaka Masanori
“Scattering of an Electron by Magnetic Domain Walls”
Department of Applied Physics, The University of Tokyo
Thursday 20 November 1997

Dr. Shigenori Hiramatsu
High Energy Accelerator Research Organization
“Free Electron Laser for Gamma Collider”
Friday 21 November 1997

Dr. Xiaozhong. Zhang
Department of Physics, National University of Singapore, Singapore
“Atomistic Simulation of High Temperature Superconductors”
Monday 24 November 1997

Dr. Hugo Christenson
Department of Applied Mathematics, Research School of Physical sciences, Australian National University, Australia
157th Colloid Science Seminar
“Surface Forces and Long Range Hydrophobic Attraction Is the Long-Range Hydrophobic Attraction Relatied to the mobility of Adsorbed Hydrophobic Groups?”
Thursday 27 November 1997

Dr. Satoru Yamada
National Institute of Radiological Sciences
“HIMAC, Accelerator for Cancer Therapy”
Friday 27, 28 November 1997

Dr. Henri Dhanzy
Centre de Recherches sur les Macromolécules Végétales, CNRS, France
“Structural Aspects of Polyaccharide Drystals”
Wednesday 3 December 1997

Dr. Dominique Bourgeois
European Synchrotron Radiation Facility, France
"The Laue Technique for Time-resolved Macromolecular Crystallography: advantage, shortcomings and associated processing difficulties"
Wednesday 3 December 1997

Dr. Giuseppe Lamanna
Italian National Institute for Nuclear Physics, Bari, Italy
“Toward Ion Beam Ordering”
Wednesday 3 December 1997

Professor Seiichi Tokura
Hokkaido University, Sapporo, Japan
Chemistry and its Application of Chitin and Chitosan
Friday 5 December 1997

Professor Eishun Tsuchida
Waseda University, Tokyo, Japan
Advanced Materials and Polymer Complexes
Friday 5 December 1997

Professor Robert Corriu
University of Montpellier II, France
“The Monophasic Hybrid Organic-Inorganic Materials”
Monday 8 December 1997

Professor Masako Kato
Department of Chemistry, Nara Women’s University
“Crystal Structures and Their Fluorescent Properties of Pt -Diimine Complexes with Multi-dimensional Interaction”
Tuesday 9 December 1997

Professor Jay S. Siegel
Department of Chemistry, University of California, San Diego, USA
"Cyclohexatriene: Kekule, Mills-Nixon, and Now"
Saturday 13 December 1997

Professor Masataka Mori
Department of Molecular Genetics, Kumamoto University, Kumamoto, Japan
"Formation of Mitochondria and Molecular Chaperon"
Monday 15 December 1997

Professor Hiroyuki Nakazumi
Osaka Prefectural University
"Preparation and Properties of Functional Dye-Incorporated Gel Films"
Friday 19 December 1997

Professor Edgar Niecke
Institut for Anorganische Chemie, Bonn, Germany
“Anions, Cations and Carbene Analogues, Containing P/N Bonds”
Monday 22 December 1997

MEETINGS AND SYMPOSIUMS

Kyoto University Centennial Commemoration Symposium

21 November 1997

1. Particle beam as an developer of future microscopic world: accelerators and their applications
   Makoto Inoue

2. How can the organic ligands recognize the metal ion sizes.
   Masakazu Matsui

3. Life chemistry in the 21st century: Visualization, manipulation and creation of genes
   Kunihiro Ueda

Tutorial on Chemistry for High-School Students

25 October 1997

1. Chemistry and green effect
   Masakazu Matsui

2. Polymer chemistry in the next age
   Takeaki Miyamoto

15th International Colloquium on Magnetic Films and Surfaces (ICMFS'97)

4-8 August 1997, Novotel Twin Water Resort, Queensland, Australia
(Organized by Institute for Chemical Research, Kyoto University)

20th Symposium on Solution Chemistry

6-8 November 1997

Organized by Japan Society of Solution Chemistry

Workshop Organized by Research Facility of Nucleic Acids

"The Frontier of Plant Science"
15 December 1997

Relationship between the genes contributing morphogenesis of apical meristem and separation of cotyledons
Mitsuhiro Aida
Faculty of Science, Kyoto University, Kyoto, Japan

Functional analysis of the CPC gene controlling root hair formation
Takuji Wada
Institute of Biomolecular Engineering, Osaka, Japan

Mutations affecting twisted characteristics of Arabidopsis thaliana
Takashi Hashimoto
Nara Institute of Science and Technology, Nara, Japan

Control of methionine biosynthesis
Satoshi Naito
Faculty of Agriculture, Hokkaido University, Hokkaido, Japan

Transcriptional regulation responsive to abscisic acid and its tissue specificity
Tsukaho Hattori
Gene Research Center, Mie University, Mie, Japan

Signal transduction system for cytokinin
Tatsuo Kakimoto
Faculty of Science, Osaka University, Osaka, Japan

Are there two-component regulatory systems universally in higher plants?
Atsuhiro Oka
Institute for Chemical Research, Kyoto University, Kyoto, Japan

MAP kinase cascade in higher plants
Tsuyoshi Mizoguchi
Institute of Physical and Chemical Research (RIKEN), Ibaraki, Japan

Signal transduction for expression of disease and wounding resistance
Yuko Ohashi
National Institute of Agrobiological Resources, Ibaraki, Japan

Isolation of genes contributing differentiation of apical meristematic cells with an equalized cDNA library
Dr. Takayuki Kouchi
Nara Institute of Science and Technology, Nara, Japan

Structural analysis of the Arabidopsis thaliana genome
Dr. Satoshi Tabata
Kazusa DNA Institute, Chiba, Japan

THESES

IWAMOTO, Chika
"Studies on Antitumor Metabolites from Marine Microorganism"
Supervisor: Professor Fuji K
23 January 1997

YAMAGUCHI Shigehiro
D Eng, Kyoto University
"Silole-Containing π-Conjugated Compounds"
Supervisor: Professor Tamao K
23 January 1997

HOSHINO, Akitaka
D Sc, Kyoto University
"Study on Organic Ultrathin-Layer Interfaces by Scanning Tunneling Microscopy"
Supervisor: Professor Kobayashi T
23 March 1997

KABETA Keiji
D Eng, Kyoto University
"Preparation, Photoreaction, and Application of Alkoxypolysilanes and Related Compounds"
Supervisor: Professor Tamao K
23 March 1997

AHN, Mija
D Pharm Sci, Kyoto University
"Studies on the Diastereoselective Reactions Using Optically Active Binaphthol"
Supervisor: Professor Fuji K
24 March 1997

HASEGAWA, Hiroshi
D Sc, Kyoto University
"Seasonal Changes in Arsenic Speciation in Hydroshere"
Supervisor: Professor Matsui M
24 March 1997

HISANO, Tamao
D Sc, Kyoto University
"Structural biological studies on dehalogenation mechanism of L-2-haloacid dehalogenase"
Supervisor: Associate Professor Hata Y
24 March, 1997

IMAJUKU, Yoshiro
D Sc, Kyoto University
"A *CDC2* Gene Family in *Arabidopsis thaliana*"
Supervisor: Professor Oka A
24 March 1997

ITO, Toshiro
D Sc, Kyoto University
"Cloning and Characterization of Genes Contributing Flower Morphogenesis in *Arabidopsis thaliana*"
Supervisor: Professor Oka A
24 March 1997

KAPIN, Valeri Vyacheslavovich
D Sc, Kyoto University
"A New Analysis of 4-rod RFQ Linac with Intrinsic Field Distortions"
Supervisor: Professor Inoue M
24 March 1997.

KUNITOMO, Jun
D Sc, Kyoto University
"Physical Properties and Stereochemistry in (Net) Hydride-Transfer Reactions of Atropisomeric Flavoenzyme Models"
Supervisor: Professor Ohno A
24 March 1997

LE Thi Hanh Quyen
D Sc, Kyoto University
"Molecular Design of Chelating Ligands with Highly Selective Recognition and Separation Function for Metali Ions"
Supervisor: Professor Matsui M
24 March 1997

NAKATSU, Toru
D Agr, Kyoto University
"Structural Studies on Asparagine Synthetase from *Escherichia coli* K-12"
Supervisor: Professor Oda J
24 March 1997

OBATA, Hajime
D Sc, Kyoto University
"Development of an Automated Analytical Method of Iron in Seawater and Studies on the Behavior of Iron in the Ocean"
Supervisor: Professor Matsui M
24 March 1997

SHIRAI, Osamu
D Sc, Kyoto University
"Voltammeric investigation on ion transport through a ligand membrane on a bilayer lipid membrane"
Supervisor: Professor Matsui M
24 March 1997

YAMAURA, Kazunari
D Sc, Kyoto University
"Synthesis and Physical Property of Layered Copperand Nickel Oxides"
24 March 1997

WAKAI, Chihiro
D Sc, Kyoto University
"Anomalous viscosity dependencies of rotational and translational coefficients of solitary water molecules in organic solvents"
Supervior: Professor Nakahara M
24 March 1997

SASAKI, Takayuki
D Sc, Kyoto University
"Studies on the Complex Formation Reaction of Metal Ions with Macrocyclic Ligands in the Aqueous Solution"
Supervisor: Professor Matsui M
23 May 1997

EMOTO, Takeshi
D Sc, Kyoto University
"Magnetism of Au/M (M=Fe, Co and Ni) Multilayers by Mössbauer Spectroscopy"
Supervior: Professor Shinjo T
23 July 1997

CHONG, Iksu
D Sc, Kyoto University
“Single Crystal Growth of Pb substituted Bi-Based Superconductors and Magnetic Property”
24 September 1997

ONOE, Jun
D Sc, Kyoto University
“Relativistic Effects on Covalent Bonding: Role of Individual Valence Atomic Orbitals”
Supervisor: Mukoyama T
24 September 1997

MATSUDA, Tsunetoshi
D Eng, Kyoto University
“Molecular Simulation Studies on Structure and Properties of Linear Polymers”
Supervisor: Professor Kaji K
24 September 1997

MIZUHARA, Hidekazu
D.Pharm Sc, Kyoto University
“Induction Mechanism of T Cell-Dependent Mouse-Hepatitis by Concanavalin A”
Supervisor: Professor Sugiura Y
24 September 1997

NAGAOKA, Makoto
D.Pharm Sc, Kyoto University
“DNA Recognition and Functinal Conversion of Zinc Finger Typed Transcription Factor Sp1”
Supervisor: Professor Sugiura Y
24 September 1997

IKEGAMI, Masanori
D Sc, Kyoto University
“Halo Formation from High Current Axial Symmetric Beams”
Supervisor: Professor Noda A
25 November 1997.

KURODA, Akio
“Studies on Optically Active 1,1'-Binaphthalene-8,8'-Diol: Applications to Asymmetric Synthesis and Molecular Recognition”
Supervisor: Professor Fuji K
25 November 1997

TANIGUCHI, Kiyoshi
“Syntheses and Structure-Activity Relationship of Cychic Amines Having Anti-Bladder Contraction Activity”
Supervisor: Professor Fuji K
25 November 1997

ORGANIZATION AND STAFF

INSTITUTE FOR CHEMICAL RESEARCH
KYOTO UNIVERSITY

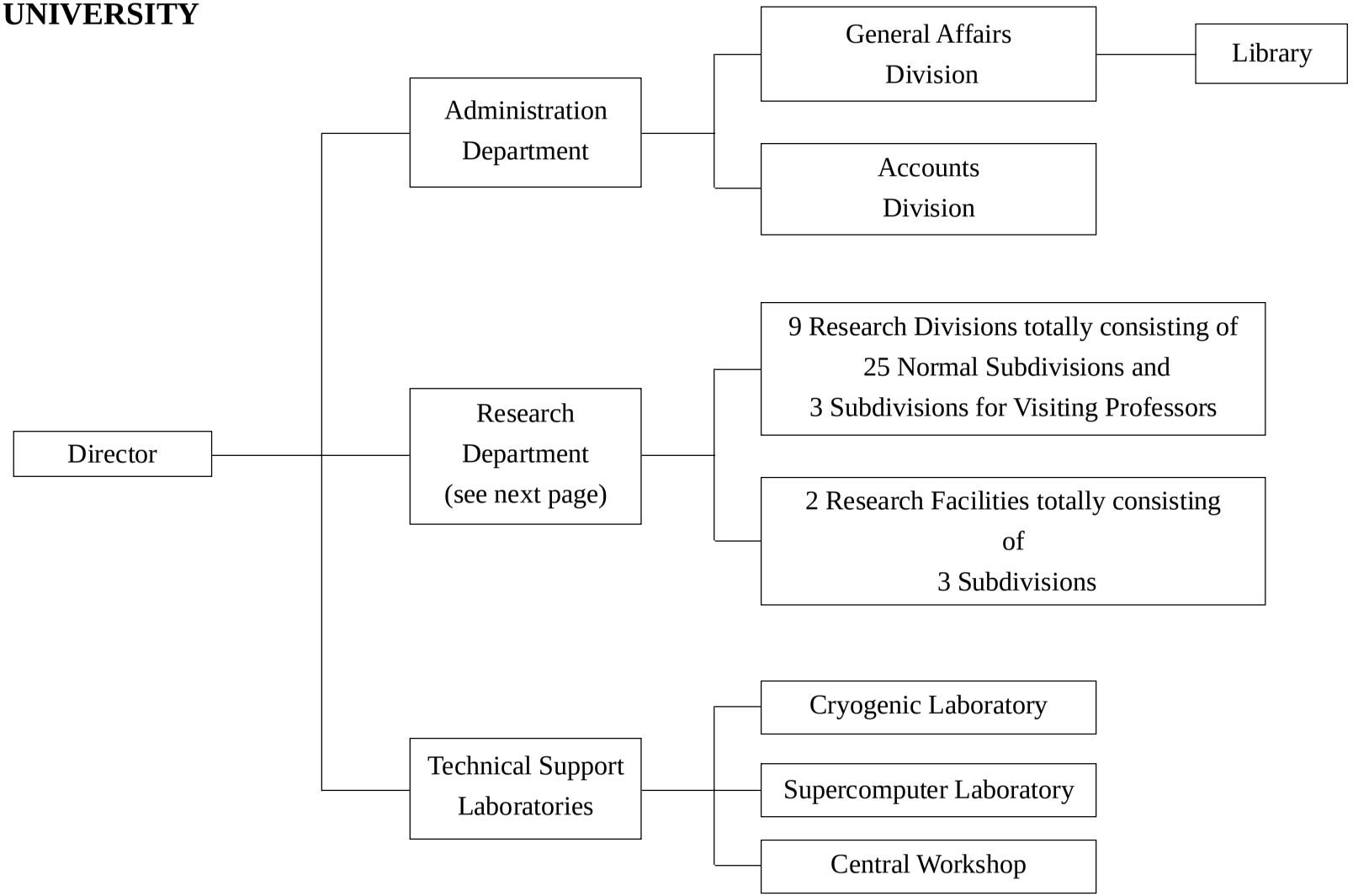

INSTITUTE FOR CHEMICAL RESEARCH, KYOTO UNIVERSITY As of 31 December 1997

RESEARCH DIVISION (G: Laboratory for Visiting Professors)

	Research Division	Subdivision (Laboratory)	Related Graduate School *Graduate School of / Division of*	Professor	Associate Professor	Instructor
Director SHINJO, Teruya	States and Structure	I. Atomic and Molecular Physics	*Science / Physics I*	MUKOYAMA, Takeshi	ITO, Yoshiaki	KATANO, Rintarou NAKAMATSU, Hirohide
		II. Crystal Information Analysis	*Science / Chemistry*	KOBAYASHI, Takashi	ISODA, Seiji	OGAWA, Tetsuya NEMOTO, Takashi
		III. Polymer Condensed States	*Engineering / Polymer Chemistry*	KOHJIYA, Shinzo	TSUJI, Masaki	URAYAMA, Kenji TOSAKA, Masatoshi MURAKAMI, Syozo
	Interface Science	I. Solutions and Interfaces	*Science / Chemistry*	NAKAHARA, Masaru	UMEMURA, Junzo	MATSUMOTO, Mutsuo MATSUBAYASHI, Nobuyuki
		II. Molecular Aggregates	*Science / Chemistry*	SATO, Naoki	ASAMI, Koji	KITA, Yasuo YOSHIDA, Hiroyuki
		III. Separation Chemistry	*Science / Chemistry*	MATSUI, Masakazu	UMETANI, Shigeo	SASAKI, Yoshihiro HASEGAWA, Hiroshi
	Solid State Chemistry	I. Artificial Lattice Alloys	*Science / Chemistry*	SHINJO, Teruya	HOSOITO, Nobuyoshi	MIBU, Ko
		II. Artificial Lattice Compounds	*Science / Chemistry*			IKEDA, Yasunori TERASHIMA, Takahito
		III. Multicomponent Materials	*Science / Chemistry*	TAKANO, Mikio	HIROI, Zenji	AZUMA, Masaki
		IV. Amorphous Materials	*Engineering / Molecular Engineering*	YOKO, Toshinobu	KOZUKA, Hiromitsu	UCHINO, Takashi LIN, Hong
		G. Structure Analysis		KOMATSU, Takayuki	TAKAGI, Hidenori	
	Fundamental Material Properties	I. Molecular Rheology	*Engineering / Molecular Engineering*	OSAKI, Kunihiro	WATANABE, Hiroshi	INOUE, Tadashi
		II. Polymer Materials Science	*Engineering / Polymer Chemistry*	KAJI, Keisuke	KANAYA, Toshiji	NISHIDA, Koji
		III. Molecular Dynamic Characteristics	*Engineering / Molecular Engineering*	HORII, Fumitaka	TSUNASHIMA, Yoshisuke	KAJI, Hironori
		G. Composite Material Properties		TANAKA, Michihiro	FUJIKI, Michiya	
	Organic Materials Chemistry	I. Polymeric Materials	*Engineering / Polymer Chemistry*	MIYAMOTO, Takeaki	FUKUDA, Takeshi	TSUJII, Yoshinobu MINODA, Masahiko
		II. High-Pressure Organic Chemistry	*Engineering / Energy & HC Chemistry*	KOMATSU, Koichi		MORI, Sadayuki KUDO, Kiyoshi NISHINAGA, Tohru
	Synthetic Organic Chemistry	I. Synthetic Design	*Engineering / Energy & HC Chemistry*	TAMAO, Kohei	TOSHIMITSU, Akio	KAWACHI, Atsushi YAMAGUCHI, Shigehiro
		II. Fine Organic Synthesis	*Pharmaceutical Sci. / Pharmac. Chem.*	FUJI, Kaoru	TANAKA, Kiyoshi	KAWABATA, Takeo
		G. Synthetic Theory		NAKATA, Tadashi	YAMADA, Haruo	
	Bioorganic Chemistry	I. Bioorganic Reaction Theory	*Science / Chemistry*	OHNO, Atsuyoshi	NAKAMURA, Kaoru	KAWAI, Yasushi SUGIYAMA, Takashi
		II. Bioactive Chemistry	*Pharmaceutical Sci. / Drug System*	SUGIURA, Yukio		MORII, Takashi
		III. Molecular Clinical Chemistry	*Medicine / Internal Medicine*	UEDA, Kunihiro	TANAKA, Seigo	ADACHI, Yoshifumi
	Molecular Biofunction	I. Functional Molecular Conversion	*Agriculture / Agricul. Chem.*	ODA, Jun'ichi	HIRATAKE, Jun	KATO, Hiroaki
		II. Molecular Microbial Science	*Agriculture / Agricul. Chem.*	ESAKI, Nobuyoshi	YOSHIMURA, Tohru	KURIHARA, Tatsuo
	Molecular Biology and Information	I. Biopolymer Structure	*Science / Biophysics*	TAKAHASHI, Sho	HATA, Yasuo	HIRAGI, Yuzuru FUJII, Tomomi AKUTAGAWA, Tohru
		II. Molecular Biology	*Science / Biophysics*	OKA, Atsuhiro	AOYAMA, Takashi	GOTO, Koji
		III. Biological Information Science	*Science / Biophysics*	KANEHISA, Minoru		GOTO, Susumu OGATA, Hiroyuki
	Nuclear Science Research Facility	I. Particle and Photon Beams	*Science / Physics II*	NODA, Akira	KAKIGI, Shigeru	SHIRAI, Toshiyuki
		II. Beams and Fundamental Reaction	*Science / Physics II*	INOUE, Makoto	MATSUKI, Seishi	IWASHITA, Yoshihisa OKAMOTO, Hiromi
	Research Facility of Nucleic Acids		*Science / Biophysics*	OKA, Atsuhiro	SUGISAKI, Hiroyuki	FUJIBUCHI, Wataru

PERSONAL

Award

Professor Emeritus Dr. Kenji SODA

(Molecular Microbial Science, Division of Molecular Biofunction)

Dr. Kenji Soda, Professor Emeritus of Kyoto University, received a Purple Ribbon Medal (Shijuhosho) on November, 1997.

Dr. Soda was born in Aichi Prefecture on February 7, 1933. He graduated from Faculty of Agricultural and Biological Chemistry, Kyoto University in 1956 and continued his studies on microbial biochemistry under the supervision of the late Professor H. Katagiri. He graduated from the Doctor Course of Agricutural and Biological Chemistry, Kyoto university, and awarded the degree of Ph.D. in 1961.

He started his academic carrier as an instructor of the Departement of Agricutural and Biological Chemistry, Kyoto University to study microbial biochemistry and biotechnology with the late Professor K. Ogata, and Professor T. Tochikura in 1962. During 1963 and 1965, on leave from Kyoto University he stayed at Tufts University School of Medicine, Boston, Mass, U.S.A. as a visiting research fellow of Department of Biochemistry, and studied the biochemstry of amino acids with Professor A. Meister. In 1965, he was promoted to an associate professor at the Laboratory of Microbial Biochemistry of the Institute for Chemical Research, Kyoto University. In 1981, Dr. Soda was appointed full professor of Kyoto University, and directed the Laboratory of Microbial Biochemistry, Institute for Chemical Research. At the Graduate School of Agriculture, Kyoto University, he gave lectures on Microbial Biochemistry and Applied Microbiology and supervised the dessertation works of many graduate students.

On the 31st of March, 1996, Dr. Kenji Soda retired from Kyoto University after having completed his 35 years of service at Kyoto University, and was honored with the title of Emeritus Professor of Kyoto University on the following day. Now, he takes a position as a professor of Kansai University.

Dr. Soda devoted himself to the Japanese Biochemical Society and officiated as President of the Society between 1992 and 1993. He was also the trustee of Japan Society of Bioscience, Biotechnology and Agrochemistry, Vitamin Society of Japan, and others. He was awarded the Prize of Agricultural Chemical Society of Japan for Young Scientists in 1969, the Prize of Vitamin Society of Japan in 1985, and the Prize of the Japan Society of Bioscience, Biotechnology and Agrochemistry in 1992.

For the past forty years, he extensively investigated various aspects of microbial biochemistry. He studied the structure and functions of biocatalysts produced by microorganisms, in particular, pyridoxal enzymes, NAD enzymes, and flavin enzymes: he characterized L-lysine ε-aminotransferase, D-amino acid aminotransferase, kynurenine aminotransferase, arginine racemase, alanine racemase, amino acid racemase with low substrate specificity, methionine γ-lyase, leucine dehydrogenase, alanine dehydrogenase, phenylalanine dehydrogenase, *meso* -α,ε-diaminopimelate D-dehydrogenase and others. He carried out also the research on the metabolism and biofunction of selenium containing amino acid and peptides. He has found new enzymes participating in the selenium metabolism such as selenocysteine β-lyase and a new pathway of the microbial fluorine metabolism. He also engaged himself in the characterization and application of new biomolecules. For example, he has elucidated the molecular structure and functions of thermostable and thermolabile enzymes and studied their application.

He discovered a few halo acid dehalogenases, and studied their structure and functions, and new oxygenases and oxidases acting on nitro compounds, and characterized. He modified and improved their properties by protein engineering and developed a new procedure to effectively decompose the nitro compounds in waste water by means of these enzymes.

Retirement

Professor Jun'ichi ODA

(Functional Molecular Conversion Laboratory, Division of Molecular Biofunction)

On the 31st of March, 1998, Dr. Jun'ichi Oda retired from Kyoto University after 33 years of service to the University and was honored with the title of Professor Emeritus of Kyoto University.

Dr. Oda was born in Kyoto on the 20th of December, 1934. After graduation from Department of Agriculture, Kyoto University in 1959, he continued his studies on the synthesis and evaluation of biologically active natural products as a graduate student. In 1965, he was appointed an instructor of the Laboratory of Plant Product Chemistry, Institute for Chemical Research, Kyoto University, under the supervision of the late Emeritus Professor Minoru Ohno. He was granted a doctoral degree from Kyoto University in 1965 for his studies on the synthesis of naturally occurring cumarane compounds. During 1968 and 1969, on leave from Kyoto University, he stayed at the Department of Chemistry, Bonn University in West Germany and studied the metabolism of chlorinated hydrocarbon insecticides with Professor F. Korte. In 1973, Dr. Oda was promoted to Associate Professor of the same laboratory. In 1984, he was appointed full Professor of Kyoto University and directed the Laboratory of Plant Product Chemistry (present name, Molecular Biofunction I), Institute for Chemical Research, Kyoto University. From the 1st of April, 1992, to the 31st of March, 1994, Dr. Oda was appointed Director of the Institute and made great contributions not only to the Institute but also to the University as a councilor.

During the past 33 years, his research interest encompassed a wide array of synthetic organic chemistry, stereochemistry, bioorganic chemistry, molecular biology and structural biology. Following his early studies on the synthesis of biologically active plant products, he developed a series of asymmetric reactions such as Simmons-Smith reactions, cyclopropanations and a sigmatropic rearrangement. He synthesized a series of chiral dihydronicotinamide (NADH) derivatives as a model study of alcohol dehydrogenase, and carried out the stereoselective reduction of ketones with high enantioselectivity. He also focused on the use of lipases as a chiral catalyst in organic synthesis and prepared several important chiral synthons. As a molecular biological aspect of his research, he cloned the gene of a microbial lipase and characterized a hitherto unknown protein which might assist the folding of the lipase. He also prepared the catalytic antibodies which are capable of stereoselective hydrolysis of esters and carbonates, and defined the mechanisms of the catalyzed reaction and product inhibition. His research interest in enzyme chemistry and structural biology was highlighted by the X-ray crystallography of ATP-dependent ligases such as glutathione synthetase and asparagine synthetase. He also designed and synthesized a transition-state analogue inhibitors of these ligases and used for the elucidation of the detailed reaction mechanisms of the ligases by inhibition kinetics and structural characterization of the enyzme-inhibitor complex, along with a time-resolved X-ray crystal analysis. For his brilliant achievements on biocatalysts, he was awarded a prize from Japan Society for Bioscience, Biotechnology, and Agrochemistry in 1996.

NAME INDEX

KEYWORD INDEX